SORPTION OF SULFATE ON IRON OXIDE MINERALS

SORPTION OF SULFATE ON IRON OXIDE MINERALS: HEMATITE AND GOETHITE

By

LAURIE JEANNE TURNER

A Thesis

Submitted to the School of Graduate Studies

in Partial Fulfilment of the Requirements

for the Degree

Doctor of Philosophy

McMaster University

DOCTOR OF PHILOSOPHY (1988)
(Geology)

McMASTER UNIVERSITY
Hamilton , Ontario

TITLE: Sorption of Sulfate on Iron Oxide Minerals: Hematite and Goethite.

AUTHOR: Laurie Jeanne Turner, B.A. (University of Maine at Farmington)
MSc. (McMaster University)

SUPERVISOR: Professor James R. Kramer

NUMBER OF PAGES: xiii, 158

ABSTRACT

The influence of sulfate on terrestrial and aquatic ecosystems depends on the mobility of the sulfate anion in soils. This mobility is determined by several factors, one being the types and amounts of soil constituents. In this study, several iron oxide/hydroxide minerals were evaluated for sulfate sorption characteristics.

Hematite and goethite were synthesized and positively identified using x-ray diffraction, mossbauer spectroscopy and scanning electron microscopy. Mineral surfaces were characterized using surface area and zero point of charge measurements, infrared spectroscopy and thermal analyses. Neutron activation and x-ray fluorescence were used to look for impurities. Samples were compared to a natural hematite sample and a synthetic jarosite.

Sorption experiments, conducted on mineral suspensions in KNO_3 media at room temperature, considered the variables time, ionic strength, solid:solution ratio, pH and sulfate concentration. Sorption was initiated by a fast reaction, followed by a longer, slower one which reached an apparent equilibrium in 24 hours. Sorption was unaffected by solid:solution ratio and decreased with ionic strength at pH 5 for goethite only.

Sorption increased with increasing sulfate concentration and decreasing pH. A sorption maximum was reached by all minerals except synthetic hematite. Under optimum pH and $[SO_4]$, approximately half of the mineral surface is covered by sulfate ions. Sulfate was sorbed irreversibly. Only a fraction of sorbed sulfate can be desorbed, an amount which increases with pH.

Thermal analyses indicate sulfate to be strongly bonded. The presence of four infrared bands on sulfate treated surfaces indicate direct coordination of the anion to the iron cation. The above evidence, including irreversibility of sorption, supports inner sphere complexing of sulfate. Sulfate sorption on iron oxide/hydroxide minerals is thus a combination of nonspecific electrostatic attraction and mono - multi ligand exchange (including binuclear bridging) which act under different system conditions to form the basis of sulfate sorption behavior.

The present observations are important in modelling of environmental systems, such as in the Direct Delayed Response Program Model, due to the significance of irreversibility of sulfate sorption on model assumptions.

ACKNOWLEDGEMENTS

I wish to express appreciation to the following persons for their assistance throughout the course of this study:

Dr. James R. Kramer for his enthusiasm and support during the supervision of this research.

Dr. H.D. Grundy and Dr. Ward Chesworth for their encouragement and advice.

Jill Gleed for assisting with A.A. analyses and chromatographic work.

Joanne Carson for her expertice with the SEM.

Marianne Crowe for assisting with XRD analyses.

Frank Gibbs for DTA and TGA work.

Ota Mudroch for XRF analyses.

Kathleen Gracey for assisting with NAA analyses.

Ian Thompson for help with IR spectroscopy.

Dr. Tom Birchall for Mossbauer Analyses.

Jack Whorwood for printing the SEM Plates.

Kathy Teeter and Steve Davies for computer advice.

Nancy Harper and Judy Gracey for proofreading the text.

I give my sincere thanks to many friends that have passed through the department and touched my life. Most of all I thank my husband, Blair Lagden, whose constant support, encouragement and optimism have enabled the completion of this thesis.

TABLE OF CONTENTS

PAGE

CHAPTER 1 INTRODUCTION 1

I. Environmental sulfur problems in soils..... 1

A. Sulfur status of soils..... 1

B. Ion mobility in soils..... 3

C. Atmospheric deposition of H_2SO_4..... 5

D. Acid sulfate soils and acid mine drainage 6

II. Summary of research objectives..... 8

A. Substrate..... 8

B. Other phases..... 9

C. Parameters..... 10

D. Proposal and research objectives..... 12

CHAPTER 2 AQUEOUS CHEMISTRY OF SULFUR AND IRON..... 14

I. Aqueous chemistry of sulfur..... 14

II. Aqueous chemistry of iron..... 15

III. Sulfur and iron...chemical relations..... 18

CHAPTER 3 LITERATURE REVIEW..... 23

I. Soil research literature..... 23

II. Oxide research literature..... 27

CHAPTER 4 OXIDE SURFACE CHEMISTRY..... 32

I. Surface groups..... 32

II. Surface charge and adsorption..... 33

III. Surface site/species determination..... 37

IV. Sorption models..... 38
V. Summary..... 38
CHAPTER 5 MINERAL PREPARATION AND CHARACTERIZATION.. 42
I. Mineral preparation methods..... 42
II. Methods of mineral characterization..... 44
A. Surface area..... 44
B. pH of zero point of charge (zpc)..... 46
C. X-ray diffraction analysis..... 49
D. Electron microscopy..... 53
E. Infrared spectroscopy..... 54
F. Thermal analysis..... 57
G. Mossbauer spectroscopy..... 65
H. X-ray fluorescence..... 69
I. Neutron activation analysis..... 69
J. Summary..... 70
CHAPTER 6 SORPTION EXPERIMENTS ON IRON OXIDES..... 73
I. Experimental procedures..... 73
II. Results obtained-general observations..... 74
CHAPTER 7 OTHER EXPERIMENTS..... 83
I. X-ray diffraction and scanning electron microscopy..... 83
II. Infrared spectroscopy..... 83
III. Thermal analysis..... 86
IV. Mossbauer spectroscopy..... 90
V. Ion concentration product..... 90
VI. Exchange capacity..... 91

VII. Hydroxide release vs sulfate sorption..... 96

CHAPTER 8 MODEL OF SULFATE SORPTION ON FERRIC OXIDES..... 100

I. Sorption summary..... 100

A. General characteristics..... 100

B. Sorption maxima..... 102

C. Isotherm comparison..... 103

D. Sorption in relation to surface area.... 105

II. Other evidence..... 106

A. OH- released / SO4 sorbed = R 106

B. Sample weight loss..... 107

C. Exchange capacity..... 109

D. Summary..... 110

III. Sorption behavior models..... 111

CHAPTER 9 ENVIRONMENTAL IMPLICATIONS..... 117

A. Sulfate sorption capacity of soils..... 117

B. Relevance to watershed acidification models..... 121

C. Other aspects..... 124

REFERENCES..... 126

APPENDIX A: SUMMARY OF OXIDE RESEARCH..... 153

Table of Figures

Figure Page

2.1 Eh-pH diagrams illustrating stability fields of aqueous species and solids at 25°C 1 atm pressure 17

2.2 Solubility diagrams for hematite, goethite, and and amorphous iron hydroxide calculated using the equations and constants from Table 2.1 21

2.3 Eh-pH diagram illustrating stability fields of solid and dissolved forms of sulfur and iron at 25°C and 1 atm pressure 22

4.1 Schematic showing the change in O^-, OH and OH_2^+ surface groups with acid/base additions and the resulting pH change with respect to zpc 35

4.2 Schematic of substrate surface electrical double layer at pH = 3 for low and high ionic strength 36

4.3 Example of mononuclear and binuclear bonding of a phosphate ion onto an iron oxide 37

4.4 Theoretical schematic of sulfate sorption on iron oxide surfaces 39

4.5 Schematic of the electric double layer at pH 3, high ionic media, with sulfate. Electrostatic attraction only 40

4.6 Schematic of the electric double layer at pH 3, high media, with sulfate. Ligand exchange 41

5.1 X-Ray diffraction patterns for synthetic hematite and goethite 51
5.2 X-Ray diffraction patterns for natural hematite and synthetic jarosite 52
Plate 5.1 SEM images of mineral samples 55
5.3 Differential thermograms of mineral samples 64
5.4 Mossbauer level splitting in ^{57}Fe and the types of spectra which arise 67
5.5 Mossbauer spectra of mineral samples taken at room temperature at maximum velocity 10.268 mm/s 68
6.1 Initial goethite experiment: pH vs Time 75
6.2 Initial goethite experiment: $[SO_4]$ vs Time 76
6.3 Percent sorbed of the original solution sulfate concentration for 4g/l iron oxide suspension 78
6.4 Amount sorbed vs equilibrium solution sulfate concentration 79
6.5 Desorption of sulfate from iron oxide surfaces: pH dependence 82
7.1 Differential thermograms of mineral samples after sulfate sorption 89
7.2 Suspension treatment for exchange capacity determination 92
8.1 Schematic illustrating the internal structure of iron oxides at the pH_{zpc} 111
8.2 Schematic of oxide surface under the system conditions pH = 3 and constant ionic strength 112

8.3 Schematic illustrating sulfate sorption onto surface sites described in Figure 8.2 116

Table of Tables

Table Page

1.1 Average concentration of sulfur, carbon and nitrogen in rocks (in ppm) 2

2.1 Equations used to draw Figures 2.1, 2.2 and 2.3 20

3.1 Investigations of sulfate sorption on iron oxyhydroxide minerals. Experimental conditions 31

5.1a Comparison of surface area values for goethite 45

5.1b Comparison of surface area values for hematite 46

5.2a Comparison of ZPC values for hematite 49

5.2b Comparison of ZPC values for goethite 49

5.3 Infrared spectral peaks obtained 58

5.4 Thermogravimetric data for sample weight losses 63

5.5 XRF analysis data of oxide samples 69

5.6 Neutron activation analysis data of oxide samples .. 70

6.1 Relationship between pH and reversibility 81

7.1 Surface group peaks in the V SO_4 region 86

7.2 Thermogravimetric data for sample weight loss 88

7.3 Exchange capacity related characteristics 94

7.4 Reported exchange capacity and surface coverage values 96

7.5 Ratio of hydrogen consumed to sulfate sorbed calculated from early raw data 99

7.6 Ratio of hydrogen consumed to sulfate sorbed from

titration data for 500 ppm initial [SO_4] 99

8.1 Sorption reaction observations 100

8.2 Sorption maxima and calculated maximum possible surface coverage by sulfate 101

8.3 Percent desorbed from equilibrium solutions 102

8.4a Langmuir isotherm data fit for oxide samples 103

8.4b Freundlich isotherm data fit for oxide samples 104

8.5 Sorption in relation to surface area 105

8.6 Ratio of hydroxyl released vs sulfate sorbed 106

8.7 Weight loss on ignition, and by thermal gravimetric analysis before and after sulfate sorption, and resulting OH/nm^2 108

8.8 Exchange capacity and efficiency 109

9.1 Estimated time required to saturate Manitoba soils with sulfate 119

CHAPTER 1 INTRODUCTION

I. ENVIRONMENTAL SULFUR PROBLEMS IN SOILS

A. Sulfur Status of Soils:

Sulfur is not a major constituent of the outer crust as only 0.06% of all sulfur is found there (Conesa et al. 1982), but it is widely distributed in reduced form in both igneous and sedimentary rocks as metallic sulfides (Hem 1970). The average composition of igneous and sedimentary rock types is given in Table 1.1. Sulfur is present in variable quantities in all soils. Carbon, nitrogen and sulfur are found in a ratio of 100:10:1 with some variation due to soil pH (Simon-Sylvestre 1969).

Goldberg (1963) reports seawater concentrations of 2,700 mg/l SO_4, 142 mg/l HCO_3 (including CO_3, H_2CO_3 and organic carbon), and 0.5 mg/l N (including NO_3, NO_2, N_2 and NH_4). Rainfall concentrations are invariably greater than 1 mg/l SO_4. Eriksson (1955, 1960) estimates the average sulfate content of rain deposited on land to be ~30 kg/hectare/yr.

As a constituent of certain amino acids, sulfur is an essential nutrient in the cultivation of crops. Sulfur deficiency is widespread, especially in highly leached

Table 1.1 Average concentration of sulfur, carbon and nitrogen in rocks (in ppm).

ELEMENT	IGNEOUS ROCKS*	SEDIMENTARY ROCKS#		
		sandstone	shale	carbonate
sulfur	410	945	1850	4550
carbon	320	13,800	15,300	113,500
nitrogen	46	-	600	-

* Horn and Adams 1966, Parker 1967
\# Hem 1970

tropical soils. In humid/semi-humid zones and arid/semi-arid regions, rainy season showers resulting in heavy leaching have been widely reported. Soil sulfur status information relating to soil characteristics is needed to prepare a guideline for fertilization programs.

Soil fertility relating to sulfur was neglected for a long time because early determinations of sulfur requirements by crops were underestimated due to the ashing techniques used. The fertilizer 'superphosphate' was thought to supply ample sulfur in conjunction with natural sources such as atmospheric deposition (Ensminger 1954, Lowe and Delong 1961). However, modern agricultural practices and improved crop varieties only intensify sulfur demand.

Recent investigations of sulfur cycling behavior have shown sulfur to be distributed between two soil fractions: organic and inorganic. Surface soils contain several organic forms of sulfur (i.e. carbon bonded sulfur and ester sulfates - Williams 1975, Fitzgerald 1978), some of which can be converted to crop available forms such as

sulfate ($SO_4^=$) by microbial decomposition (Ensminger 1954). Inorganic soil sulfur is found as sparingly soluble minerals like elemental sulfur, sulfides and sulfates, as well as in ionic forms ($SO_4^=$) in soil solution and sorbed onto soil colloids. Generally a higher proportion of inorganic sulfur is found in subsoil than in surface soil (Harward and Reisenauer 1966). The water soluble sulfate pool in surface soils (whose concentration fluctuates due to uptake by biota, mineralization, and leaching from the system) is thought to be active in sulfur cycling, whereas the water insoluble subsurface sulfate is an inactive long term sulfur reserve (Johnson and Henderson 1979).

B. Ion Mobility in Soils:

Sulfur budgets for forest ecosystems indicate net sulfate accumulations in old, highly weathered soils, and balances between inputs and outputs in young, less weathered soils. Kamprath et al. 1956, Chao et al. 1962, Barrow 1967, Haque and Walamsley 1973 and Sanders and Tinker 1975 all show that sulfate adsorption capacity is related to pH and to the amount of sesquioxides contained in the soil. The sesquioxide content is determined by the parent rock composition, the soil age, and the extent of weathering.

Ion mobility in soil depends on soil characteristics such as composition (solid phases present), pH, presence of other ions (e.g. phosphate from fertilizers), the pattern,

amount and velocity of water movement, and the ion concentration. The interactions of these factors determine the fate of sulfate; its distribution in the profile, availability to biota, and magnitude of losses to drainage water (Harward and Reisenauer 1966).

It has been well established through field and laboratory studies that soils differ markedly in their ability to retain sulfate. A variety of sulfate leaching losses have been reported for lysimeter percolates (MacIntire et al. 1941,1952, Stauffer and Rust 1954, McKell and Williams 1960, Pratt and Chapman 1961, Harward and Reisenauer 1966). Superphosphate applications and liming have been shown to cause soils to lose some of their ability to retain sulfate, after which leaching can begin (Ensminger 1954, Kamprath et al. 1956).

Johnson and Cole (1980) propose cation nutrient transport from soil profiles to be regulated by soil solution anions which maintain electroneutrality. Normally, bicarbonate ions (from soil CO_2 pressure and pH) play the major role, with organic anions, Cl^-, NO_3^-, HPO_4^- and $SO_4^=$ taking up the slack. But activities which change the normal balance of soil anions such as the management practices of fertilization, harvesting and fire, and forms of pollution (e.g. acid rain) can greatly change cation transport in the system. When soil solution anions are retained, nutrient

cations can also be held; when mobile and leached, they can take nutrient cations with them.

C. Atmospheric Deposition of H_2SO_4:

The potential of acid precipitation to increase nutrient leaching in ecosystems and possibly adversely affect productivity is causing much concern. Acid rain affect on nutrient status of many forest sites is being evaluated by estimating wet and dry atmospheric deposition, nutrient cycles and hydrologic fluxes. Examples of sites where sulfate outputs have been found to exceed inputs (leaching occurs) are the Thompson Site WA. (Cole and Johnson 1977), Hubbard Brook Watershed N.H. (Likens et al. 1977) and Haney Forest B.C. (Feller and Kimmins 1979). Those sites where sulfate inputs exceed outputs (net accumulation occurs) are the Solling Site in Germany (Heinrichs and Mayer 1977), Walker Branch Watershed TN. (Shriner and Henderson 1978), the La Selva Site in Costa Rica (Johnson et al. 1979), the Bowl Site N.H. (Martin 1979) and the Coweeta Watershed N.C. (Swank and Douglas 1977).

Acid input (H^+) to a system has several possible fates:

(a) neutralization by strong base cations (Ca^{2+}, Na^+), which come from sources such as mineral weathering.

(b) passage to ground waters (for soils already acidic or low in cation exchange capacity, CEC). Acidification of

natural waters is of great concern because a drop in pH can cause the concentration of toxic forms of elements such as aluminum to increase to the point where biota are threatened.

(c) entrance into exchange reactions with cations present on soil colloids (McFee et al. 1976). Soil acidification, which occurs once the soil buffer capacity is exceeded by acid inputs, is also of great concern in areas where acid precipitation is prevalent. Soils with low CEC and moderate pH are quite sensitive to acidification.

The net effect of acid deposition on an ecosystem will thus depend on certain site-specific factors such as present nutrient status (base saturation/buffer capacity), present H+ content, ion sorption and desorption, mineralogy, composition and the amount of atmospheric acid input.

D. Acid Sulfate Soils and Acid Mine Drainage:

Acid sulfate soils and acid mine drainage caused by sulfide mineral weathering are an environmental concern. Acid sulfate soils develop on waterlogged pyritic sediments and mine tailings when the water level falls below the pyritic substratum. Sediments can be exposed through natural causes such as decreased sea levels or water tables or through human interferences. Diking, for example, has caused severe acidification of tidal sediments (Van Breeman 1982). Extended exposure to the atmosphere allows oxidation of pyrite to iron (II) sulfate and sulfuric acid. Bacterial

oxidation of iron (II) to iron (III) continues the reaction. The sediment water pH may drop to 4 or lower.

Ions released during sulfide mineral weathering undergo various reactions:

H^+ - some is partly inactivated by ion exchange and other weathering reactions.

- some is lost to waters where it can lower their pH.

Fe^{2+} - oxidizes to Fe^{3+} which precipitates as oxides, and basic Al^{3+} and Fe^{3+} sulfates such as jarosite.

$SO_4^=$ - a large percentage remains in solution to be removed by leaching along with cations obtained from ion exchange and weathering.

- some is precipitated as basic Al^{3+} and Fe^{3+} sulfates and possibly as temporary water soluble hydrated ferrous sulfates (melanterite, copiapite) which are responsible for increased acidity in receiving streams during rain events (Nordstrom 1982).

- some is adsorbed onto mineral surfaces.

There are millions of hectares of potentially or currently acidic sulfate soils in recent coastal plains (Van Breeman 1982). Marine sediments are neutral to alkaline when submerged, but when drained (e.g. tidal marshes) iron and sulfur oxidation occurs causing acidification. On resubmerging, a certain amount of these elements will be reduced to sulfide again (Harward and Reisenauer 1966).

In mines such as the California Iron Mountain

watershed copper mines, a variety of sulfide minerals are weathering to produce highly acidic mine water. Both oxidized and reduced iron minerals can be present as efflorescences and precipitates in or near the acid mine waters (Nordstrom 1982). Acid mine drainage is especially characteristic of coal mining, with pyrite being the usual source of acid weathering products.

II. SUMMARY OF RESEARCH OBJECTIVES

Retention and leaching of cations and anions are significant in the processes of soil formation, geochemical circulation of nutrients, fertilization and pollution of soils and waters. The influence of sulfate on terrestrial and aquatic ecosystems depends on sulfate mobility. The difference between a soil that retains sulfate and one that does not is dependent on environmental conditions and site characteristics with a major influence being played by soil constituents (hydroxides and clays).

A) Substrate:

Natural whole soil samples are a complex mixture of surfaces with a variety of organic and inorganic species in the soil solution. They have been examined for sorption characteristics, but do not readily allow evaluation of sorption mechanisms due to their complex nature. The sorption mechanisms of the individual constituents can be

interpreted with less difficulty since they can be more thoroughly characterized than whole soil samples. Extrapolation of experimental results must be done with caution because when placed back into the natural environment, constituent behavior is modified by interaction with other substrate components. The iron oxide hematite, and hydroxide goethite, referred to collectively as oxides or oxyhydroxides throughout the text, were chosen for substrate materials in this study for several reasons. First, they are common to many soils. Second, they have been widely studied and are easily prepared and characterized. Lastly, they are important soil constituents which do sorb sulfate.

B) Other phases:

The concentrations of ions such as sulfate in solution are influenced by precipitation and dissolution as well as sorption and desorption reactions. It is generally difficult to tell which process is predominant unless a precipitating phase is visible. Sorption and precipitation are closely related. Sorption onto surfaces, which is site dependent, is the first step in solid phase precipitation, which is dependent on solution concentration. If nucleation, growth, and dissolution rates are slow, the process will approximate sorption behavior. That is, there may not be a distinctive boundary between 'pure sorption' and 'pure

precipitation' (Nordstrom 1982). But a lower limit of the boundary can be set, assuming that saturation with respect to the solid phase is required for nucleation, because if the solubility product (K_{so}) is exceeded, there is the possibility of precipitation. In this study, the potassium iron sulfate mineral Jarosite was examined as a possible precipitant on the oxide surfaces under the experimental conditions. Jarosite was chosen because it is often found in acid sulfate soils and acid mine spoils.

C) Parameters:

A general knowledge of substrate sorption characteristics and consideration of the factors which influence sorption are prerequisite to the modelling of natural sorption in soils.

a) Substrate parameters:

i) Purity - surface impurities often can mask the sorption characteristics of the substrate of interest.

ii) Pretreatment - pretreatments which may have been performed to remove surface impurities may in effect alter the surface by creating new sites or destroying true sites and thus change the original sorption characteristics.

iii) Surface area - surface area is determined by grain size, shape and crystallinity and ultimately determines the number of available surface sites.

b) Substrate : solution ratio - may effect sorption at low substrate concentrations.

c) Salt concentration (or ionic strength) - when in high concentrations, salts can displace electrostatically held ions. Salt concentration may influence flocculation. Coagulation into flocs may enhance sorption by increasing the ion concentration in interstitial waters, or may decrease sorption by blocking sorption sites.

d) Complexing ligands - when present, complexing ligands complicate sorption reactions. If the ligands have an affinity for the surface, they will enhance sorption. If not, they will effectively reduce the ions concentration in solution and decrease sorption.

e) Other ions - when other ions are present, sorption can be complicated. There may be competition for sorption sites by surface and solution complexation and formation of precipitates.

f) Sorbate concentration - anion sorption increases with concentration. At lower concentrations it may increase linearly, with the isotherm being best described by a distribution coefficient, K_d. At higher concentrations a nonlinear isotherm with no maximum, often described by the Freundlich equation, may be observed. At even higher concentrations a nonlinear isotherm with a maximum, commonly described by Langmuir equations, can be found.

g) pH - affects H^+ as a counterion in nonspecific

sorption. Substrate stability and surface charge and sorbate speciation are dependent on pH .

h) Time - if sorption is considered an equilibrium process, then the time required to achieve equilibrium is important. The kinetics of the reaction will determine if the process will be slow, or fast, or if in fact it is an equilibrium process at all.

D) Proposal and Research Objectives:

This project attempts to characterize clearly sulfate sorption on iron oxides. If the process on the individual soil constituents can be clarified, then parallels in whole soil behavior may be defined. An increased understanding of the interaction between soils and sulfate would contribute to existing knowledge of the sulfur cycle and would aid in recognition and evaluation of the environmental effects of anthropogenic inputs to ecosystems.

General Objective: to contribute to the knowledge of reactions at solid-liquid interfaces, especially with respect to the fate of sulfate ions in soils.

Specific Objectives:

- to prepare and characterize several iron oxyhydroxide minerals and compare them to a natural sample.

- to examine sulfate sorption characteristics of the

iron oxides and hyroxides in relation to the variables time, pH, ionic strength, solid:liquid ratio, and sulfate concentration.

- to examine reversibility (desorption).

- to examine the relation between sorbed sulfate and the oxide surface. Are there any indications for precipitation?

- to propose a model for the sorption process.

CHAPTER 2 AQUEOUS CHEMISTRY OF SULFUR AND IRON

I. Aqueous Chemistry of Sulfur

In natural water, dissolved sulfur is found in the following thermodynamically stable forms (25°C 1 atm):

$$HSO_4^-,\ SO_4^=,\ S^o,\ H_2S,\ HS^-,\ S^=$$

Several intermediate oxidation species (ex. thionate, $S_4O_6^=$; sulfite, $SO_3^=$) have been reported in thermal springs (Hem 1970).

The conversion of oxidized to reduced sulfur forms is slow; inorganic chemical conversion is not completed. Thus nonequilibrium forms can persist for a long time. In many cases bacteria, of the Thiobacillus genus, are required to catalyze the conversion.

An Eh-pH stability diagram for sulfur can be prepared using equilibrium assumptions and the equations and constants in Table 2.1. (see Figure 2.1). This diagram does not present a completely true picture of sulfur behavior because of the presence of nonequilibrium conditions in the true system, but is valuable for predicting general boundary conditions so approximations of oxidation state and species present can be made. Note, the boundaries in a stability field diagram are drawn at equal ion activities, and the only boundary that will change on

increasing or decreasing the total sulfur concentration will be those around solid sulfur.

In aerated water (25° C, 1 atm., pH 4-9 and Eh 0.4 volts), the most chemically stable form of sulfur is the sulfate anion. It forms ion pairs with common cations such as Ca^{++}, Na^{+}, K^{+} and Mg^{++} as well as forming salts with certain metals.

Sulfate reduction occurs when the system is depleted of oxygen (ex. anoxic conditions in lake sediments). The reduction requires bacteria and produces sulfides which precipitate out as sulfide minerals such as pyrite (FeS_2) and pyrrhotite (FeS).

II. Aqueous Chemistry of Iron

As the fourth most abundant element in the earth's crust, iron is an important metal in soils, sediments and natural water systems. Its chemical behavior involves oxidation and reduction, precipitation and dissolution, and hydrolysis reactions.

In the absence of strong complexing ligands (organics), iron cations in solution will react with water through stepwise hydrolysis. When polymers are not considered, hydrolysis equilibrium can be established quickly. Reduced "ferrous" iron will occur in the forms Fe^{2+}, $FeOH^{+}$ and $Fe(OH)_2$ (aq). Oxidized "ferric" iron will

occur as Fe^{3+}, $FeOH^{2+}$, $Fe(OH)_2^{+}$, $Fe(OH)_3$ (aq), $Fe(OH)_4^{-}$ and in polymeric forms. The hydrolysis process is pH dependent and is limited by the precipitation of oxyhydroxide phases.

Using chemical equilibrium assumptions and the equations and constants in Table 2.1, solubility diagrams can be prepared for the different naturally occurring solid phases (ex. Figure 2.2a - amorphous solid, 2.2b - goethite and 2.2c - hematite). These diagrams are used to predict saturation under the specified conditions. They illustrate conditions under which a particular solid phase predominates.

In order to examine the whole picture, an Eh-pH diagram illustrating fields of stability of solids and predominant oxidized and reduced ionic species can be prepared (see Figure 2.1b). Again, boundaries are at equal ion activities and can shift around the solid phases with changing total iron concentration.

Standard conditions in aerated water are 25°C, 1 atm., Eh 0.4 volts and pH 4-9. At lower pHs, iron will be reduced (Fe^{2+}), at higher pHs oxidized (Fe^{3+}) and most likely complexed into oxide and hydroxide species.

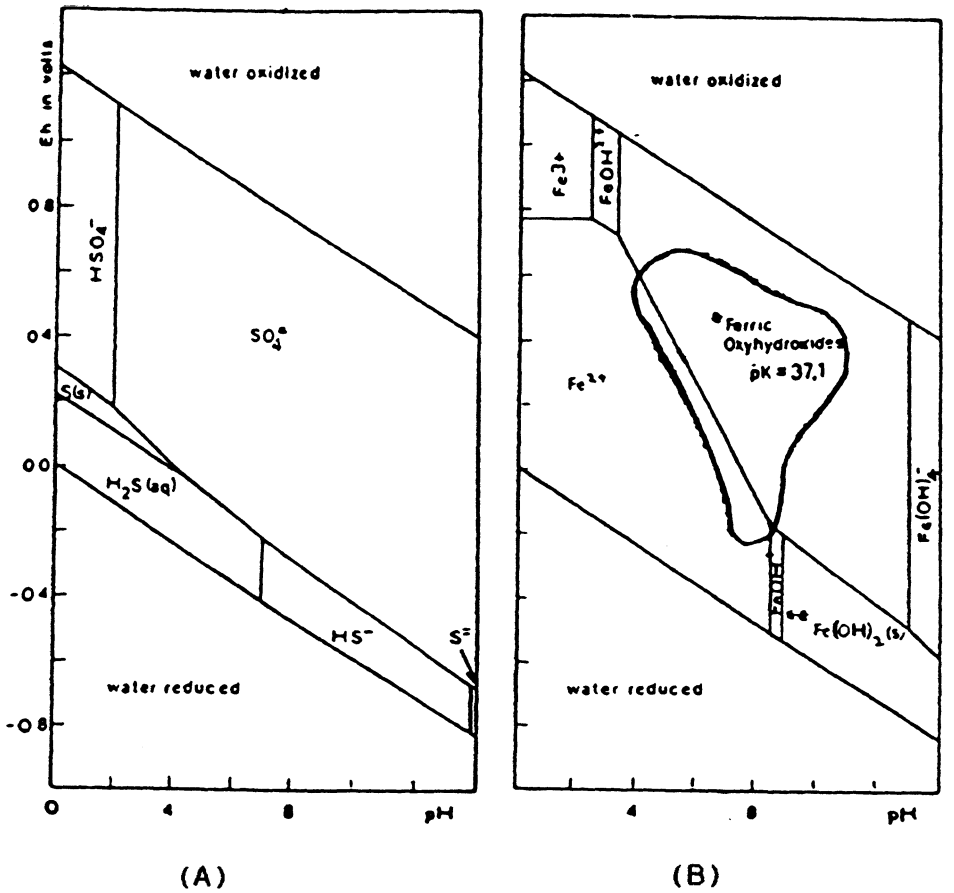

Figure 2.1 Eh-pH diagrams illustrating stability fields of aqueous species and solids at 25°C 1 atm pressure.

A. Sulfur species predominance regions assuming total dissolved sulfur = 10^{-3} M as sulfate. (From Hem 1970).

B. Iron species predominance regions assuming dissolved iron = 10^{-4} M and assuming a pK of 37.1 for the ferric oxyhydroxide - Fe^{2+} boundary. This boundary will move towards the left with increasing pK values. (Adapted from Langmuir and Whittemore 1971)

* The ferric oxyhydroxide field shown represents areas which may be occupied by ferrihydrite, goethite, or hematite. The area occupied by most soils is also outlined.

** The $Fe(OH)_2$ (s) field also may be occupied by magnetite.

III. Sulfur and Iron . . . . Chemical Relations

The iron cycle begins with the weathering of iron containing minerals. Silicate minerals weather slowly, but sulfides such as pyrite weather quickly due to bacteria such as Thiobacillus and Ferrobacillus ferrooxidans which catalyze the oxidation. Pyrite weathering releases iron and sulfate to the environment through the following overall reaction:

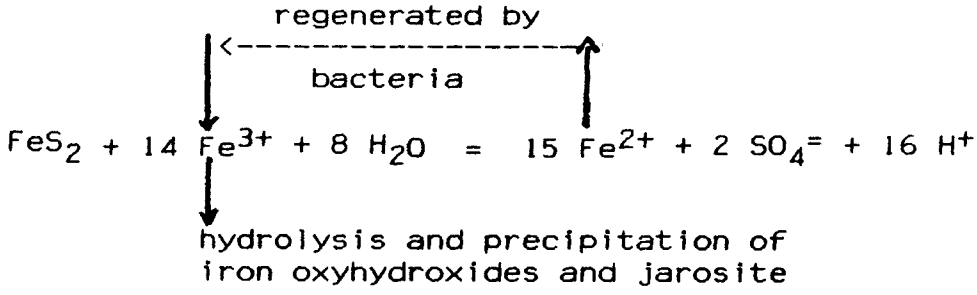

which, in large amounts, can lead to the formation of acid mine drainage and acid sulfate soils. The acidity comes from S_2 (II) oxidation and Fe (III) hydrolysis. One mole of pyrite can release 4 equivalents of acidity, two equivalents can be released from S_2 (II) oxidation, and two from Fe(II) oxidation (Stumm and Morgan 1981). Bacteria perpetuate the reaction until the pyrite is used up or the water leaves the sulfide surfaces. Once the solution has been removed, it will fully oxidize and hydrolyze to form the various ferric minerals.

Figure 2.3 depicts conditions occuring when sulfur is taken into account in preparing an iron stability field

diagram. This diagram considers solid sulfur, ferric oxides and hydroxides, jarosite and the sulfide mineral pyrite, as being present under the system conditions of 25°C, 1 atm., and fixed Fe, K and S activity. It illustrates that iron is relatively insoluble except under low pH conditions. In cases of:

a) strong reduction, pyrite is stable,

b) moderate oxidation, ferric oxides and hydroxides are stable.

In aerated water (Eh 0.4 volts) pyrite is unstable, but iron oxides and hydroxides are stable.

Note: The diagram summarizes aqueous chemistry in a system which considers only the minerals listed as being present. The system is assumed to be at equilibrium, with no other complexing agents (such as organics) present.

Table 2.1 Equations used to draw Figures 2.1, 2.2 and 2.3

EQUATION:	LOG K @25°C, 0 IS:
$H^+ + S^= = HS^-$	13.9
$H^+ + HS^- = H_2S$	-6.9
$H^+ + SO_4^= = HSO4^-$	2.0
$S(s) + 2\ H^+ + 2\ e^- = H_2S\ (aq)$	4.8
$S(s) + 1\ H^+ + 2\ e^- = HS^-$	-2.2
$S(s) + 4\ H_2O = SO_4^= + 8\ H^+ + 6\ e^-$	-36.2
$S(s) + 4\ H_2O = HSO_4^- + 7\ H^+ + 66\ e^-$	-34.2
$SO_4^= + 9\ H^+ + 8\ e^- = HS^- + 4\ H_2O$	34.0
$SO_4^= + 8\ H^+ + 8\ e^- = S^= + 4\ H_2O$	20.1
$SO_4^= + 10\ H^+ + 8\ e^- = H_2S\ (aq) + 4\ H_2O$	41.0
$Fe^{++} + S^= = FeS(s)$	-18.1
$Fe^{++} + 2H_2O = Fe(OH)_2(s) + 2H^+$	-12.8
$Fe^{+++} + 3H_2O = Fe(OH)_3(s) + 3H^+$	>-12
$Fe^{+++} + 2H_2O = \alpha\text{-}FeOOH(s) + 3H^+$	-0.5
$Fe^{+++} + 2H_2O = am\text{-}FeOOH(s) + 3H^+$	-2.5
$Fe^{+++} + 3/2\ H_2O = 1/2\ Fe_2O_3(s) + 3H^+$	0.7
$Fe^{++} + H_2O = FeOH^+ + H^+$	-9.5
$Fe^{+++} + H_2O = FeOH^{++} + H^+$	-2.2
$Fe^{+++} + 2H_2O = Fe(OH)_2^+ + 2H^+$	-5.7
$Fe^{+++} + 4H_2O = Fe(OH)_4^- + 4H^+$	-21.6
$Fe(OH)_3(s) + H_2O = Fe(OH)_4^- + H^+$	-19.2
$Fe^{++} + H_2O = FeOH^{++} + H^+ + e^-$	15.2
$Fe^{++} + 3H_2O = am\text{-}Fe(OH)_3 + 3H^+ + e^-$	16.0
$Fe(OH)_2(s) + H_2O = Fe(OH)_3(s) + H^+ + e^-$	4.3
$Fe^{+++} + e^- = Fe^{++}$	13.0

References: Stumm and Morgan 1970/1981, Sillen and Martell 1971, Parks and DeBruyn 1962

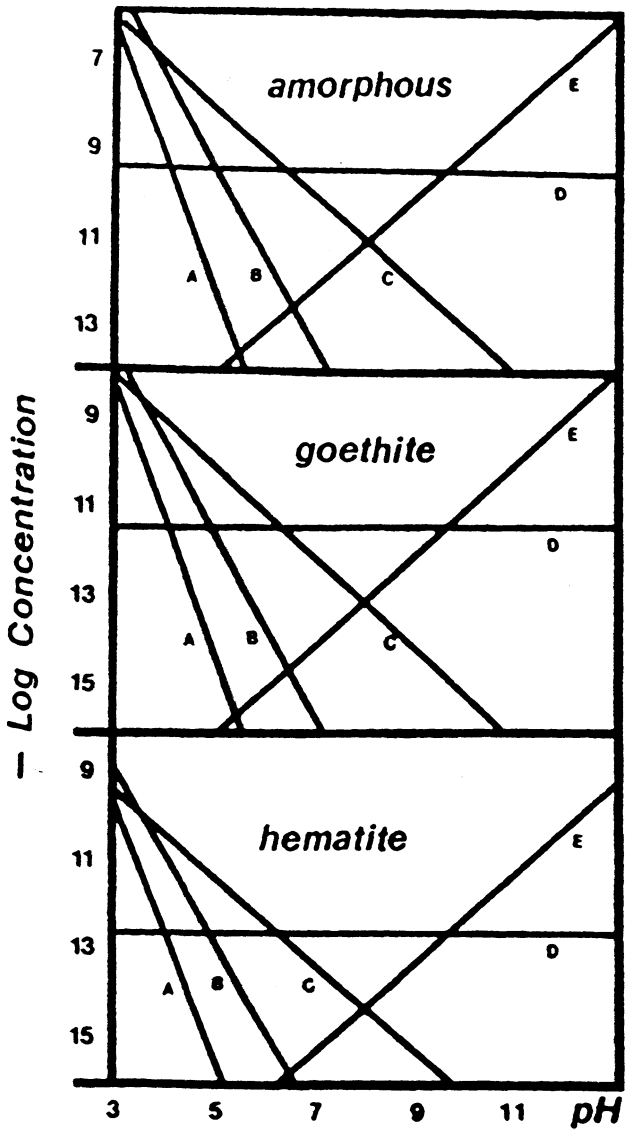

Figure 2.2: Solubility diagrams for hematite (α-Fe_2O_3), goethite (α-FeOOH) and amorphous iron hydroxide (FeOOH) calculated using the equations and constants from Table 2.1.

A = Fe^{3+}
B = $FeOH^{2+}$
C = $Fe(OH)_2^{+}$
D = $Fe(OH)_3^{-}$
E = $Fe(OH)_4^{-}$

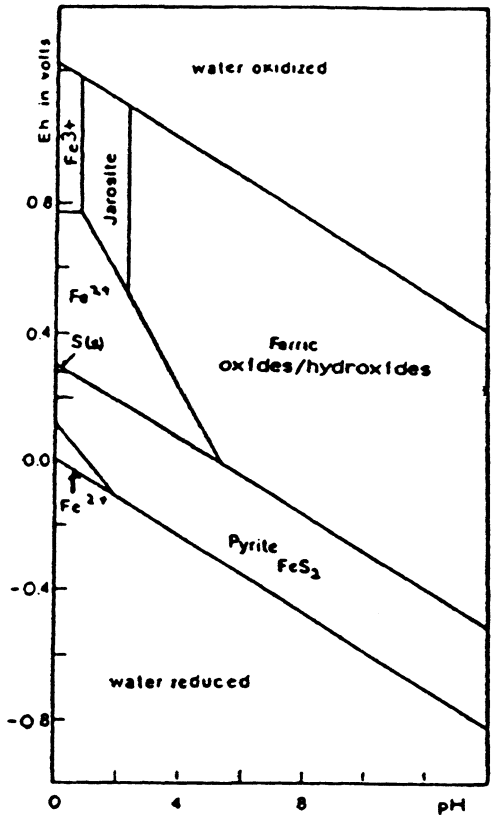

Figure 2.3 Eh - pH diagram illustrating stability fields of solid and dissolved forms of sulfur and iron at 25°C and 1 atm pressure.

Included are fields of solid sulfur, pyrite, jarosite and ferric oxides/hydroxides whose boundaries will be determined by the solubility products. The ferric oxide/hydroxide field generalizes the location where goethite, hematite and ferrihydrite are found. Activities of dissolved species are Fe = 10^{-4} M, total S = 10^{-2} M and K^+ = 10^{-3} M. (Adapted from Garrels and Christ 1965, Hem 1960, 1970, Van Breeman 1982 and Nickel 1984).

CHAPTER 3 LITERATURE REVIEW

I. SOIL RESEARCH LITERATURE

Many soils have exhibited the ability to retain sulfate as shown in investigations performed by the following:

Kamprath et al. 1956
Liu and Thomas 1961
Chao et al. 1962
Fang et al. 1962
Chang and Thomas 1963
Bornemisza and Llanos 1967
Barrow 1967, 1972
Barrow et al. 1969
Hasan et al. 1970
Mekaru and Uehara 1972
Hague and Walmsley 1973
Gebhardt and Coleman 1974
Sanders and Tinker 1975
Couto et al. 1979

whose works have been reviewed by Harward and Reisenauer (1966). Sulfate sorption isotherms have been obtained by the above researchers for some soils.

A soil's capacity to retain sulfate has been shown by the above authors to vary widely with soil properties: (a) content and nature of clay minerals, (b) hydrated aluminum and iron oxides, (c) organic matter, (d) pH, (e) sulfate concentration, (f) accompanying cations and (g) other anions present. Surface soils, which are higher in organic matter than subsoils, tend to sorb less sulfate and desorb it to water easily. Subsoils, which are higher in sesquioxide content than surface soils, sorb more sulfate. Sorption increases with decreasing soil pH and with increasing sulfate concentration, although a smaller

percentage is sorbed at higher sulfate concentrations. Efficiency of sorption of sulfate follows the order of chemical valency of the accompanying cation (e.g. 2 valent $CaSO_4$ > 1 valent K_2SO_4). Retention strength of anions follows the order $PO_4^{=}$ > $SO_4^{=}$ > NO_3^{-} = Cl^{-}, meaning that phosphate sorbs more strongly than sulfate. That is, the presence of phosphate decreases the amount of sulfate that can be sorbed and it will increase desorption by replacing a large percentage of sulfate already sorbed onto soils.

Sulfate sorption in soils is initiated by a rapid reaction, followed by a longer slow reaction whose time to equilibrium, if ever reached, is not resolved. Chao et al. (1962) and Sanders and Tinker (1975) suggest that a steady state is achieved after 4 hours of reaction time, but Barrow (1967) states that it takes more than 48 hours; Chang and Thomas (1963) and Liu and Thomas (1961) conclude that it takes more than 5 and 8 weeks respectively before equilibrium is attained.

As sulfate is being sorbed, pH increases due to consumption of H^{+} (or production of OH^{-}). But the amount of hydroxyl released to sulfate sorbed is not constant.

Barrow (1967) is the only investigator to examine sulfate sorption in soils for soil/solution ratio and ionic strength effects. Although he observes no influence on sorption of sulfate by soil/solution ratio, there is a

noticeable decrease in sorption with increasing ionic strength up to 0.01 M. Above this concentration, no effect is observable. Barrow also observes an increase in sulfate sorption with temperature.

Many studies show that the sulfate sorbed by soils can only be partially desorbed. Surface soils, containing a water soluble pool, desorb sulfate more readily than subsoils (Couto et al. 1979). Sorption reversibility increases as time periods diminish from the order of days to the order of hours (Rehm and Caldwell 1968), and as equilibrium concentrations diminish (Barrow 1967). For example, Sanders and Tinker (1975) observed greater reversibility over a sorption period of hours when less than 15 mg/l of sulfate was used in the sorption step. Desorption of sulfate, by washing with water or solutions of NaCl or $NaNO_3$, is not as efficient as washing with solutions containing phosphate (KH_2PO_4) (Ensminger 1954, Chao et al. 1962). Bornemisza and Llanos (1967) observed that in three extraction steps, water and phosphate removed <65% and >80% of sorbed sulfate respectively. Yet phosphate did not completely desorb (replace) all sulfate sorbed by soils.

Sorbed sulfate is in equilibrium with solution sulfate, as shown by isotopic exchange studies with $^{35}SO_4$ (Chao et al. 1962). Sorption behavior on some soils conforms to the Langmuir adsorption equation, with its sorption maximum, especially at lower sulfate

concentrations. For example, Kamprath et al. (1956) find their data fit Langmuir behavior up to and above 300 mg/l equilibrium solution sulfate concentration. Data of Couto et al. (1979) also fit Langmuir behavior. Haque and Walmsley (1973) find their data to obey the Langmuir equation, but only at low sulfate concentrations (<100 mg/l). Barrow (1967) also finds that parts of his data are defined by the Langmuir equation. On the other hand, investigators such as Fang et al. (1962) find isotherms to follow Freundlich behavior, with no sorption maximum, more closely. Chao et al.'s (1962) data also show no sorption maximum, at least not up to 500 mg/l sulfate. Bornemisza and Llanos (1967) find no sorption maximum up to 1000 mg/l sulfate, the highest sulfate concentration used in their studies.

Sorption Mechanisms:

There are several possible mechanisms which lead to sulfate retention in soils and can be used to explain the above observations:

I) incorporation into soluble and insoluble sulfate minerals through precipitation.

Adams and Rawajfih (1977) propose sulfate precipitates as insoluble basic aluminum and iron sulfate minerals in soils.

II) interaction with sesquioxides (hydrous oxides and clays) through:

i) nonspecific electrostatic sorption, and

ii) specific sorption involving chemical coordination. Most investigators believe mechanisms in addition to nonspecific sorption occur due to a) changes in pH upon sorption and b) the inability of solutions such as KNO_3 to remove all sorbed sulfate. Some authors suspect that more than one mechanism is working (Aylmore et al. 1967), or that more than one site is being activated (Fang et al. 1962, Barrow 1967, 1969, Haque and Walmsley 1973, Muljadi et al 1966) due to a) deviations in behavior from the Langmuir equation, b) changes in behavior on exchange with $^{35}SO_4$, and c) inability of phosphate to replace all sorbed sulfate.

The most accepted specific sorption mechanism involves protonation of Al and Fe bearing mineral surfaces forming aluminol and ferrol groups, followed by ligand exchange of $SO_4^=$ for OH^- to allow coordination of the anion with the metal cation at the surface (Aylmore et al. 1967, Hingston et al. 1967, Gebhardt and Coleman 1974).

II. OXIDE RESEARCH LITERATURE

There are many investigations which examine the sorption of anions on oxyhydroxide minerals. As with sorption on whole soil samples, sulfate sorption on iron oxyhydroxides is a) pH dependent (increases with decreasing pH), b) concentration dependent (increases with

concentration) and c) time dependent. The high affinity isotherm produced often reaches a plateau or maximum thus showing apparent Langmuir behavior over the concentration ranges studied (Aylmore et al. 1967).

Previous studies on anion sorption produced many isotherms but few structural models. Studies on sorption rates and isotopic exchange rates, determination of area covered by sorbed anions, along with crystal morphology and infrared studies of surface groups give the data used to propose sorption mechanisms and structural models.

Due to the rate and extent of sorption of anions on goethite in comparison to chromic oxide (αCr_2O_3) (phosphate sorbs quickly on both, sulfate and nitrate slower on both), Yates and Healy (1975) conclude that sulfate is not significantly involved in direct exchange with surface groups on iron oxides and suggest it to be non-specifically sorbed much like nitrate.

On the other hand, high affinity for sulfate, inability of non specifically sorbed ions such as NO_3^- and Cl^- to desorb sulfate, and strong pH dependence of sorption, suggests sulfate to be specifically sorbed on iron oxides and hydroxides. Shifts in oxide zero point of charge (zpc) accompanying sorption also indicates specific sorption of anions. Sulfate sorption increases the pH_{zpc} of goethite (Yates and Healy 1975, Sigg and Stumm 1981) and hematite (Breuwsma and Lyklema 1973).

Parks and DeBruyn (1962), Yopps and Fuerstanau (1964), Breuwsma and Lyklema (1973), Rajan et al. (1974), Ryden and Syers (1975) and Parfitt and Russel (1977) all agree that sulfate ligand exchanges with surface OH and H_2O groups to form chemical bonds with oxide metal ions. This is supported by commonly observed variations in adsorption capacity with pH. A few investigators (Hingston et al. 1972, Atkinson et al. 1967, Bowden et al. 1973) propose that a relationship between pK_a of the sorbing acid (H_2SO_4) and pH of optimum sorption exists. Sigg and Stumm (1981) give evidence that sorbed sulfate forms an inner sphere complex because the complexing tendency in solution (with free Fe^{3+}) and on the surface is similar. They found a correlation between the formation constant of the ligand with Fe^{3+} in solution and the equilibrium constant of the surface complex.

When anions such as sulfate and phosphate are sorbed in amounts > 100 μmol/g, infrared spectra show that sorption sites for carbonate become blocked (Parfitt and Russell 1977). Infrared spectra also indicate that A-type (singly bonded) hydroxyl groups, on hematite 1010 and goethite 100 and 010 faces, are lost on sorption of these anions. Unlike phosphate, sulfate sorption bands do not shift after D_2O treatment and evacuation, indicating that the sorbed sulfate species is not protonated ($SO_4^=$ vs HPO_4^-). Atkinson et al. (1974) and Russell et al. (1974)

used this information and the irreversibility of the sorption to propose a binuclear bridging complex mechanism for $SO_4^{=}$ and HPO_4^{-} sorption. The binuclear bridging complex forms when one anion adsorbs onto the oxide surface and coordinates to a metal cation by ligand exchanging with two adjacent surface hydroxyl sites. Ions complexed in this way are more strongly held than those involved in mononuclear bonding.

Table 3.1 summarizes the studies of sulfate sorption on hematite and goethite which report sorption maxima. Although the table shows increasing sorption with decreasing pH, the theoretical sorption maximum of 200 μmol/g (Parfitt and Smart 1977) is never achieved. This is because the minerals are not stable at the pH required for 'maximum' sorption (pH < 0) and start to dissolve under such conditions.

Table 3.1 Investigations of sulfate sorption on iron hydrous oxide minerals. Experimental conditions.

INVESTIGATOR	SA	ZPC	SM	IS	pH	T
HEMATITE STUDIES						
Aylmore et al. 1967 Synthetic Sample	26.7	-	67 (2.50)	-	4.6	20
(note irreversible: only desorbed ~15 μmol/g)						
Parfitt Smart 1978 Synthetic Sample	22	-	85 (3.86)	KCl	3.5	26
Wootton 1985 Natural Sample	12.0	-	46 (3.83)	0.01 NaCl	3	20
			35 (2.92)		5	
			25		7	
GOETHITE STUDIES						
Hingston et al. 1972 and 1974 Synthetic Sample	81	8.0	150 (1.85)	0.1 NaCl	3.0	20-23
			110 (1.36)		4.0	
			60 (0.74)		5.0	
Parfitt Smart 1977/78 Synthetic Sample	90	-	125 (1.39)	KCl	3.4	26
			75 (0.83)		5.1	

SA = surface area in m^2/g IS = ionic strength
T = temperature in ^oC ZPC = zero point of charge
- = Not reported SM = sorption maximum in μmol/g (μmol/m^2)

CHAPTER 4 OXIDE SURFACE CHEMISTRY

Oxide properties are influenced by their precipitation conditions, crystalline structure, and morphology. Their surface chemistry is determined by their large surface area and electrical charge.

I. SURFACE GROUPS

Some oxides are naturally hydroxylated (contain surface OH), while others are not:

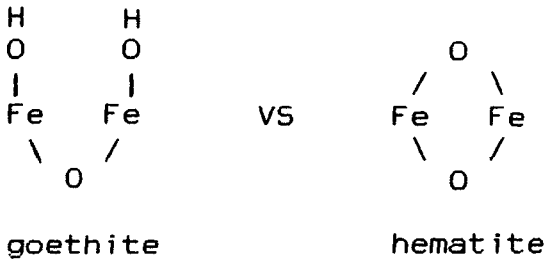

goethite hematite

Chemisorption of water can occur due to hydroxylation leading to completion of coordination shells (Breuwsma 1973). Depending on the oxide type (hydrous versus anhydrous) and its surface area, additional water may be sorbed beyond hydroxylation of the surface (Parks 1965) by hydrogen bonding to structural or surface hydrogens. This is referred to as 'physical adsorption' (Breuwsma 1973).

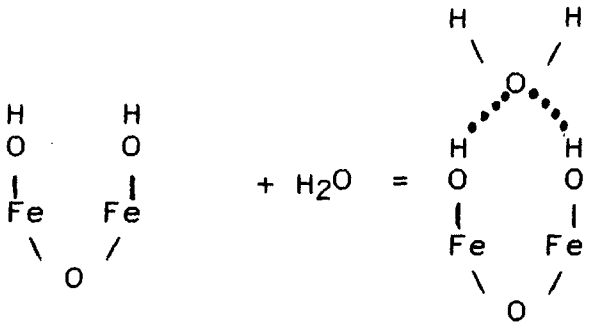

The reactivity of oxide surfaces are determined by this chemically and physically sorbed water.

The common surface structures on hydroxides and oxides are terminal aquo ($-M-OH_2$) and hydroxo ($-M-OH$) groups, of which the hydroxo group can be singly, doubly, or triply bound, as well as

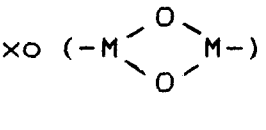 and 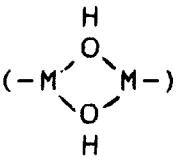 groups (Harward and Reisenauer 1966).

II. SURFACE CHARGE AND ADSORPTION

The proportions of different surface groups found on an oxide surface are determined by suspension pH, which in turn determines surface charge. At the zero point of charge (zpc), the net positive and net negative groups are equivalent for a given substrate. The pH_{zpc} of an oxide will depend on the relative properties of the oxide with respect to acidity and basicity, where variables such as hydration state and ion arrangement play a role. Parks

(1965) proposed that strongly amphoteric oxides like hematite (Fe_2O_3) have zpc near neutral pH.

Surface charge can be made positive or negative by raising or lowering, respectively, the pH relative to the zpc (see Figure 4.1). Excess surface charge is balanced by an equivalent amount of counter-ions [anions (A^-) or cations (C^+)] which diffuse into the surrounding medium forming an electric double layer near the surface (see Figure 4.2).

The phenomenon whereby ions are adsorbed in the outer double layer in proportion to the equilibrium activity, is an example of nonspecific electrostatic adsorption. Chemisorption or specific adsorption, mentioned above for water, results when ions are held more strongly to the structural cation by covalent bonds via O and OH groups, or exchange with these ligands in order to penetrate the coordination shells of the cation (Fe^{3+}). The amount sorbed will depend on many factors such as the specific ion, its concentration and pH.

Surface charge can be measured by:

(1) potentiometric titration in indifferent electrolyte such as KNO_3 (Parks and DeBruyn 1962),

(2) adsorption of indifferent ions at a range of pH values (Bolland et al. 1976).

Figure 4.1 Schematic showing the change in O^-, OH and OH_2^+ surface groups with acid/base additions and the resulting pH change with respect to zpc.

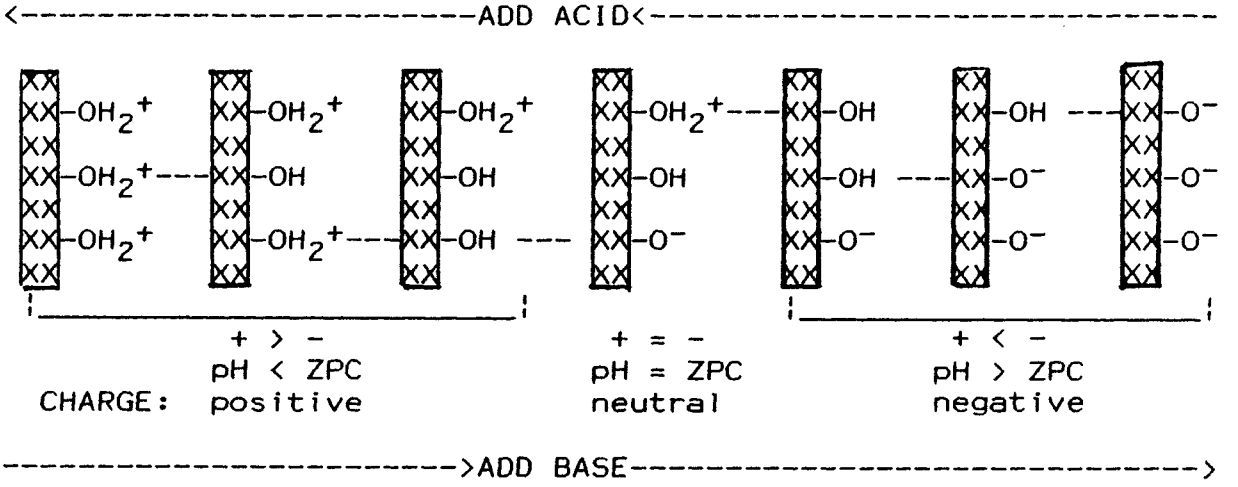

Titration Situations:

1. At ZPC:
   + ACID) surface --> positive, pH decreases
   + BASE) surface --> negative, pH increases

2. At pH < ZPC:
   + ACID) surface --> positive, pH decreases
   + BASE) surface --> zpc or above thus becoming negative
   pH increases

3. At pH > ZPC:
   + ACID) surface --> zpc or below thus becoming positive
   pH decreases
   + BASE) surface --> negative, pH increases

Figure 4.2 Schematic of substrate surface electrical double layer at pH=3 for low and high ionic strength. (σ_o, σ_1 and σ_d represent surface charges of the surface layer, inner helmholtz plane and diffuse layer or outer helmholtz plane respectively).

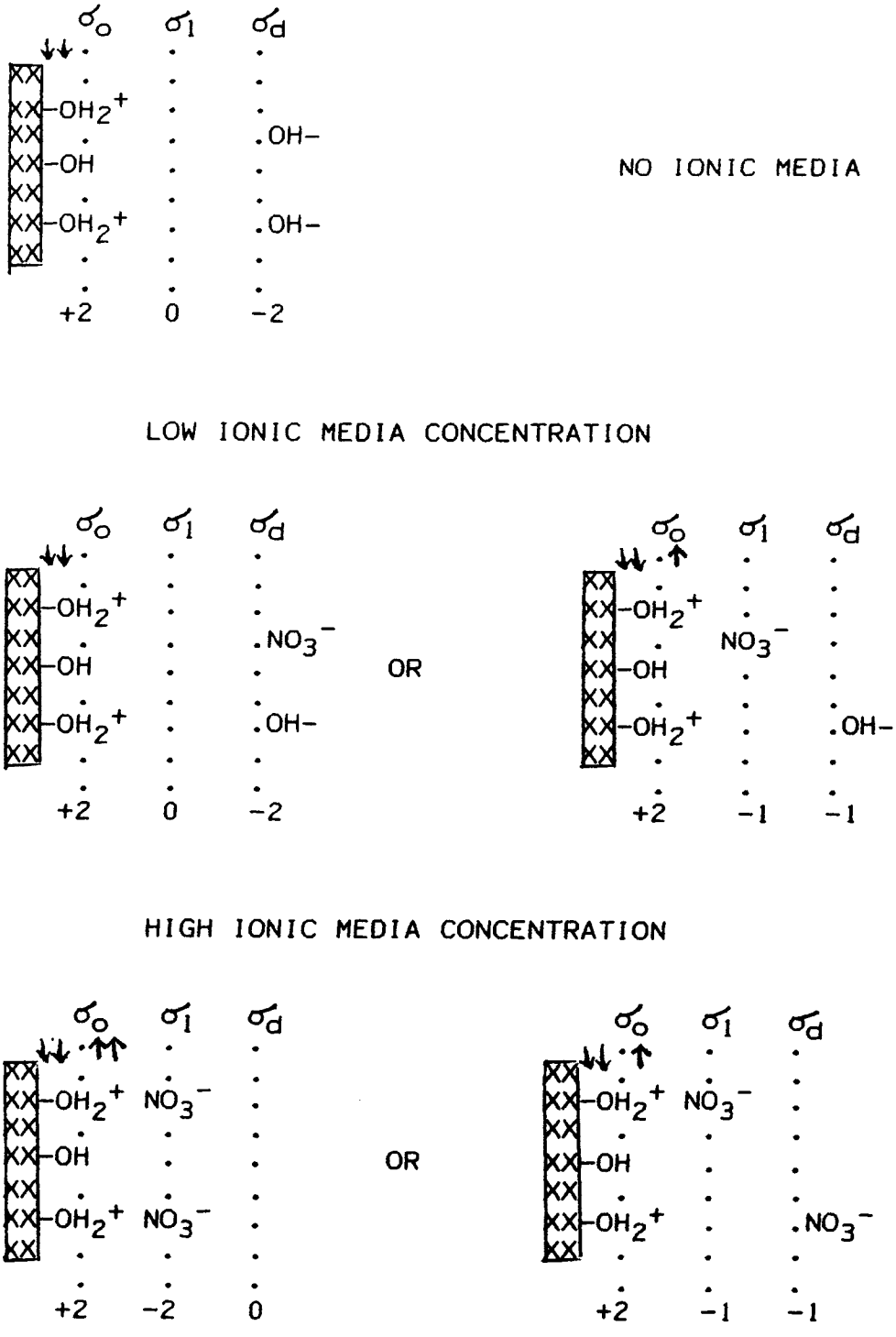

Figure 4.3 Example of mononuclear and binuclear bonding of a phosphate ion onto an iron oxide.

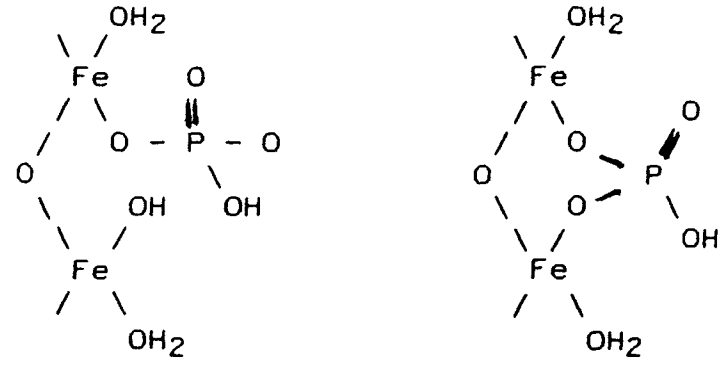

III. SURFACE SITE AND SPECIES DETERMINATION

The number of surface sites can be estimated by ligand exchange through exchange capacity titrations. The species occupying surface sites can often be identified by infrared spectroscopy. Sorbed ions exhibit characteristic spectrum peaks. Changes in spectrum after ion sorption gives clues to the sorption mechanism. For example, infrared evidence (Atkinson et al. 1974, Russell et al. 1974, Parfitt et al. 1975, 1976, Parfitt and Atkinson 1976, Parfitt and Russell 1977, Parfitt and Smart 1977, 1978) has indicated the formation of binuclear bridges in the cases of phosphate and sulfate adsorption on iron oxide surfaces, which may explain the partial irreversibility seen for these and other specifically sorbed ions (see Figure 4.3).

IV. SORPTION MODELS

Figure 4.4 summarizes general models for sulfate sorption on oxide surfaces. The sulfate anion can be a) electrostatically held to a positively charged surface site, or b) chemically held by replacement of one or more surface ligands. The ratio of ligands replaced to the number of anions held ($R = \{OH\}/\{SO_4\}$), can be used to define the nature of the reaction of $SO_4^=$ and OH^- (or H^+).

Figure 4.5 illustrates nonspecific electrostatic reactions which may occur under solution conditions of high ionic strength and low pH as used in this study. Generally electrostatic attraction does not give an R index value above 0. Figure 4.6 illustrates several possible ligand exchange reactions. Note that two types of sites, -OH and $-OH_2^+$, can be replaced, and that R can range from 0 to 2 meaning mononuclear and/or binuclear bonding can occur.

V. SUMMARY

Iron oxide and hydroxide sorptive properties depend strongly on the reactivity of their hydroxylated surfaces. Their zero points of charge are determined by the net amounts of different surface groups. Ions may be loosely sorbed through non-specific electrostatic attraction (Figure 4.5), an outer sphere phenomenon; or more strongly held by

specific sorption, an inner sphere phenomenon (Figure 4.6). Ligand exchange with two surface groups, called binuclear bridging, is the strongest form of specific sorption. Although all ions can be held electrostatically, few ions are known to be involved in specific sorption.

Figure 4.4 Theoretical schematic of sulfate sorption on iron oxide surfaces. R = [OH] / [SO_4]

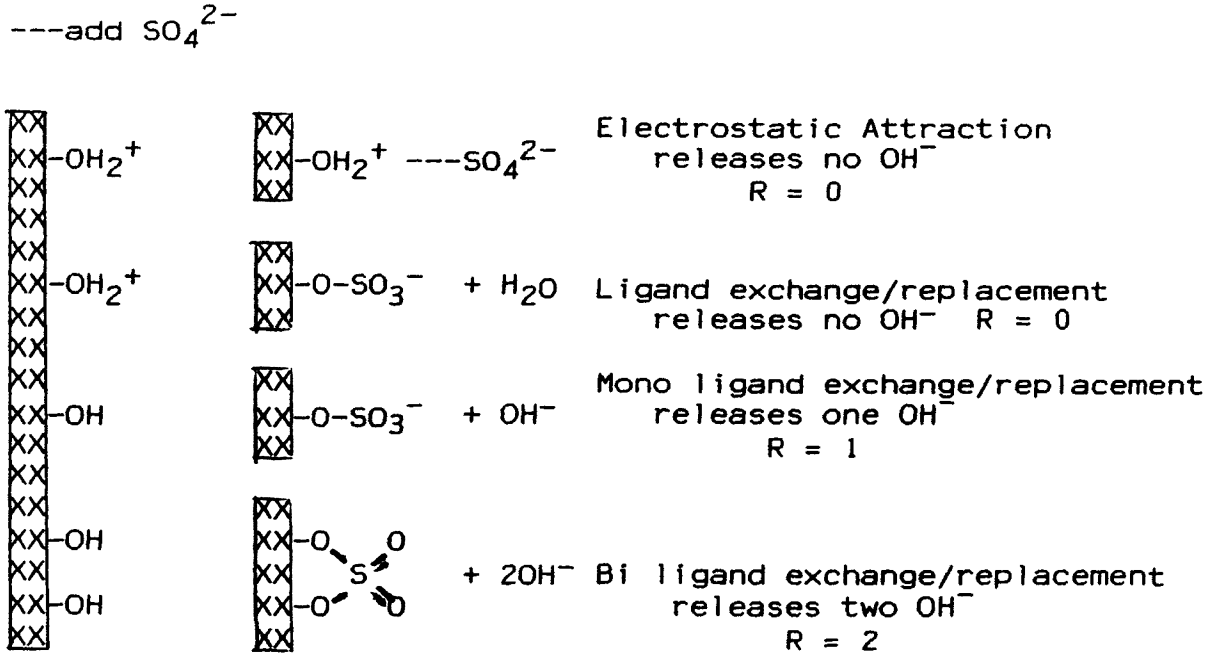

Figure 4.5 Schematic of the electric double layer at pH 3, high ionic media, with sulfate. Electrostatic attraction only.

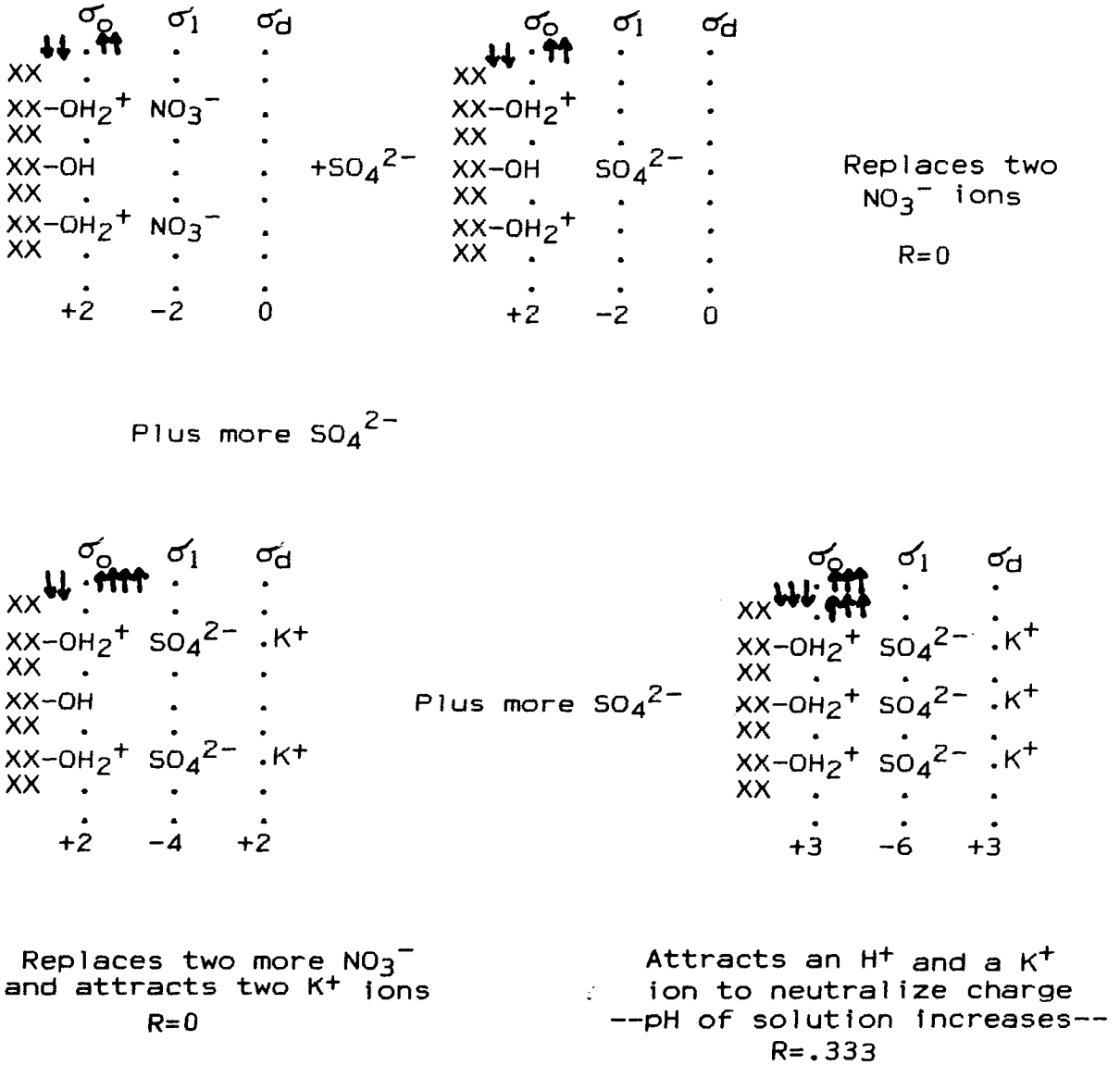

Figure 4.6 Schematic of the electric double layer at pH 3, high ionic media, with sulfate. Ligand exchange.

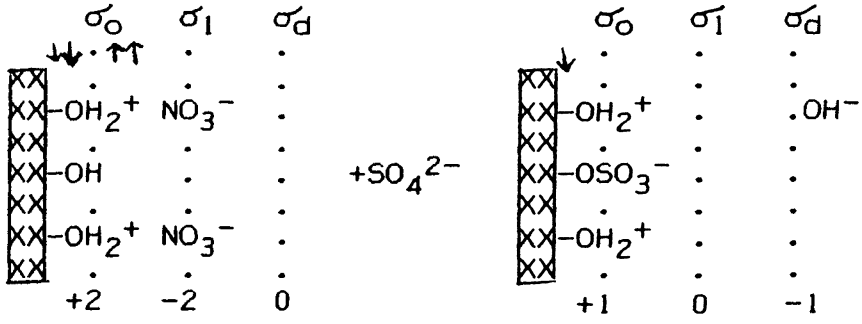

*O O= attaches directly to the surface
S expels one hydroxyl ion thus
O O giving R = {OH}/{SO4} = 1

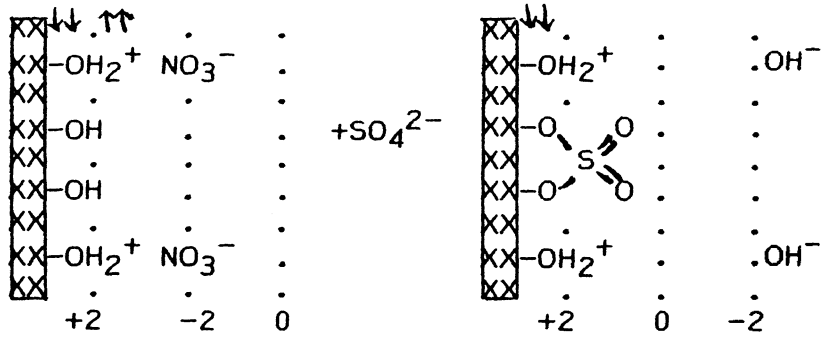

*O O= attaches directly to the surface
S and expels two hydroxyl ions
*O O giving R = {OH}/{SO4} = 2
(Note: the OH- in the double layer can be NO_3^- as well).

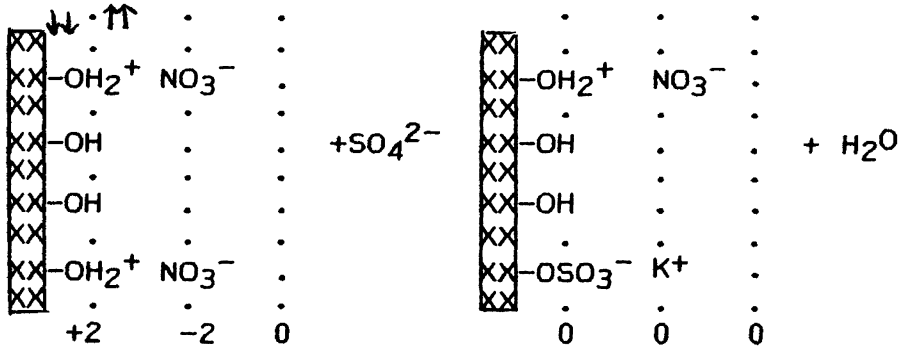

*O O= attaches directly to the surface
S and expels one water
O O giving R = {OH}/{SO4} = 0

CHAPTER 5 MINERAL PREPARATION AND CHARACTERIZATION

The following sections discuss the general characteristics of two iron oxides and an iron sulfate mineral which are important for either identification or surface reactivity determination with respect to sorption. The simplest, yet most reproducible mineral preparation synthesis procedures for the three minerals concerned are given first, then methods of characterization are discussed, along with literature and experimental results.

I. MINERAL PREPARATION METHODS

GOETHITE - the following procedure was initially used by Atkinson et al. 1967, and followed by many other authors.

200 mls of 2.5 N KOH are added to 50 g of $Fe(NO_3)_3 \cdot 9H_2O$ in 800 mls of MilliQ water giving the solution a final pH of 12. This solution is aged in an oven at 60°C for > 1 day in linear polyethylene bottles. The resulting precipitate is washed by centrifugation, decantation and finally by filtering (0.45 µm millipore filter) then either oven, hot plate or vacuum dried.

$$Fe(NO_3)_3 * 9\ H_2O + 3\ KOH = FeOOH + 3\ KNO_3 + H_2O$$

HEMATITE - the procedure whereby ferric nitrate is hydrolyzed at the boiling point of water (Parks and DeBruyn 1962, Atkinson et al. 1967, 1968, and Parfitt et al. 1975) was used to prepare hematite.

A solution of 20 g of $Fe(NO_3)_3 \cdot 9H_2O$ in 200 mls of MilliQ water is prepared at room temperature, then boiled at >100°C for 18 days in a sand bath. This is performed under reflux conditions to ensure that the HNO_3 formed by hydrolysis is prevented from escaping by vaporization and results in a final pH of around 1. The precipitate is then washed, filtered and dried in an oven or on a hot plate.

$$2\ Fe(NO_3)_3{*}9\ H_2O + 3\ H_2O = Fe_2O_3 + 6\ HNO_3$$

JAROSITE - the following procedure was used on suggestion of Ivarson (private communication).

A saturated solution of $Fe(SO_4)_3{*}nH_2O + K_2SO_4$ adjusted to a pH between 1.8 and 3 is allowed to age overnight at room temperature, then is warmed on a hot plate to facilitate crystal production. The precipitate is filtered and washed on a 0.45 μm millipore filter then oven or hotplate dried.

$$6Fe(SO_4)_3{*}6H_2O + K_2SO_4 + H_2SO_4 = 2KFe_3(SO_4)_2(OH)_6 + 16H_2SO_4 + 6H_2O + 18OH$$

II. METHODS OF MINERAL CHARACTERIZATION

Mineral samples prepared in this study were identified and characterized using the following techniques:

X-Ray Diffraction - crystalline identity
Electron Microscopy - morphology
Surface Area, Zero Point of Charge, Infrared Spectroscopy and Thermal Analyses - surface properties
Mossbauer Spectroscopy - internal structure
Neutron Activation Analysis and X-Ray Fluorescence - purity
Thermal Analyses (Differential Thermal Analysis, Thermo-Gravimetric Analysis and Loss on Ignition) - water content

The methods and results are described in detail below.

A) SURFACE AREA -

The classic BET-N_2 adsorption method (Brunauer, Emmett and Teller 1938) is used for surface area determination of natural and prepared samples. In BET theory, gases adsorb in multi- molecular layers. There is a vapor pressure of N_2 at which the surface, in equilibrium with the N_2 gas, will adsorb a monolayer. Performing adsorption at this pressure of N_2 will result in adsorption of a monolayer coverage. The total surface area per unit of material can be calculated knowing the total amount of gas adsorbed and the diameter of the N_2 molecule.

The BET method requires drying the material prior to the adsorption process. There is some argument against the use of this method because the drying process may alter the surface area or structure.

A Micrometrics BET Surface Area Analyzer is used for the analysis.

EXPERIMENTAL RESULTS:

Of twenty different preparations of goethite, the surface areas vary between 32.3 (the lowest) and 90.8 m^2/g (the highest), but most give values in the 40's. A group of goethite samples, most similar in characteristics, was mixed together for use in sorption experiments. This mixture exhibited a surface area of 44.1 m^2/g.

Table 5.1a Comparison of surface area values for goethite.

SA m^2/g	Investigator		SA m^2/g	Investigator	
70.9	Atkinson et al.	1967	78	Mackenzie et al.	1981
48.5	Balistreri/Murray	1981	70.5	Madrid/Arambarri	1978
82	Bleam & McBride	1985	84	Madrid & Posner	1979
16	Borggaard	1983	74	Madrid et al.	1984
82	"		80	Parfitt et al.	1975
87.4	Cabrera et al.	1977	90	Parfitt && Smart	1977
54.4	"		50	Pritchard & Ormerod	1976
112	Evans et al.	1979			
89	Forbes et al.	1974	50	Rendon & Serna	1981
17	Hingston et al.	1968	60	Russel et al.	1974
28	1972, and	1974	96.2	Sibanda & Young	1986
32	"		28	Sigg & Stumm	1981
81	"		29	"	
16.2	Jurinak	1964	11	Tipping	1981
32	Landa and Gast	1974	18	"	
86	Lumsdon et al.	1984	48	Yates & Healy	1975
44.1	This study (synthetic sample)				

Table 5.1b Comparison of surface area values for hematite.

SA m^2/g	Investigator		SA m^2/g	Investigator	
23	Albrethson	1963	1.2	Cabrera et al.	1977
36.4	Atkinson et al.	1967	17.3	"	
34.1	"		9.60	Jurinak	1964
43.5	"		110	Madrid et al.	1983
44.6	"		10	McCafferty and Zettlemoyer	1971
26.7	Aylmore et al.	1967			
14	Borggaard	1983	18.0	McLaughlin et al.	1981
36	"		21	Onoda & DeBruyn	1966
64	"		22	Parfitt et al.	1975
56	Boehm	1971	22	Parks and DeBruyn	1962
18	Breuwsma & Lyklema	1973	43.2	This study, synthetic sample	
12.0	This study, natural sample				

Surface areas ranged from a low of 27.9 to a high of 43.2 m^2/g for the various preparations of hematite. Due to its similarity in surface area to goethite, the hematite preparation having the surface area of 43.2 m^2/g was used in sorption experiments. The surface area of a natural hematite sample was 12 m^2/g.

B) pH of Zero Point of Charge (ZPC) -

Solid particles such as oxides develop surface electrical charges in aqueous solution by adsorption or desorption of potential determining ions (p.d.i.). By definition, potential determining ions for oxides such as Fe_2O_3 are the lattice constituents Fe^{3+} and O^{2-}, and ions such as H^+ and OH^-, which are in equilibrium with them. Knowing that H^+ and OH^- are p.d.i. for the iron oxide

surfaces:

$$MeOH_2^+ = MeO^- + 2H^+$$

Surface charge measurements can be obtained through adsorption and desorption measurements for H^+ ions, as carried out by potentiometric titration of oxide suspensions in an indifferent electrolyte of various ionic strengths (Parks and DeBruyn 1962).

$\sigma s = F (z^+ \Gamma^+ + z^- \Gamma^-)$

where σs = surface charge,
z^+ (z^-) = valence and sign
Γ^+ (Γ^-) = adsorption density of p.d.i.

The pH_{zpc} is the pH, or concentration of potential determining H^+ ions, at which the net surface charge is zero ($\sigma s = 0$).

Procedure:

The zpc of the ferric oxyhydroxide and oxides are determined by an adsorption method utilizing potentiometric titration of an aqueous suspension of each mineral at several ionic strengths (10^{-4} to 1 M) at 25°C using a Ross Orion Microelectrode. Standardized 0.1 M KOH and HNO_3 are used as titrants and KNO_3 as the indifferent electrolyte because it is unlikely to complex Fe(III). A 125 ml teflon bottle, used as a titration vessel, is sealed with parafilm and placed in a thermostated water jacket to maintain constant temperature. The vessel is purged with argon to remove traces of CO_2 and stirred with a teflon coated stirring bar.

The titration procedure consists of adding 100 g of suspension (0.4 g of oxide per 100 ml KNO_3 media) to the vessel and degassing for approximately 15 minutes. Then aliquots of acid or base are added to cover a titration range of pH 5 to 10.

Adsorption density (Γ) of OH^- or H^+, being the excess of one over the other ($\Gamma H - \Gamma OH$) in meq/g, is determined by the difference between total titrant added (acid or base) and the equilibrium concentration ($[H^+]$ and $[OH^-]$) in the suspension in comparison with blank solution titrations. Reproducibility is established by multiple titration runs.

The pH_{zpc} is determined by the intersection of the adsorption curves for the various ionic strengths used. The surface density of charge (σ) can also be calculated if the surface area (in m^2/g) is known through:

$$\sigma = 1/A \ (\Gamma H^+ - \Gamma OH^-) \ \mu eq/cm^2$$

where A is the surface area

EXPERIMENTAL RESULTS:

The zero points of charge for the synthetic goethite and hematite preparations and natural hematite used in later sorption experiments are determined to be 7.1, 8.0, and 8.8, all $\pm$ 0.05 respectively.

Table 5.2a Comparison of ZPC values for hematite.

ZPC	Reference		ZPC	Reference	
5.3±.05	Ahmed & Maksimov	1968	8.5±.2	Breuwsma & Lyklema	1973
5.7±.1	"		6.45	Cabrera et al.	1977
8.7	Albrethson	1963	6.77	"	
8.90±.15	Atkinson et al.	1967	8.6	Hazel & Ayres	1931
8.45±.20	"		8	Jurinak	1966
9.27±.10	"		6.7	Madrid et al.	1983
8.60±.20	"		8.5	Parks & DeBruyn	1962
7.3	Borggaard	1983	8.3	Troelstra & Kruyt	1942
5.9	"				
7.1	"				
8.0±.05	This study (synthetic)		8.8±.05	This study (natural)	

Table 5.2b Comparison of ZPC values for goethite.

ZPC	References		ZPC	References	
7.55±.15	Atkinson et al.	1967	8.71	Madrid & Arambarri	1978
7.5	Balistreiri & Murray	1981	8.0	Madrid & Posner	1979
7.2±.3	Borggaard	1983	8.5	Madrid et al.	1983
7.6±.3	"		7.0	Sigg & Stumm	1981
8.45	Cabrera et al.	1977	7.5	Yates & Healy	1975
8.75	Evans et al.	1979	7.1±.05	This study	
8.0	Hingston et al.	1972/74			
7.8	"				
8.3	"				

C) X-Ray Diffraction Analysis -

The basic structural units in both goethite and hematite consist of hexagonal close packed oxygen coordinated with Fe^{3+} in various octahedral positions (i.e. in 2/3 of the octahedral positions in the interstices for hematite), often viewed as assemblages of $[FeO_6]$ octahedra.

Generally four major d-spacing values are used to characterize minerals, although cryptocrystalline particles

with very small particle sizes may appear amorphous to XRD because of reduced coherent scattering of the x-rays. The Joint Committee on Powder Diffraction Standards (JCPDS) d-spacings for the Fe(III) oxides are:

MINERAL	CRYSTAL SYSTEM	d1(in Å)	d2	d3	d4
Goethite	orthorhombic	4.18x	2.693	2.452	4.98
Hematite	hexagonal (Rh)	2.69x	1.696	2.515	3.66
Jarosite	hexagonal (Rh)	3.08x	3.110	5.090	5.93

with the cell dimensions:

MINERAL	JCPDS File	a_o	b_o	c_o	cell volume $Å^3$
Goethite	17-536	4.596	9.957	3.021	
Hematite	24-72	5.038		13.772	
Jarosite	22-827	7.29		17.16	
s-Goethite	\	4.60 ±.01	9.99±.02	3.025±.004	139.11
s-Hematite	\this	5.029±.001		13.738±.003	300.856
n-Hematite	/study	5.0 ±.2		13.6 ± .5	291.2
s-Jarosite	/	7.33 ±.02		16.72 ±.05	778.16

Procedure:

X-ray analyses were performed on smear samples of goethite, hematite and jarosite scanning a range of 5 ° < 2θ < 75 ° (with 2θ being the irradiation angle) with Cu/K2 α radiation on a Philips diffractometer. The diffraction patterns are shown in Figures 5.1 and 5.2.

EXPERIMENTAL RESULTS:

Those iron oxide samples chosen for use in later sorption experiments give x-ray diffraction peaks which match the above four d-spacings obtained from JCPDS powder diffraction files. The hematite diffraction pattern shows

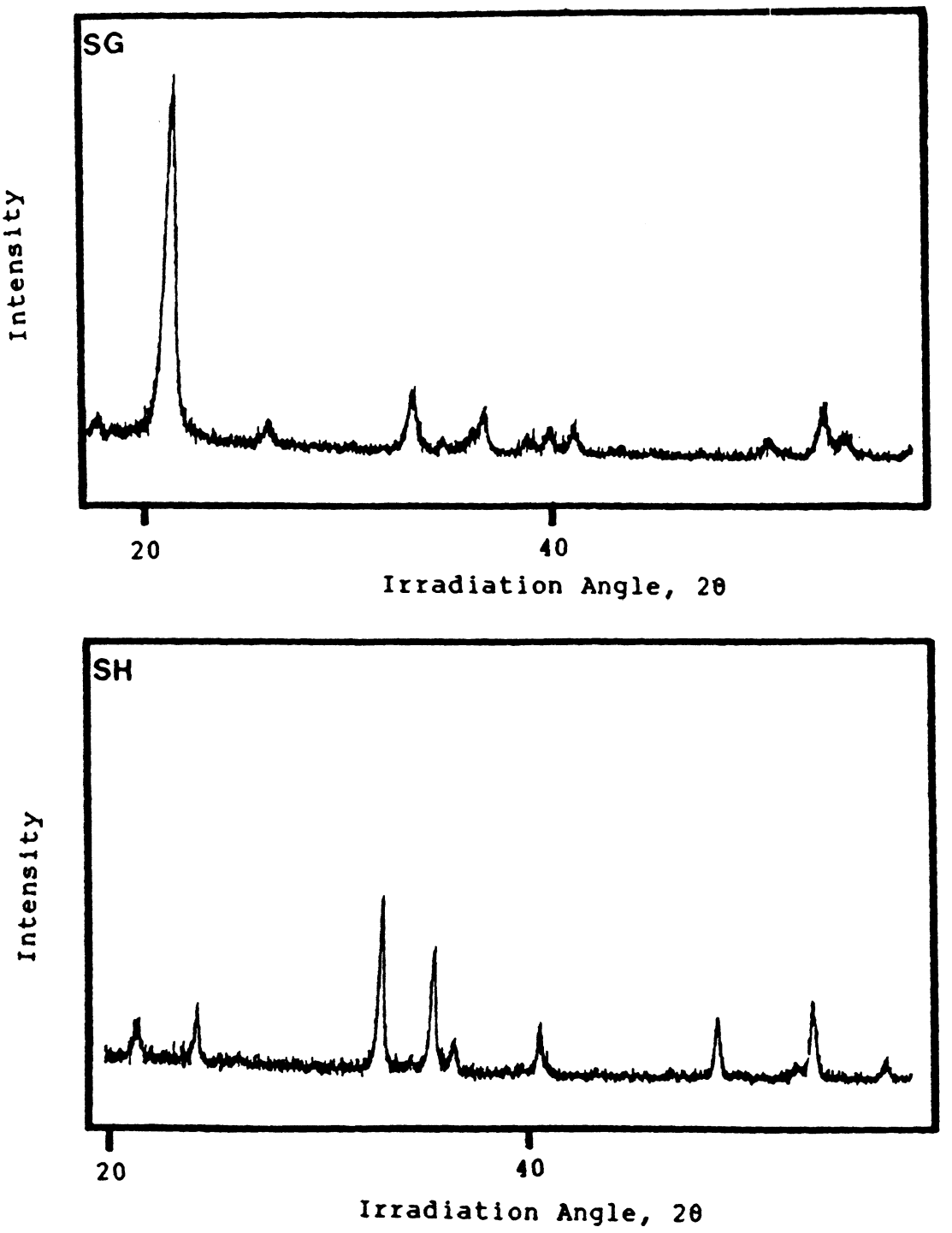

Figure 5.1 X-Ray diffraction patterns for synthetic hematite and goethite.

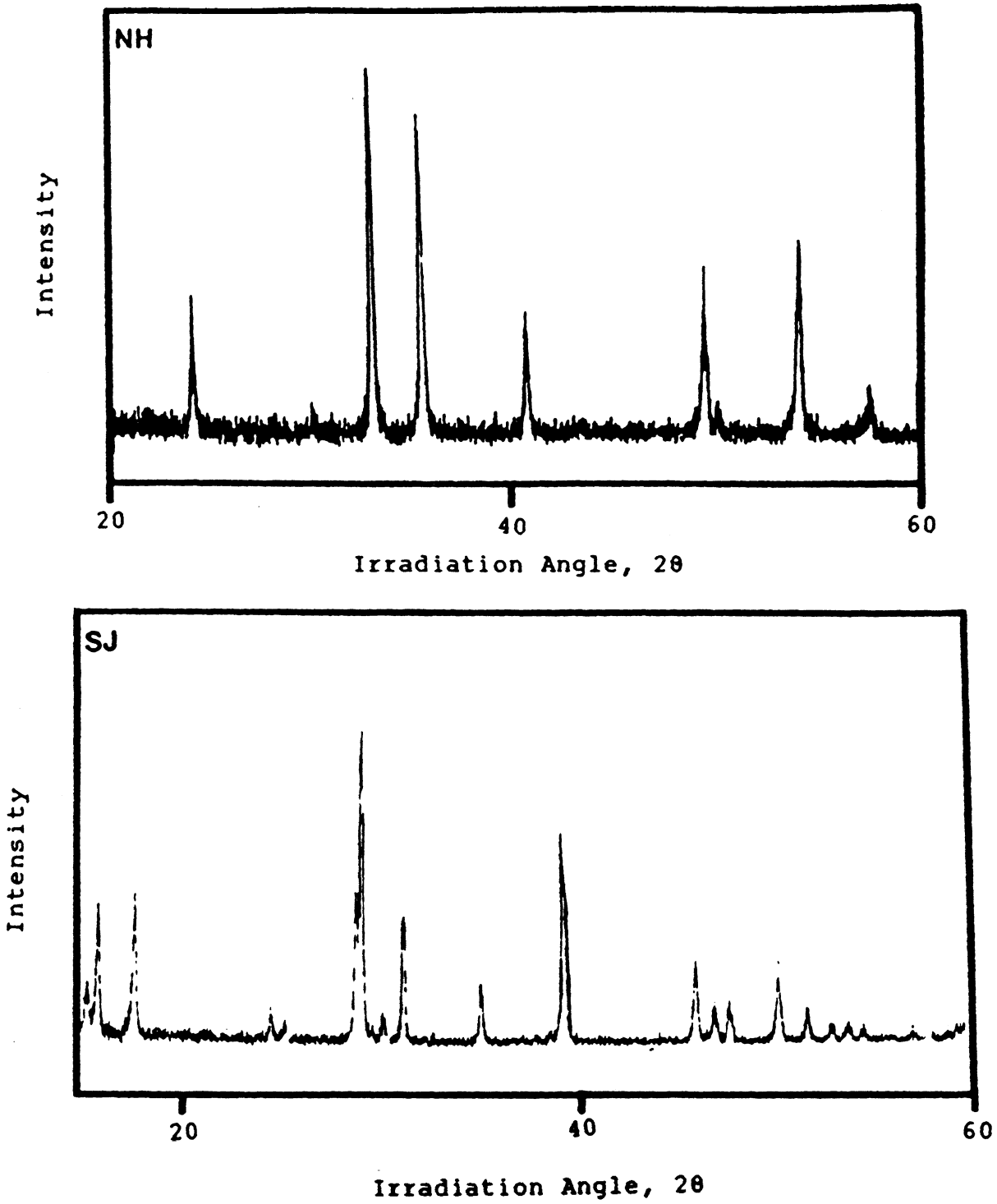

Figure 5.2 X-Ray diffraction patterns for natural hematite and synthetic jarosite.

a minor amount of goethite by exhibiting a small peak for the 4.18 d-spacing. The d-spacings of the jarosite sample diffraction pattern also match with the JCPDS values.

Experimental d-spacings were used to calculate the cell parameters for the four samples. Results, in angstroms, are listed above with the JCPDS values. Calculated cell parameters are in fair agreement with JCPDS standard cell parameters and literature values.

D) Electron Microscopy -

Scanning Electron Microscopy is used to examine morphologies for various natural and synthetic mineral samples. SEM is used to compare particle size and shapes for different preparations to help assess reproducibility of the preparation methods via duplicate samples.

Orthorhombic goethite commonly forms in an acicular habit, with needles being 0.1 to 1μm long, and often twinned. Hematite and jarosite commonly form small thick hexagonal tabular crystals.

Procedure:

Suspensions of samples approximately 0.02% in Fe are transferred with a pipette to nucleopore filters mounted on small brass stubs. These are air dried at room temperature, then coated with gold in a Polaron Sputter Coater.

Samples are examined on an ISI DS-130 Scanning Electron Microscope at 20,000 to 60,000 times

magnification.

EXPERIMENTAL RESULTS:

Under SEM, goethite (Plate 5-1a) appears as well formed 1 μm long laths, as observed by other investigators who have prepared the oxide using a similar procedure (Atkinson et al 1968 and Landa and Gast 1973). Hematite (Plate 5-1b), on the other hand, is poorly formed and has much smaller and more equi-dimensional crystals (as shown here and in the literature). Jarosite crystals (Plate 5-1d), also poorly formed, are much larger and more developed than the hematite preparations. The natural hematite sample (Plate 5-1c) shows no characteristic structure or grain size due to being a crushed whole rock sample.

E) Infrared Spectroscopy -

Infrared Spectroscopy is used to examine surface group characteristics to aid in the identification of natural and synthetic oxide and jarosite preparations. Particular surface groups presence and location are used as diagnostic indicators of mineral identification and purity, although exact peak locations depend on variables such as mineral size, shape and composition (Rendon and Serna 1981).

Goethite displays several identifying peaks which distinguish it from other iron oxides. The three most important of these are located at approximately 890, 795

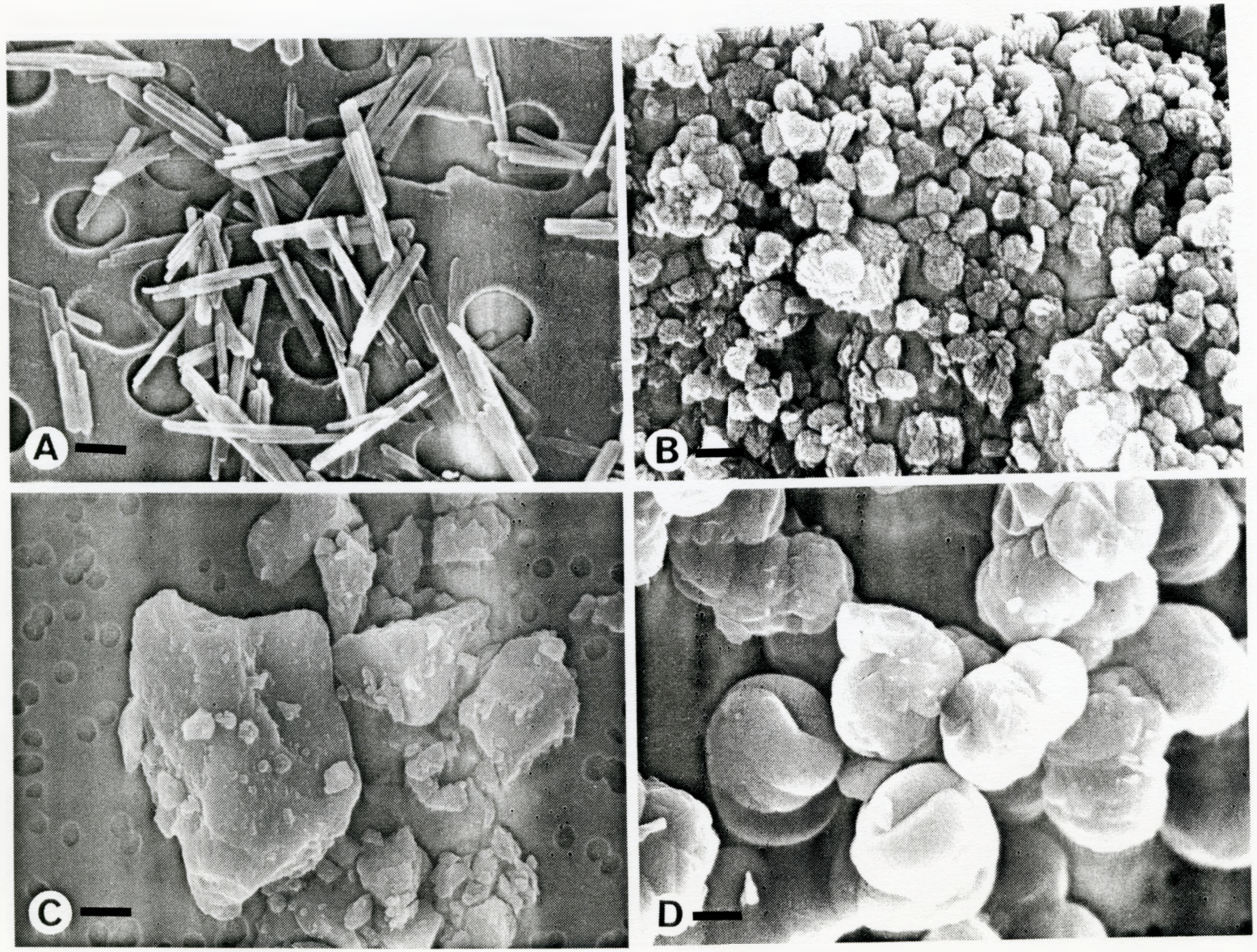
A
B
C
D

Plate 5.1 SEM images of mineral samples:

A) Synthetic goethite @ 20 KV and 30.4 KX
marker = 329 nm

B) Synthetic hematite @ 15 KV and 30.4 KX
marker = 329 nm

C) Natural hematite @ 20 KV and 10.1 KX
marker = 990 nm

D) Synthetic jarosite @ 15 KV and 7.99 KX
marker = 1.25 μm

and 640 cm^{-1} on IR spectra. Hematite's three major identifying peaks are found at approximately 560, 465 and 340 cm^{-1}. Jarosite has lattice vibration peaks at 560 and 465 cm^{-1} as does hematite, but also shows a 500 cm^{-1} lattice peak and several sulfate vibration peaks.

Oxide surface hydroxyls, which have been studied through deuteration procedures (Verdonck et al. 1982, Parfitt et al. 1976, Rochester and Topham 1979), have characteristic locations in IR spectra which are described in great detail in the literature. The high end of the spectrum (3000-4000 cm^{-1}) contains a group of peaks ascribed to free hydroxyl stretching. The size of these peaks, and thus the amount of the particular hydroxyl type present, differs for each oxide due to the nature of their surfaces. Many researchers consider iron oxides to have three main types of surface hydroxyls (A=singly, B=doubly and C=triply bonded) which are progressively difficult to remove, by heat or ion exchange, due to their bonding. These hydroxyl types give rise to separate identifiable peaks in the upper spectrum. The most important of these, the A=type at ~ 3440 cm^{-1}, is considered the active site and is monitored during sorption processes.

Procedure:

Approximately 1 mg of powdered oxide sample is ground in a porcelain mortar with approximately 400 mg of

dry KBr until it is equally distributed. The mixture is compressed into a disk and placed in a holder for analysis. The IR spectra are recorded on a Perkin-Elmer 283 double beam Spectrophotometer at a speed of 12 cm/min using air as a reference and on a Nicolet FT-IR Infrared Interferometer using an N_2 atmosphere as a reference.

EXPERIMENTAL RESULTS:

Peaks observed in the IR Spectra for analyzed oxide samples are listed in Table 5.3. The IR spectra positively identify the mineral samples and show all but the synthetic hematite to be pure. The synthetic hematite exhibits some small peaks indicative of goethite as an impurity.

F) THERMAL ANALYSIS

Thermal analyses of oxide samples can give much information on the stoichiometry and stability of surface hydroxyls. Several types of thermal analyses can be employed for direct and indirect surface studies (Paterson 1980, Paterson and Swaffield 1980, Mackenzie et al. 1981). Two types are used here:

(a) Differential Thermal Analysis (DTA)

Mineral thermograms obtained from DTA indicate temperature regions where endothermic (ex. phase transitions and dehydration) and exothermic (ex. [re]crystallization, decomposition, and oxidation) transitions occur, including regions where chemisorbed surface water is removed, as well

Table 5.3 Infrared spectral peaks obtained.

IR1	IR2		A) SYNTHETIC GOETHITE SAMPLE
3531 cm^{-1}	\		
3423	>---------V	OH	O-H stretch of free hydroxyls
3141	3120/		
2919			???
2849			???
	1780\		
1650	1650 >----------		H-O-H bend of water
1600	/		
1541	1540----------		NO_3^- adsorption band
1464	\		
1428	>----------		$CO_3^=/NO_3^-$ adsorption bands
1384	1385/		
1120	\----------		O-H deformation
	1045/		
889	882----------	OH δ	O-H in plane bend
794	790----------	OH γ	O-H out of plane bend
721----------			$CO_3^=/NO_3^-$ adsorption band
658----------			$CO_3^=$ adsorption band
640	630----------V	Ls	Fe-O lattice bond symmetrical
494	\		stretch
447	[450] \--------V	La	Fe-O asymmetrical stretch vibration
	[400] /		multiplet
	[360]/		
	254----------V	Ls	Fe-O lattice symmetrical stretch

IR1	IR2		B) SYNTHETIC HEMATITE SAMPLE
3596 cm^{-1}	\		
3471	3470 \		
3408	>--------V	OH	O-H stretch of free hydroxyls
3167	/		
3113	3120/		
2929	2940		???
2851	2855		???
1648	1650\----------		H-O-H bend of water
1604	/		
1539----------			NO_3^- adsorption band
1383	1385----------		$CO_3^=/NO_3^-$ adsorption band
	1030----------		O-H deformation
890	888		Goethite δ OH in plane bend
855----------			$CO_3^=/NO_3^-$ adsorption band
800	795		Goethite γ OH out of plane bend
	602------A2v		O- displacement mode /where A=longitu-\
564	567------Ev		O- displacement mode \dinal adsorption/
467	470------Ev		" "
	410------A2v		" " where E = transverse
	345------Ev		" " adsorption

C) NATURAL HEMATITE SAMPLE

IR1	IR2		
3830 cm^{-1}	\		
	3640 \	V OH	O-H stretch of free hydroxyls
3526	3520 /		
3444	3460/		
2951	2970		???
2919	2930		???
2870			???
2840			???
1650	\		H-O-H bend of water
1604	/		
1456	1460\		$CO3^{=}/NO3^{-}$ adsorption bands
1376	/		
1199	\		O-H deformation
1160	1160/		
1070	\		$CO3^{=}$ adsorption bands
1080	1080/		
1018	1030\		O-H deformation
970	/		
799			$CO_3^{=}/NO_3^{-}$ adsorption band
616	600	A 2v	O-- displacement mode
546	555	E v	O-- displacement mode
464	467	E v	" "
420	420	A 2v	" "
	332	E v	" "

D) SYNTHETIC JAROSITE SAMPLE

IR1			
3387		V OH	O-H stretch of free hydroxyls
2161			???
2077			???
2020			???
1971			???
1633			H-O-H bend of water
1182\		V3 SO_4	
1140/		V3 SO_4	
1002			O-H deformation
629		V4 SO_4	
569\			
506 >			FeO_6 octahedral vibrations
471/			

IR1 = Peaks from Infrared Interferometer (Range 400-4000 cm^{-1})
IR2 = Peaks from Infrared Spectrophotometer (Range 200-4000 cm^{-1})

as regions where structural dehydroxylation takes place. Thermograms are dependent upon particle size and crystallinity (Derie et al. 1976, Patterson and Swaffield 1980, Mackenzie et al. 1981). Large goethite particles tend to give two endothermic peaks between 250-400°C, small particles one sharp peak accompanied by shoulders. DTA thermograms also often exhibit effects at 670-680°C where the goethite dehydroxylation product hematite undergoes some magnetic changes.

EXPERIMENTAL RESULTS

Results found in this study are illustrated in Figure 5.3. Synthetic goethite exhibits three endothermic peaks. A small peak (A) at 85°C represents removal of surface waters. A large peak at 290°C (B) indicates removal of structural waters (dehydroxylation 2 FeOOH -> Fe_2O_3 + H_2O). The last small peak (C) at 620°C represents changes in the hematite dehydroxylation product.

Synthetic hematite exhibits three endothermic peaks. The first peak (D) at 100°C arises from surface water removal, the second peak (E) at 290°C indicates structural water removal. This peak has a shoulder at 340°C and is much smaller than the corresponding peak in the goethite spectrum. A small inflection (F) at high temperatures (>700°C) indicate magnetic transitions, which occur in ferro-magnetic materials at iron's curie temperature of ~780°C.

The natural hematite sample also has three endothermic peaks. Surface water removal occurs around 90°C (G), structural water removal at 280°C (H) with shoulders at 235 and 295°C and magnetic effects at 720°C (I).

Synthetic jarosite loses surface water at 114°C (J). Peaks at 455 (L) and 675°C (N) and inflections at 230 (K) and 560°C (M) indicate structural water removal and phase changes. Several investigators (Kerr and Kulp 1948, Kulp and Adler 1950, Caillere and Henin 1954) attribute the 400-450°C endothermic peak to decomposition to K_2SO_4 and $Fe_2(SO_4)_3$, the 500-550°C peak to crystallization of Fe_2O_3 and the 650-700°C peak to decomposition of $Fe_2(SO_4)_3$.

(b) Thermogravimetric Analysis (TGA)

TGA thermograms indicate temperature regions and weight loss resulting from physical and chemical bond destruction and formation whereby volatile products, including surface and structural water, are released.

Paterson (1980) and Paterson and Swaffield (1980) determined experimental dehydroxylation weight losses of 11.8% on synthetic goethites. Schwertman et al. (1985) found structural losses of OH^- on a series of synthetic goethites of different sizes, surface areas and crystallinity and observed a range of 10.34 to 12.00 % weight loss. All of these results reflect an OH^- excess over the theoretical structural dehydroxylation loss value

of 10.1%. Excesses such as this have generally been attributed to either (a), protonation of surface oxide ions, or (b), a contribution from water coordinated to exposed Fe(III) at crystal edges. From their TGA data Schwertman et al. (1985) calculated an average area of 8 $Å^2$ per water molecule. This is slightly less than the monolayer coverage of 10 $Å^2$ per water molecule as determined by Gast et al. (1974).

EXPERIMENTAL RESULTS:

In this study all three oxide samples and jarosite are analyzed by Thermogravimetric methods. TGA data are given in Table 5.4. From experimental data the surface area covered by surface water molecules can be calculated (or surface 'density' = molecules per surface area):

Oxide Sample	$Å^2/H_2O$	(H_2O/nm^2)	ZPC
goethite	6.7	15.3	7.1
hematite	5	19.7	8.0
natural hematite	3.3	29.6	8.8

Notice that the higher the pH of zpc, the more water molecules per surface area are found. The hydration state (and charge) when the oxides are analyzed is therefore important. At the analysis pH the mineral farthest from zpc may have the most hydroxyls or waters on its surface.

The synthetic goethite and hematite are uncrushed samples formed in an aqueous environment whose surfaces are able to fully hydroxylate. The large dry natural hematite sample increased its surface area per gram of sample on

grinding. Crushing may produce surfaces which are unable to equilibrate (hydroxylate) to their fullest potential since they are kept dry. This is indicated by data for weight loss on ignition. But experimentally, TGA shows natural hematite to hold twice as much water as goethite and a third more than the synthetic hematite. For comparison:

Oxide Sample	$Å^2/H_2O$	(H_2O/nm^2)	Reference
goethite	8	13	Schwertman et al. 1985
goethite	10	10	Gast et al. 1974

Table 5.4 Thermogravimetric data for sample weight losses.

Sample	ΔT °C	%loss	DTA peak #	Comments**
Synthetic	70-231	2.0	41-237 A	surface H_2O/OH^-
Goethite	231-665	10.0	237-370 B	structural OH^-
	665-750	2.3	612-637 C	full dehydroxylation
	Total =	14.3		of hematite product
Natural	196-254	1.0	41-231 D	surface H_2O/OH^-
Hematite	254-446	2.5	231-330 E	structural OH^-
	(end 500)	inflection	720 F	
	Total =	3.5		
Synthetic	55-232	2.5	65-242 G	surface H_2O/OH^-
Hematite	232-320	3.0	242-361 H	structural OH^-
	(end 650)	inflection	710 I	
	Total =	5.5		
Synthetic	50-195	3.8	35-195 J	surface H_2O/OH^-
Jarosite	195-374	1.7	195-269 K\	
	374-524	11.9	387-479 L \	structural OH^-
			535-582 M /	
	Total =	17.4	642-698 N/	

Notes: 1) total structural losses for goethite are close to Schwertman et al.'s (1985) theoretical value of 10.1%.

2) Weight loss on ignition indicates synthetic goethite, hematite and natural hematite to be 15.3, 5.5 and 0.85 weight percent water respectively.

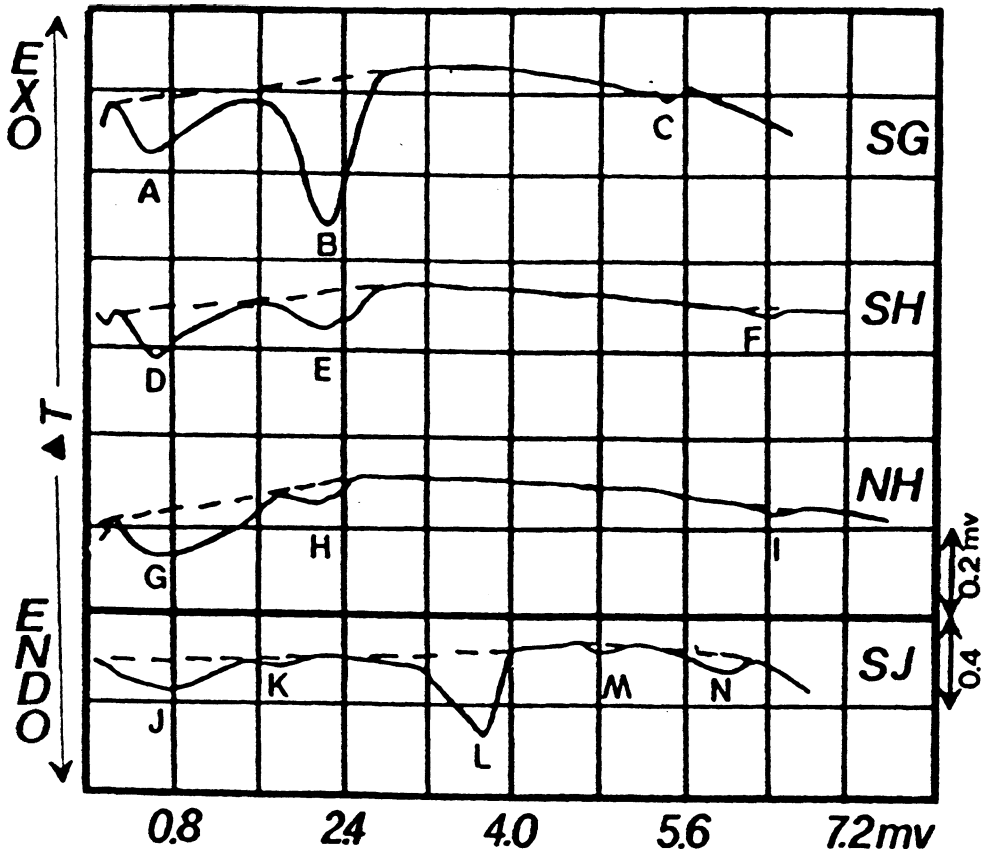

Figure 5.3 Differential Thermograms of mineral samples.

SG = synthetic goethite
SH = synthetic hematite
NH = natural hematite
SJ = synthetic jarosite

A-N designate DTA peaks as listed in Table 5.4

Literature values of water per surface area are lower than those experimentally determined by TGA. Later titration data calculations (Chapter 7) give approximately 9 OH/nm^2 (or 11 $Å^2/OH-$) which is in better agreement with the literature than TGA data.

G) Mossbauer Spectroscopy -

Due to its specificity towards iron, Mossbauer spectroscopy is a useful tool in the study of iron containing minerals (Goodman 1980, Bowen and Weed 1981, Amarasirwardena et al. 1986). Hematite and goethite, in particular, possess distinctly different magnetic hyperfine fields allowing easy identification. Figure 5.4 illustrates the splitting of Mossbauer levels in different ^{57}Fe substances and the resulting spectra.

Room temperature Mossbauer spectra of hematite and goethite should consist of six Lorentzian shaped resonant peaks indicating magnetic splitting, but hydration state, particle size, nonstoichiometry, ion substitution by aluminum and other structural defects can lower the spectra quality (Murad 1979, 1982). The sextet could collapse into a doublet, indicating quadrupole splitting, in which case temperatures as low as that of liquid nitrogen or helium would be required to observe the magnetic hyperfine splitting. But generally, several slightly different fields will superimpose so that the hyperfine magnetic field

distributions are skewed downwards from the upper limiting value for the perfectly crystallized mineral (i.e. 382 kilo-oersted (kOe) for goethite), thus giving rise to the more typical asymmetrically broadened resonant lines (Murad 1982).

Both hematite and goethite spectra display an isomer shift (δ) with respect to metallic iron of approximately +0.36 mm/s, typical of high spin octahedral Fe^{3+}. Goethite, which has a lower Neel temperature (400 K) and internal hyperfine field distribution than hematite (956 K), displays a quadrupole moment (Q) of approximately -0.3 mm/s, whereas the hematite quadrupole moment is approximately -0.2 mm/s (Bowen and Weed 1984).

EXPERIMENTAL RESULTS:

Mossbauer spectra of synthetic and natural samples are taken at room temperature using a $^{57}Co/Rh$ source. All spectra display the Fe^{3+} isomer shift (no Fe^{2+} present). Internal hyperfine field and quadrupole moment values positively identify hematite and goethite. Natural hematite is fitted with a single hematite sextet (Figure 5.5C). Synthetic hematite (Figure 5.5A) displays two sextets, one for hematite, the other for goethite (approximately 5%). Synthetic goethite (Figure 5.5B) exhibits 3+ goethite sextets, indicating that several iron sites are contained in the mineral. Jarosite is fitted with a doublet (Figure 5.5D) indicating quadrupole splitting at one iron site.

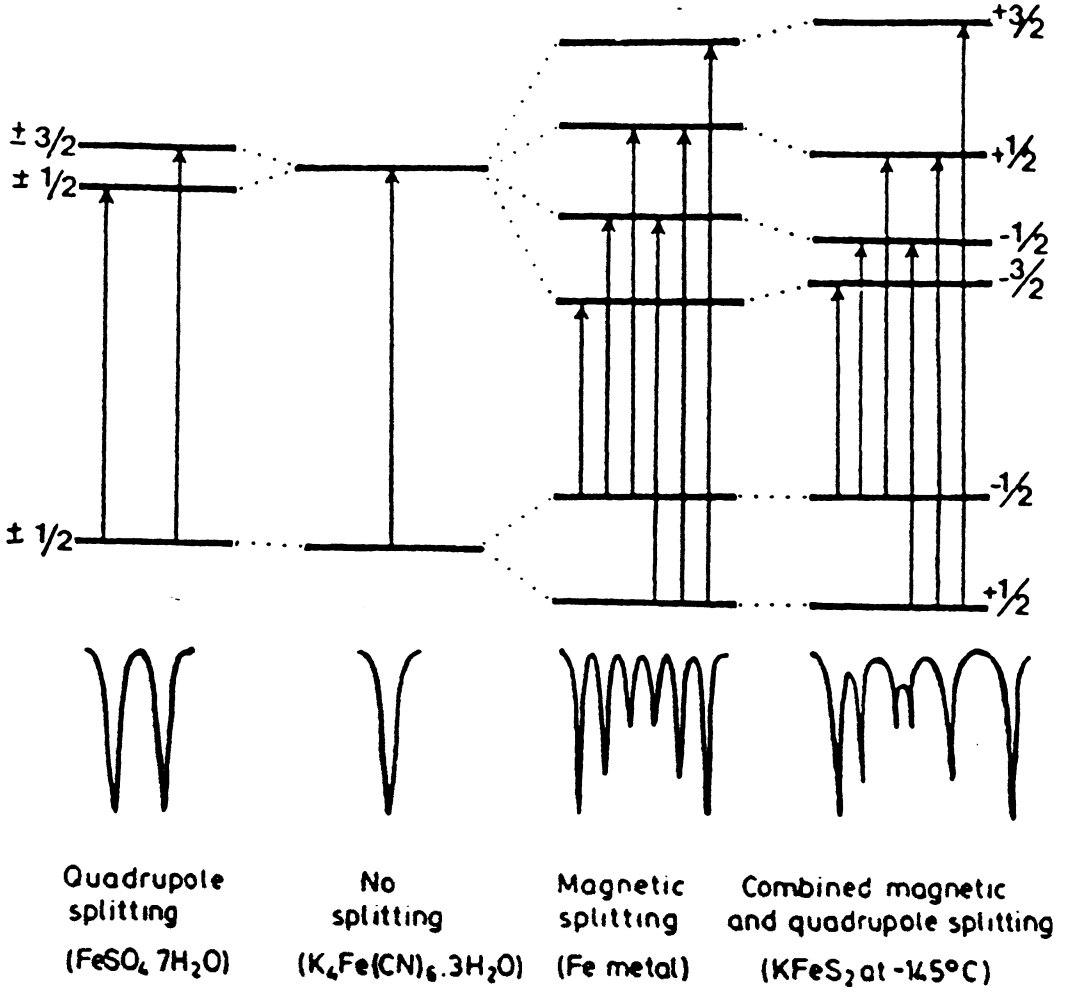

Figure 5.4 Mossbauer level splitting in ^{57}Fe and the types of spectra which arise. Examples of substances giving such spectra are named. These spectra are illustrative only. The spacings are not intended to be comparable.
(From McKay 1971)

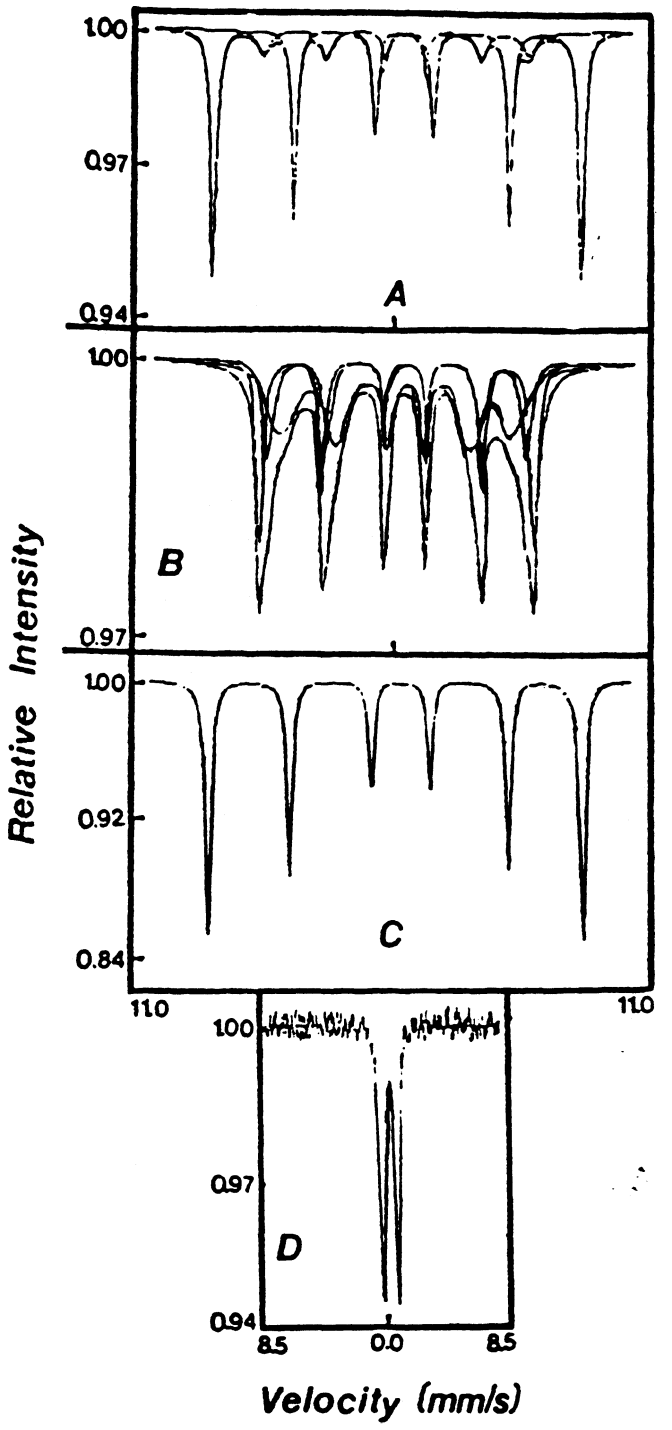

Figure 5.5 Mossbauer Spectra of mineral samples taken at room temperature at maximum velocity 10.268 mm/s.

a) synthetic hematite exhibits magnetic splitting of hematite and goethite (~ 5% impurity)
b) synthetic goethite exhibits > = 3 magnetic splitting sites.
c) natural hematite exhibits magnetic splitting only.
d) synthetic jarosite exhibits quadrupole splitting only.

H) X-RAY FLUORESCENCE -

The three oxide samples are analyzed for major elements using X-Ray Fluorescence. Results are listed in Table 5.5. As expected, the natural hematite sample contains the highest percentage of impurities. NOTE: the high potassium of the goethite sample is due to inadequate rinsing of the sample when separated from the KNO_3 media.

Table 5.5 XRF analysis data of oxide samples.

	Natural Hematite		Synthetic Hematite		Synthetic Goethite	
	wt. %	ions in formula	wt. %	ions in formula	wt. %	ions in formula
SiO2	3.35	0.08 Si	.80	0.02 Si	.3	0.00
Al2O3	2.63	0.08 Al	.05	0.00	.02	0.00
MgO	1.01	0.04 Mg	.03	0.00	.06	0.00
CaO	.23	0.01 Ca	.02	0.00	.01	0.00
Na2O	.03	0.00	.06	0.00	.03	0.00
K2O	.03	0.00	.03	0.00	3.21	0.06 K
TiO2	.25	0.00	<.01	0.00	<.01	0.00
MnO	.09	0.00	.05	0.00	.03	0.00
P2O5	.04	0.00	.01	0.00	<.01	0.00
H2O*	.85	0.14 OH	6.62	1.03 OH	15.34	1.41 OH
Fe2O3	91.49	1.72 Fe	92.32	1.63 Fe	80.93	0.84 Fe

* Water content is measured by loss on ignition (LOI).

Note: The number of ions in the mineral formula are calculated from XRF and LOI data using methods outlined by Deer et al. (1966). The minerals calculated formulas are approximately $Fe_{10}OH$, Fe_3OH_2, and $FeOH_2$ for natural hematite, synthetic hematite and synthetic goethite respectively.

I) NEUTRON ACTIVATION ANALYSIS -

The three oxide samples are analyzed by neutron activation analysis. Data are listed in Table 5.6. As

Table 5.6 Instrumental neutron activation analysis data of oxide samples. Standard deviation and detection limits are shown.

	Natural Hematite conc (ppm)	det.	Synthetic Hematite conc (ppm)	det.	Synthetic Goethite conc(ppm)	det.
Co	19.0±1.5	4	0 0	0	33.2 ± 1.8	3.3
Ti	430 ± 60	176	167 ± 19	50	163 ± 33	100
Br	22 ± 5	15	38 ± 5	7	42 ± 5	9
Na	222 ± 39	120	395 ± 25	40	195 ± 28	70
K	0 0	0	0 0	0	24000 ± 4000	4000
Cl	0 0	0	75 ± 17	50	0 0	0
Al	3910 ±130	21	69.6 ± 29	1.9	129 ± 6	3.1
Mn	447 ± 32	6	62 ± 5	2.2	68 ± 6	3.4
Cl	43 ± 9	24	54 ± 10	22	87 ± 16	28
I	0 0	0	7.4 ±1.8	1.9	0 0	0
Ca	1510 ±130	140	0 0	0	0 0	0

found in XRF analyses, the natural hematite sample exhibits the most impurities, with aluminum being most prominent.

J) SUMMARY -

Data from analysis of surface area, zero point of charge, x-ray diffraction patterns, infrared spectra, Mossbauer spectra and electron microscope observations can be summarized as follows:

SAMPLE	XRD	MOSS	IR	ZPC	SA~	SEM	TGA&DTA
Goethite	G	G	G	7.1	44.1	orth	G
Hematite	G/H	G/H	G/H	8.0	43.2	hex.	G/H
(Natural Hematite)	H	H	H	8.8	12.0	hex?**	H
Jarosite	J	J	J	-	-	hex?**	J

~ units = m^2/g ** Indistinguishable
G, H and J indicate positive mineral identification

Main observations are as follows:

-Iron oxide mineral samples are fairly easy to prepare, with synthetic hematite being the most difficult because its purity is hard to maintain.

-Experimentally determined surface areas and pH_{zpc} are within the range reported in the literature.

-X-ray analysis reveals mineral identities and indicates impurity of synthetic hematite. Calculated cell parameters agree with standard cell parameters and literature values.

-Electron microscopy shows morphologies that indicate synthetic goethite to be more physically developed than synthetic hematite and jarosite.

-Infrared spectroscopy confirms mineral identities and reveals information about surface groups.

-Thermogravimetric analysis and differential thermal analysis give information on surface and structural water content, surface hydroxyl stability and mineral stability (i.e. transition regions). Goethite, hematite, natural hematite and jarosite are 14.3, 5.5, 3.5 and 17.4 wt % water respectively, of which 10.0, 3.0, 2.5 and 13.6 wt % is structural water.

-Mossbauer spectroscopy confirms mineral identities and reveals information about iron sites. Jarosite is the only mineral which displays a doublet instead of a sextet indicating no magnetic splitting. All the minerals exhibit one iron site, except synthetic goethite, which shows at

least three.

-X-ray fluorescence gives concentrations of major elements in the minerals thus, along with loss on ignition, allows calculation of mineral formulas and indicates impurities. Calculations give synthetic goethite as $FeOH_2$, synthetic hematite as Fe_3OH_2 and natural hematite as $Fe_{10}OH$.

-Loss on Ignition indicates synthetic goethite, hematite and natural hematite to be 15.3, 5.5 and 0.85 wt % water respectively.

-Neutron activation analysis gives concentrations of elements in mineral samples also indicating impurities. These samples have negligible aluminum substitution, a common impurity in iron oxides and hydroxides (Yapp 1983, Norrish and Taylor 1961, Nahon et al. 1977, Fitzpatrick and Schwertman 1982).

CHAPTER 6 SORPTION EXPERIMENTS ON IRON OXIDES

Sulfate sorption experiments on goethite and hematite are described. Experiments dealing with ionic strength, pH, soil/solution ratio, sulfate concentration and reversibility are examined.

I. EXPERIMENTAL PROCEDURES

Basic Procedure for both Goethite and Hematite

Oxide suspensions of constant ionic strength (KNO_3 media) are equilibrated for 24 hours at an adjusted pH value. A known amount of sulfate is added as a K_2SO_4 solution and allowed to react. At pre-set time intervals, the pH is recorded and a sample of the suspension removed and filtered through 0.45 μm millipore filter paper. The filtrate is saved for later sulfate concentration analysis using a Wescan ion chromatograph.

Variations in Procedure:

(1) TIME- sorption in initial experiments is monitored at the time intervals .5, 1, 6, 24 and 48 hours to determine the attainment of equilibrium or steady state with respect to time (kinetics).

(2) pH- experiments are performed at three pH levels (3, 5 and 7) to examine pH effects.

(3) SULFATE CONCENTRATION- a range of original sulfate

concentrations from 0 to 500 ppm are covered to look for sorption maxima.

(4) IONIC STRENGTH- experiments are run in 10^{-2}, 10^{-3} and 10^{-4} M KNO_3 media to examine ionic strength effects on sorption of sulfate.

(5) SOLID/SOLUTION RATIO- both 0.1 g oxide to 25 mls media (1:1) and 0.1 g oxide to 50 mls media (1:2) are used in order to look for the effects of soil/solution ratio on sulfate sorption onto these oxides.

(6) REVERSIBILITY- In order to examine the reversibility of sorption in these systems, some sorption experiments are followed by desorption experiments. The procedure consists of resuspending an oxide to which a known amount of sulphate is sorbed in an ionic media of which pH is known and controlled. After a reaction time of 48 hours, as was used in the sorption experiments, the suspension is filtered and the filtrate examined for sulfate content.

II. RESULTS OBTAINED - General Observations

(1) TIME-The sorption process is initiated by a rapid (instantaneous) reaction followed by a longer slow one. After 24 hours of reaction time, a steady state or apparent equilibrium condition is reached with respect to pH and sorption. That is, no more changes in pH or sorption are observed after the 24 hour reaction period. See Figures 6.1 and 6.2.

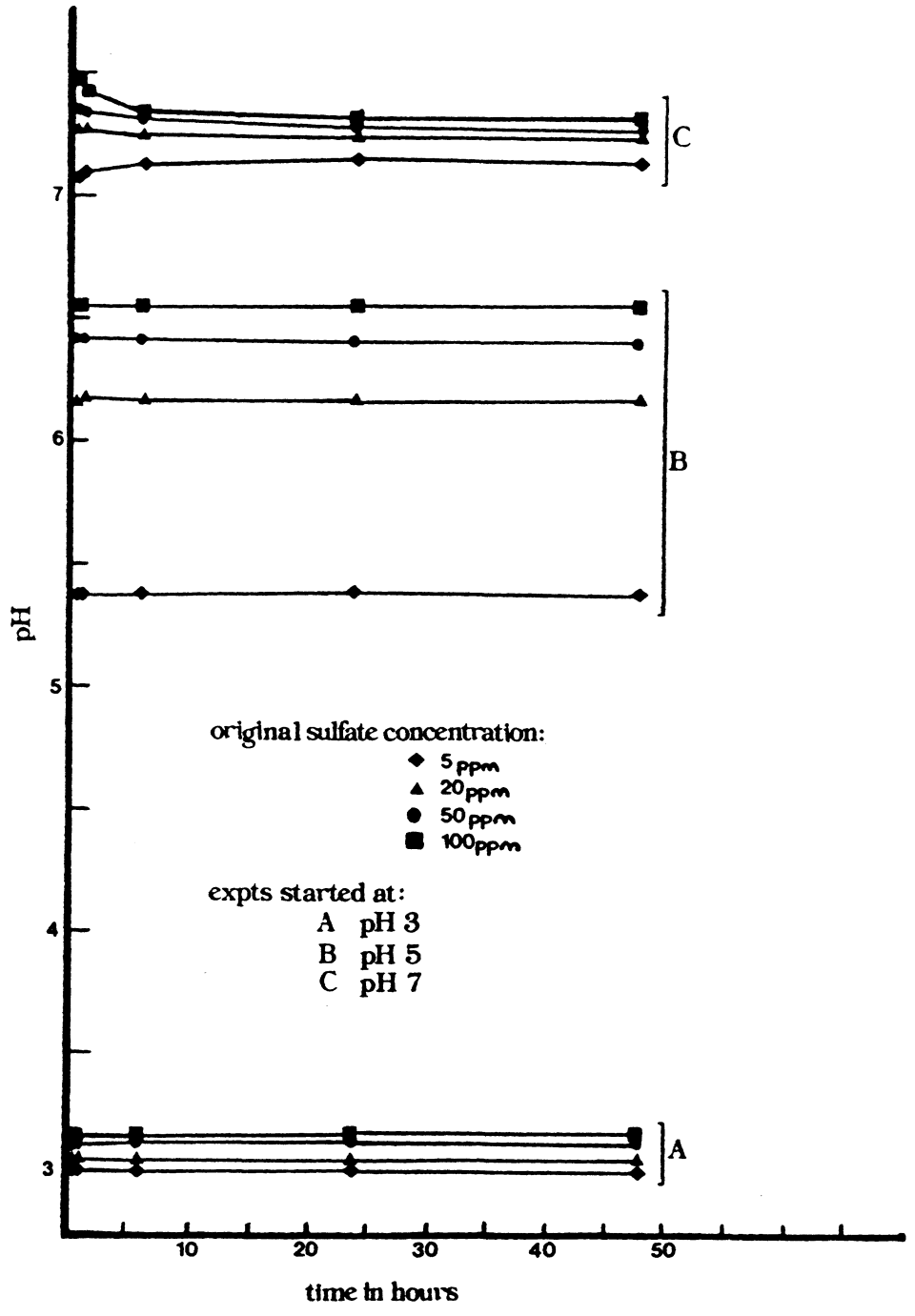

Figure 6.1 Initial goethite experiment: pH vs Time.

Notice the instantaneous pH change and the apparent equilibrium reached after 24 hours.

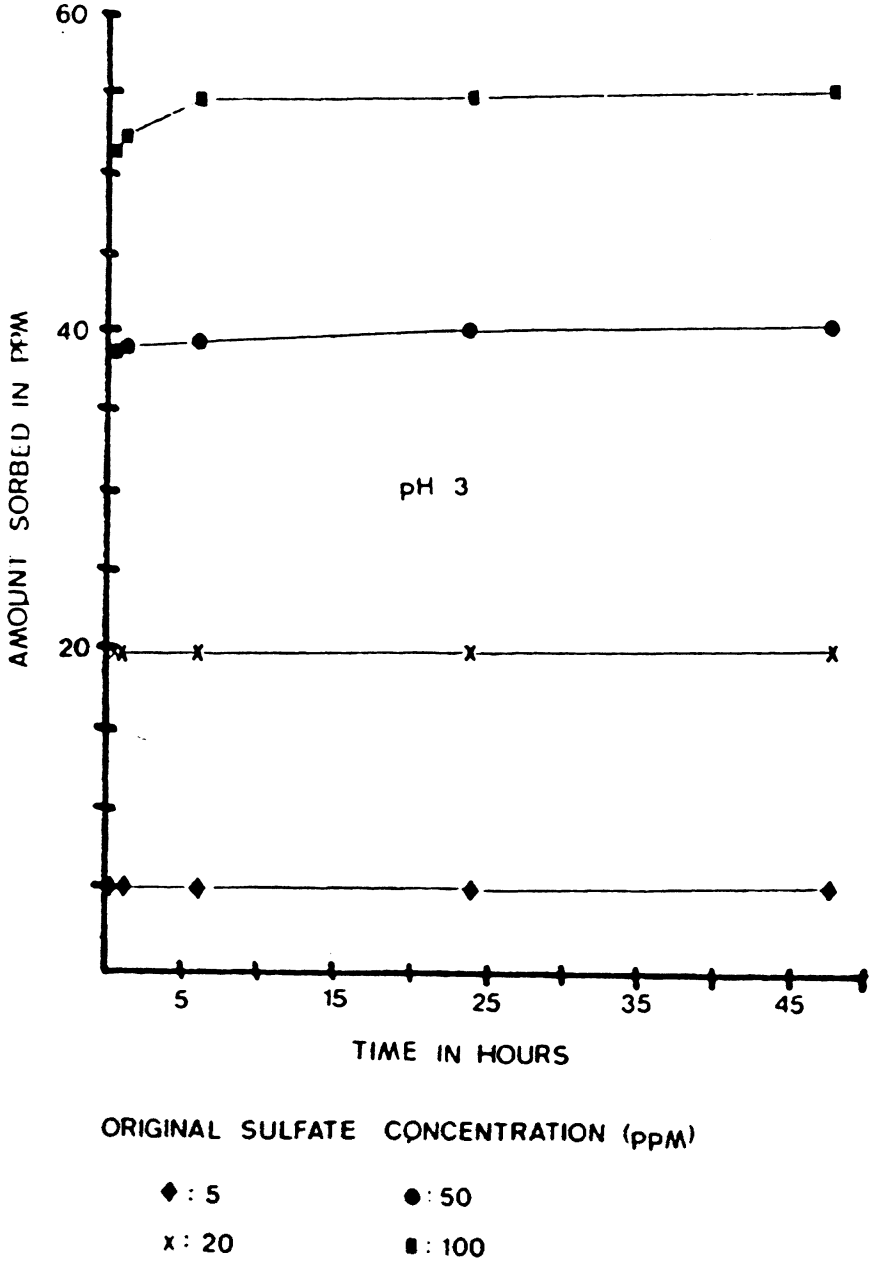

Figure 6.2 Initial goethite experiment: $[SO_4]$ vs Time.

Notice the instantaneous sorption and apparent equilibrium reached after 24 hours.

(2) pH- In all cases, the oxides sorbed increasing amounts of sulfate as pH decreased. See Figures 6.3 and 6.4.

(3) SULFATE CONCENTRATION-

a) Percent sorption vs original solution concentration - Figure 6.3. For both oxides, the percentage of sulfate sorbed decreases with increasing original solution sulfate concentration. pH 3 experiments exhibit the highest % sorbed for any original [SO_4], pH 7 experiments show the lowest sorption, pH 5 experiments lie midway between.

b) Amount sorbed vs equilibrium solution concentration- Figure 6.4. The amount sorbed increases with solution concentration. pH 3 experiments exhibit the highest ppm (or umol/g) removed from solution, pH 7 experiments show the lowest amount sorbed. Looking at the goethite data, an apparent sorption maximum is observed after a certain solution concentration for each pH level, with pH 7 experiments reaching the maxima at the lower concentration of sulfate. On the other hand, the synthetic hematite data appear to reach a maximum only in the pH 7 experiments over the concentration range studied. pH 3 and 5 data show a continuing increase in sorption with concentration with no sorption maxima plateau present. In comparison, a natural hematite sample examined at pH 3 is found to reach a maximum, and at a much lower concentration level than the synthetic hematite.

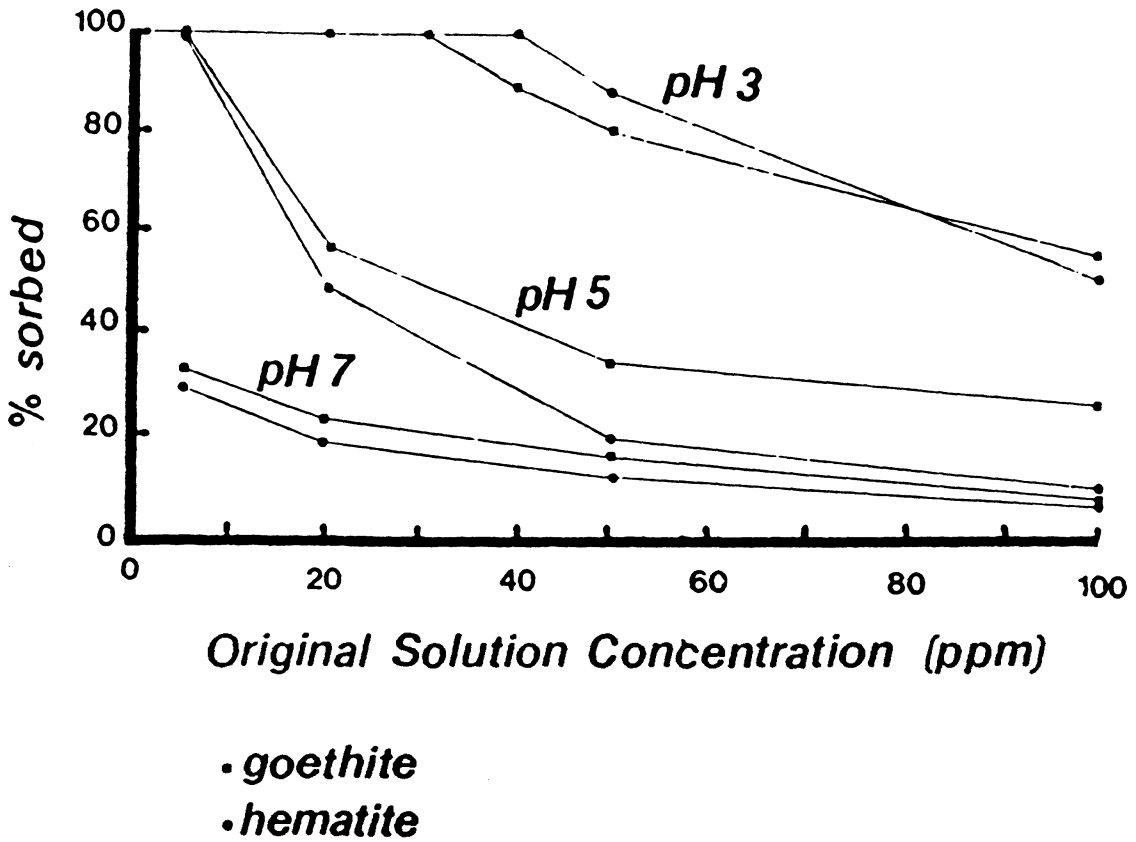

Figure6.3 Percent sorbed of the original solutionsulfate concentration for 4 g/l iron oxide suspension.
(A) Synthetic Goethite
(B) Synthetic Hematite

Notice as pH decreased the total amounts sorbed increased.

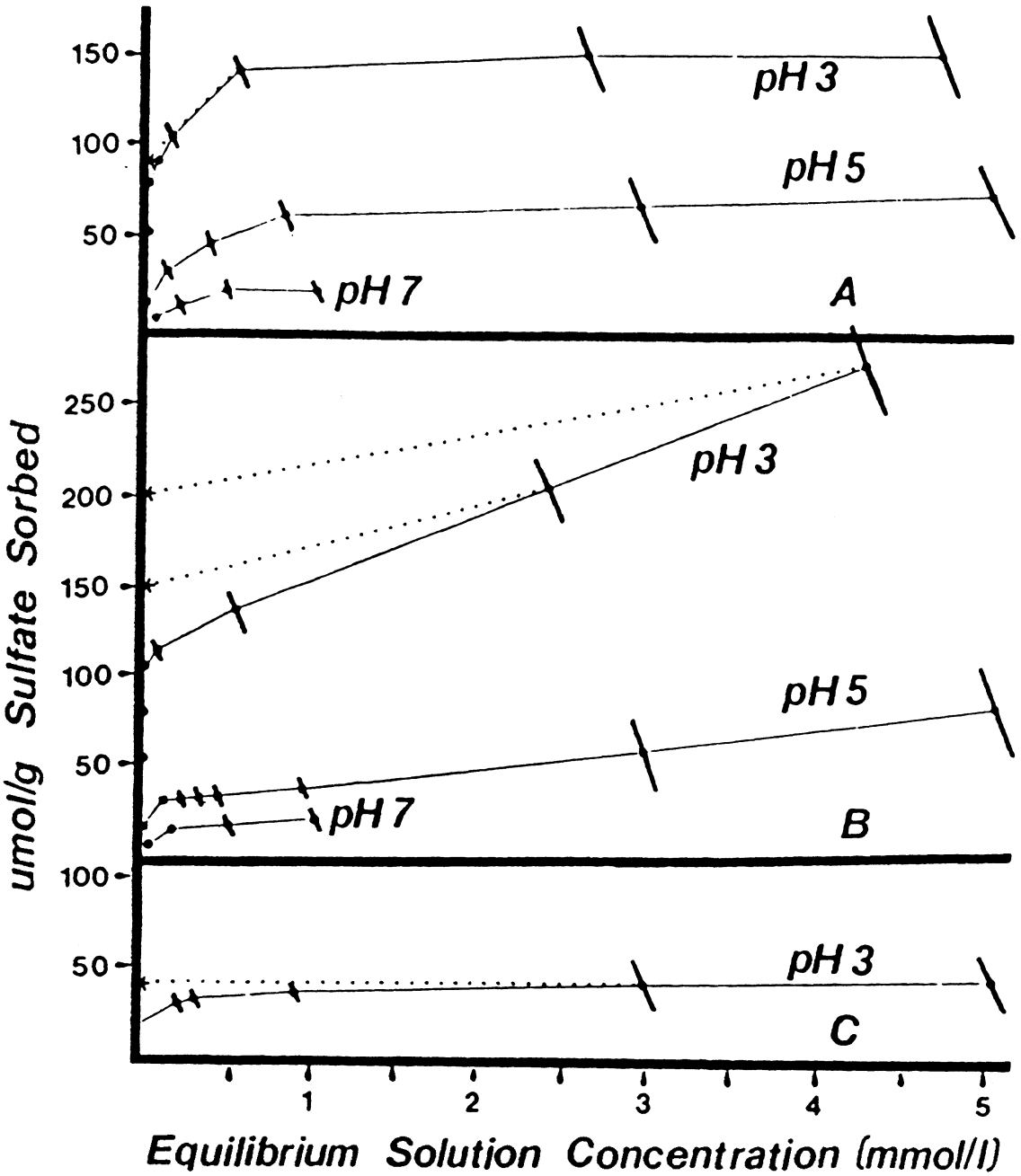

Figure 6.4 Amount sorbed vs equilibrium solution concentration for:
(A) Synthetic Goethite
(B) Synthetic Hematite
(C) Natural Hematite

Notice as the pH decreased, the total amount sorbed increased. Both goethite and natural hematite display apparent sorption maxima whereas synthetic hematite shows a maximum only at the highest pH used in the study. Sorption also appears to have poor reversibility.

(4) IONIC STRENGTH- For goethite, experiments held at pH 3 do not show an ionic strength effect at the 10^{-3}M KNO_3 level. However, at pH 5, sorption is slightly less at the 10^{-3}M ionic strength, than at 10^{-2}M. At 10^{-4}M KNO_3 goethite sorbs even less sulfate. Thus, sorption decreases with decreasing ionic strength. In synthetic hematite experiments no effect of ionic strength is observed at either pH 3 or 5, for 10^{-2}, 10^{-3} or 10^{-4}M ionic strength. Natural hematite also shows no ionic strength effect at pH 5 for 10^{-2} or 10^{-4}M ionic strength.

(5) SOLID/SOLUTION RATIO- Solid concentration effects are examined at pH 5, for goethite, but none are seen. Hematite is examined at both pH 3 and 5, and also shows no effect.

(6) REVERSIBILITY- Sulfate sorption is largely irreversible. Only the sorption/desorption isotherms at pH 3 appear reversible. There is no measurable desorption (0 %) of sulfate at pH 5 and 7.

Reversibility strongly depends upon the pH of sorption and desorption (see Table 6.1). It appears that the sorption pH strongly controls the desorption. Sulfate sorbed at low pH is generally more desorbable than that sorbed at a higher pH because a larger percentage of sulfate sorbed at higher pH is strongly bound compared to that sorbed at lower pH. pH of desorption is also important in

that more sulfate is desorbed as desorption pH increases. For example, sulfate sorbed at a pH of 3 and desorbed at pH 7 shows more sulfate desorbed than for a desorption pH of 3. Figure 6.5a shows goethite to desorb the largest percentage of its sorbed sulfate and natural hematite the smallest. Figure 6.5b indicates that synthetic goethite and hematite actually desorb about the same μmoles of sulfate per gram of oxide, whereas the natural hematite releases much less (4 μmol/g versus 60 μmol/g).

Raising solution pH shifts surface charge on these oxides towards the zero point of charge, making the surface less positive and thus less attractive to electrostatically held negative ions. A rise in pH also increases the hydroxyl ion concentration with respect to other anions in solution with more competition for non-specific sites. The present evidence suggests sorption of sulfate at higher pH to be mostly specific in nature, whereas at lower pH nonspecific sorption and specific sorption are important.

Table 6.1 Relationship between pH and reversibility.

Sorption pH/Desorption pH	Amount of Desorption
Low/Low	Low
Low/Neutral	Higher
Neutral/Neutral	Nil
Neutral/Low	Nil

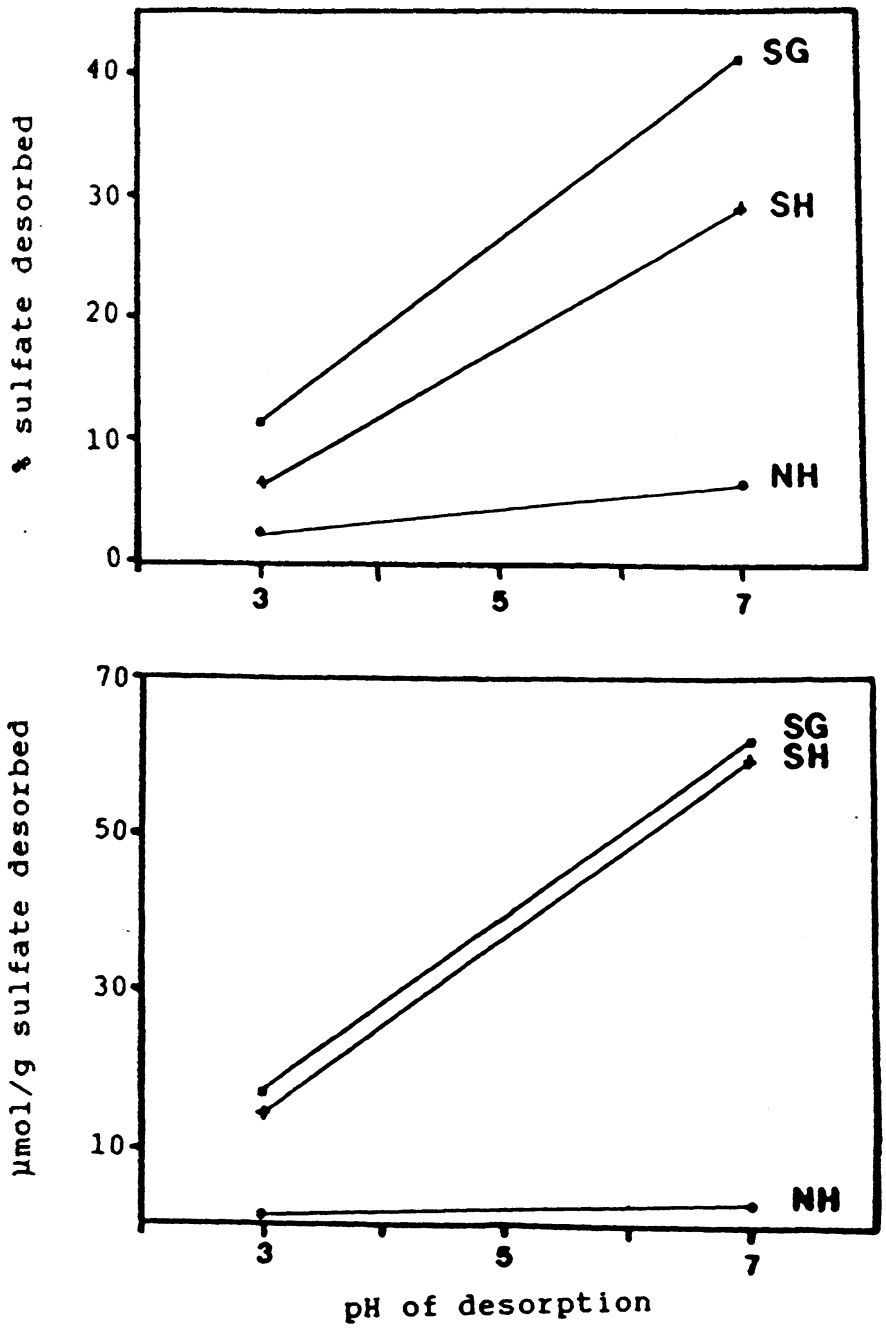

Figure 6.5 Desorption of sulfate from iron oxide surfaces: pH dependence.

a. pH vs percentage of sulfate desorbed.
b. pH vs µmol/g of sulfate desorbed.

SG = synthetic goethite
SH = synthetic hematite
NH = natural hematite

CHAPTER 7 OTHER EXPERIMENTS

I. X-Ray Diffraction and Scanning Electron Microscopy -

After sorption experiments, suspension samples are filtered. The filtrates are examined for sulphate and iron concentration by ion chromatography and atomic absorption. The oxides are examined by X-ray diffraction and electron microscopy. Diffraction spectra and SEM images taken before and after sorption experiments are compared for changes in composition (crystallography) and morphology.

Experimental results:

No differences in XRD spectra are observed. All XRD peaks can be attributed to the original minerals. No new surface structures or crystals are observed in the SEM image, thus giving no evidence for precipitation.

II. Infrared Spectroscopy -

The free divalent sulfate anion $SO_4^=$ is tetrahedral (T_d) in symmetry. It exhibits two infrared bands; the stronger one (V_3) at 1060 to 1140 cm^{-1} and the weaker one (V_4) at 580 to 650 cm^{-1}. The univalent ion HSO_4^- has C_{2v} symmetry. It exhibits four infrared bands; the strongest (V_4) at 570 to 600 cm^{-1} and three weaker ones at 850 to

880, 1050 to 1090 and 110 to 1200 cm^{-1} respectively.

Infrared spectroscopy has been used to assess the bonding of oxyanions, such as sulfate, with hydrous ferric oxides (Harrison and Berkheiser 1982). When a tetrahedral oxyanion coordinates with a surface as in sorption, the symmetry decreases causing the V_3 infrared adsorption band to split. The extent of splitting depends on the point group symmetry of the ion in its bound state (Nakamoto 1978). If a unidentate complex forms, two new bands appear (C_{3V} symmetry); if a bidentate complex forms, three new bands appear (C_{2V} symmetry) (Harrison and Berkheiser 1982).

The V SO_4 region (S-O stretch) is found between 900 and 1300 cm^{-1} with exact peak locations being dependent on the amount of surface sulfate present and the surface water content. In sulfate sorption, 4 bands are observed to arise in the V SO_4 region from V_1 and the splitting of triply degenerate V_3 vibrations (reduced C_{2V} symmetry). Their locations on goethite and hematite surfaces have been reported by investigators such as Parfitt and Smart (1977, 1978). The presence of 4 infrared bands clearly indicates direct coordination of the sulfate anion to the metal cation on the surface (Harrison and Berkheiser 1982).

Experimental results:

Compensation spectra of samples, taken referenced to air or N_2 gas, then referenced to blank oxide samples,

clarify the location of sulfate related peaks from the basic oxide spectrum. Table 7.1 lists experimental peak locations observed for sulfate.

All IR spectra indicate the presence of sulfate on the sample surfaces after sorption. Another important observation is the reduction in size of the A-type OH peak on each oxide sample, thus showing sulfate replacement of those particular hydroxyl groups. But not all the A-types have been replaced, even though some samples have sorbed their maximum amount of sulfate. As sulfate progressively replaces hydroxyl groups it becomes increasingly difficult to continue replacement, due to steric hinderance between sulfate groups on an increasingly crowded surface.

The above evidence, along with incomplete reversibility of sulfate sorption, indicates variability in bond strengths. Some sulfate ions may sorb onto more than one site, as in binuclear bridging, forming strong bonds and effectively covering large surface areas. Other ions form weak bonds with one site or are only electrostatically held to one site.

Table 7.1 Surface group peaks in the V SO_4 region.

	Sorbed Sulfate		Sample		Evaporated Sulfate		Sample	
	V3	V3	V3	V1	V3	V3	V3	V1
				Synthetic Goethite				
*	1210	1130	1025	obscured	1220	1108	1030	obscured
#	1220	1130	1049	965	1226	1123	1053	obscured
!	1219	1138	1038	966	1260	1144	1050	935
				Synthetic Hematite				
*	1260	1145	1015	965	1260	1140	1012	945
#	1162	1125	1040	982	1230	1155	1023	obscured
!	1242	1159	1041	948	obscured	1120	1040	obscured
				Natural Hematite				
*	1255	1130	1030	950	1245	1140	1030	980
#	1160	1127	1029	972	1199	1153	1024	973
!	obscured	1168	1000	obscured	obscured	1137	1012	975

* Compensation spectra peaks from Spectrophotometer
# Peaks from Interferometer using N_2 as a reference.
! Compensation spectra peaks from Interferometer

III. Thermal Analysis -

When present on mineral surfaces, anions often influence the DTA and TGA thermograms. Initial dehydroxylation stages for treated and untreated goethite and hematite appear identical, but later stages often show observable differences. For example, on NO_3^- and $SO_4^=$ treated samples, endothermic peaks at 410 and 660°C have been reported in DTA thermograms along with extra weight loss in 400-500°C and 600-700°C regions in TGA thermograms (Patterson and Swaffield 1980).

In this work, DTA and TGA thermograms are obtained for mineral samples before and after sulfate sorption to look for the evidence of anions influences.

Experimental Results:

DTA thermograms for mineral samples before sulfate sorption are shown in Figure 5.3. Results obtained after sulfate treatment are illustrated in Figure 7.1.

DTA thermograms for sulfate treated iron oxide mineral samples show no modifications in the 600°C region, but differences in thermograms do occur in other temperature regions. Synthetic goethite's thermogram displays an inflection at 390°C (Figure 7.1 point A). An enhanced exothermic peak appears on synthetic hematite's thermogram at 318°C (point 1), along with an endothermic peak at 530°C (point B). The natural hematite thermogram also displays exothermic peaks, with a larger one located at 230°C (point 2) and a smaller one at 335°C (point 3). An endothermic peak at 496°C (point C) is also observed. Low temperature endothermic peaks (80-150°C), near the boiling point of water, represent regions of surface dehydration. Endothermic peaks at higher temperatures (>200°C) represent structural dehydration and phase transitions. These temperatures, being greater than surface dehydration temperatures, indicate stronger bonding which requires more energy to break. Exothermic peaks indicate oxidation, crystallization and, as in the present case, decomposition, with breakdown and removal of sulfate ions from the surface. Exothermic peaks in Figure 7.1 occur at temperatures above that of surface dehydration also indicating the strength of the bonds

involved to be greater than that holding surface waters.

A DTA thermogram of synthetic jarosite (Figure 5.3) can be compared to the iron oxide mineral samples. It shows endothermic peaks at 455 and 675°C, a shoulder at 412°C and an inflection at 560°C. These correspond to the surface groups which give weight losses in the 400-500°C and 600-700°C regions as mentioned above.

TGA thermogram data for the oxide minerals after sulfate sorption is found in Table 7.2. When compared with the data from oxide samples before sorption experiments (Table 5.4), it is seen that both hematite samples lose a larger percentage of weight when sulfate is sorbed on their surfaces and removed through heat treatments. This is because the sulfate ion is heavier than the hydroxyl ion.

Thermogram data determined for the minerals under study indicate that sulfate sorbed on their surfaces is held by strong bonds, thus suggesting inner sphere complexing.

Table 7.2 Thermogravimetric data for sample weight loss.

Sample	ΔT °C	% loss	DTA peaks	Comments
Synthetic	65-231	0.6	35-252	surface H_2O/OH^-
Goethite	231-800	13.8	252-330	structural OH^-
	Total =	14.4	Inflection @ 390	
Natural	150-231	3.3	33-202	surface H_2O/OH^-
Hematite	231-560	3.6	255-319\	structural OH^-
	Total =	6.9	350-650/	
Synthetic	28-250	6.5	20-259	surface H_2O/OH^-
Hematite	250-325	3.6	259-361\	structural OH^-
	(end @ 500)		361-720/	
	Total =	10.1		

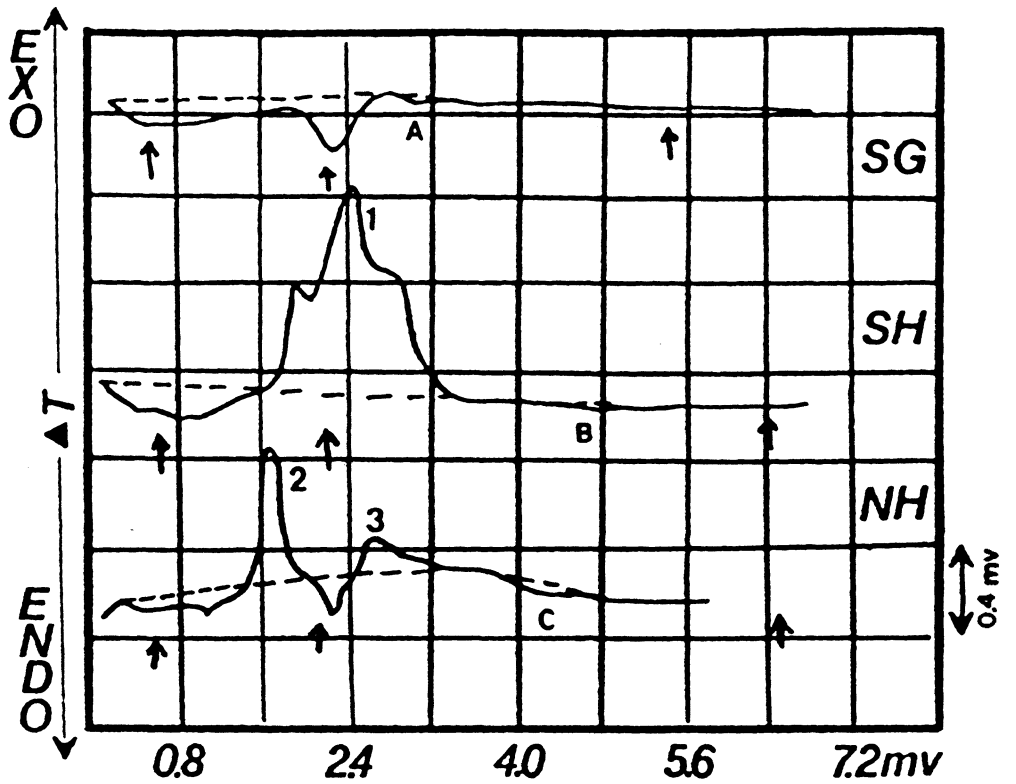

Figure 7.1 Differential thermograms of mineral samples after sulfate sorption.

SG = synthetic goethite
SH = synthetic hematite
NH = natural hematite

1, 2 and 3 are exothermic peaks
A, B and C are endothermic peaks
↑ indicate peak positions before sorption.

IV. Mossbauer Spectroscopy -

Mossbauer spectra of the three oxide samples, previously treated with sulfate, are taken at room temperature and compared with spectra obtained from untreated samples (see Figure 5.5). Spectra are taken at several velocities to get a clearer view of areas which might be obscured at normal velocities.

No changes in the spectra from those of untreated samples are observed. No doublet arising from jarosite quadrupole splitting of possible precipitants is observed in any of the oxide spectra.

V. Ion Concentration Product -

Experimental oxide suspensions contain ions with known or controlled concentrations ($[K^+] = 10^{-2}$ M, $[OH^-] = 10^{-11}$ M, $[SO_4^=] = x$). Iron content of suspensions measured by atomic absorption is 10^{-5} M for hematite and 10^{-6} M for goethite. Ion concentration products (ICP) can be compared to known solubility products to determine if mineral precipitation is possible under said conditions.

Jarosite $\{KFe_3(SO_4)_2(OH)_6\}$, suspected of precipitating on iron oxide surfaces, has a solubility product (pK_{SO}) of 98.56 (Vlek et al. 1974).

$$[K^+][Fe^{3+}]^3[SO_4]^2[OH^-]^6 = ICP$$

In solution, if:

ICP < K_{so}, no precipitation occurs (undersaturation).

ICP = K_{so}, saturation.

ICP > K_{so}, precipitation is possible (supersaturation).

For saturation with respect to jarosite, the system requires a minimum concentration of 3 ppb and 30 ppm sulfate ion for hematite and goethite respectively at pH 3. In present experiments, all solutions were saturated with respect to jarosite at pH 3. However, no evidence of a precipitant is observed.

VI. Exchange Capacity -

The titration of a blank (KNO_3) sample is completely reversible. But when an oxide is added to the solution, the system changes. Some H^+ (or OH^-) remains on the surface and is removed with the oxide when the suspension is filtered and is thus unavailable for back titration (Figure 7.2).

If experimental exchange capacity titrations are performed on an oxide at its zero point of charge, it is expected to treat excess amounts of acid and base similarly because at the zpc there are equal amounts of positive and negative charges on the surface. That is, the surface is expected to retain/release similar amounts of H^+ ions upon acid/base addition:

<u>SURFACE:</u> $Fe\text{-}OH_2^+ \xleftrightarrow[+OH^-]{+H^+}$ start Fe-OH zpc $\xleftrightarrow[+OH^-]{+H^+} Fe\text{-}O^-$

(also see Figures 4.1 and 4.2)

It must be kept in mind that this system is a suspension, with a solid and a liquid part, and that this solution must be considered when examining exchange capacity. The pH_{zpc} of goethite is about 7. This is the point where $[H^+] = [OH^-]$ in solution and excess amounts of added acid or base should behave similarly. But the hematite zpcs are higher (8-8.8) and $[OH^-] > [H^+]$ in solution. At a pH below their zpc, these oxides will have net positive sites on their surface and will be in an environment where $[H^+] = [OH^-]$ or $[H^+] > [OH^-]$, thus having excess H^+ in solution. In solutions where pH is not neutral, ions may not be treated similarly.

Figure 7.2 Suspension treatment for exchange capacity determination.

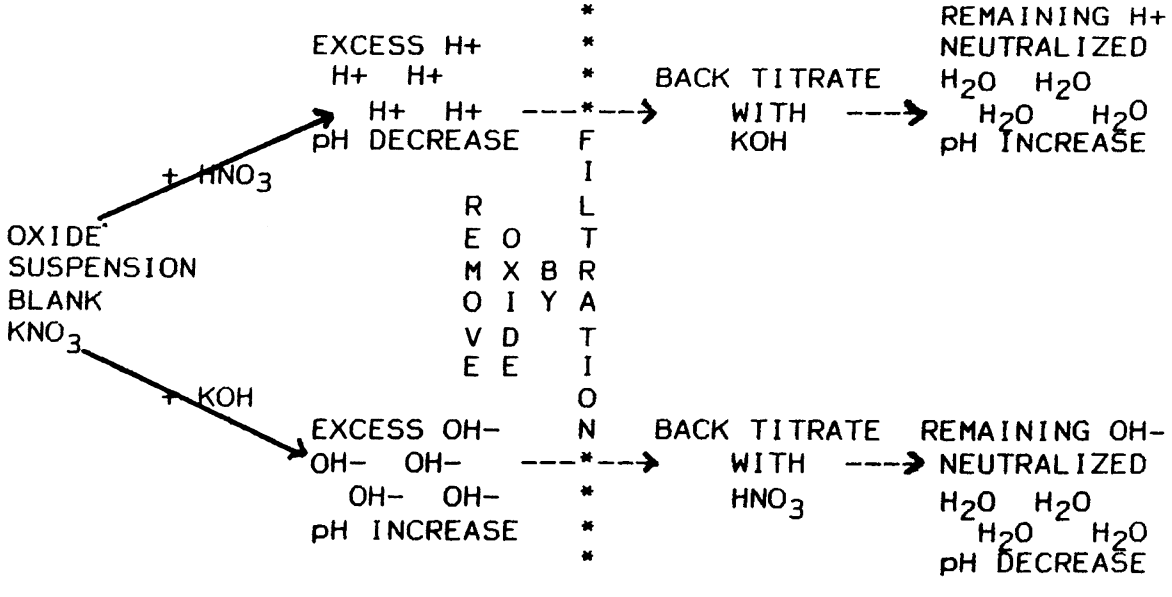

Short (pH 3-7) and long (pH 3-11) titrations are performed on all oxides. For short A/B and B/A titrations (where A=acid, B=base and / designates a filtration step) started at neutral pH on oxides of neutral pH_{zpc}, the oxide is expected to exchange equal amounts of acid or base. Experimentally, short titrations show a smaller exchange capacity and hydroxyl surface coverage in A/B runs, where the surface is loaded with H^+, than in B/A runs, where the surface is loaded with OH^-. However, short titrations still give an unclear picture of exchange capacity. For example, goethite is the only oxide shown to hold H^+ on its surface. To get a better view, extended titrations (covering pH 3 to 11) are performed. Here the initial pH is unimportant as it is adjusted to 3 or 11 with the first titrant. In AB/A the surface is loaded with OH^-, in BA/B the surface is loaded with H^+ before filtering and back titration.

From Table 7.3, it is seen that although exchange capacity titrations start on the hematites at pH < zpc and on goethite at a pH > zpc, all hold OH^- on their surfaces in an extended titration pH range. The titrations give differing results in that AB/A show more hydroxyls being exchanged for synthetic minerals and BA/B show more hydroxyls exchanged for natural hematite. This indicates the possibility of several surface sites which are being activated under differing conditions. Note there is no pattern between oxide zpc and exchange capacity for AB/A vs

Table 7.3 Exchange capacity related characteristics.

SAMPLE	ZPC	BET-SA m^2/g	EXCH-CAP μmoles/g	ion/nm^2	Comments
Synthetic Hematite pH_i 6.6	8.0	43.2	3.150 OH	0.04	A/B Sorbs more
			205.8 OH	2.9	B/A SO_4 than
			733.5 OH	10.2	AB/A NH
			412.3 OH	5.8	BA/B
Natural Hematite pH_i 6.5	8.8	12.0	174.8 OH	8.8	A/B Sorbs
			196.0 OH	9.8	B/A least SO_4
			408.3 OH	24.3	AB/A of oxides
			498.5 OH	24.8	BA/B examined
Synthetic Goethite pH_i 8, 9	7.1	44.1	74.70 H	1.0	A/B Sorbs less
			230.5 OH	3.2	B/A SO_4 than
			1316 OH	18.0	AB/A SH
			1229 OH	16.8	BA/B

/ designates where filtering took place pH_i = initial pH

BA/B. Synthetic hematite, with the mid value zpc, has exchange capacity measurements which differ most for the two extended titrations.

Total exchange capacity is the maximum number of exchangeable hydroxyl groups at the oxide surface ($=FeOH_T$) in μmol/g. When normalized to surface area (groups/nm^2), it can be compared to literature values listed in Table 7.4. Experimentally determined values are observed to be higher than most literature reports. Close agreement is seen between Yates (1975) goethite data and that of this study.

CALCULATION:

Approximate exchange capacity can be calculated by assuming the oxide surface to be covered by spheres of the hydroxyl ion radius 1.85 Å. Hydroxyl ions should cover

approximately 10.8 x10-2 nm^2, meaning there are approximately 9.26 OH per 100 $Å^2$ (= 9.26 OH/nm^2). Using the surface areas of the oxide minerals determined in Chapter 5, the approximate exchange capacity for synthetic hematite is 664 μmol OH/g, for natural hematite is 186 μmol OH/g and for synthetic goethite is 678 μmol OH/g. Remember these approximations do not consider surface sites, which should change the numbers significantly.

Experimentally derived data may differ from theoretically calculated values due to the differences in the types and reactivities of OH^- groups, including binding and repulsive effects. Experimental values (Table 7.3) for synthetic oxide samples examined here are lower for synthetic hematite and goethite in short titrations, but extended titrations give values generally higher than calculated approximations. Different results for short and long, acid and base, titrations indicate the possibility of activation of more than one phase or site under differing pH conditions.

Thermogravimetric data on the removal of surface water can also be compared to exchange capacity results. TGA shows 15, 20 and 30 OH/nm^2 (versus 18.0, 10.2 and 25.0 OH/nm^2 as reported in Tables 7.3 and 7.4) for synthetic goethite, hematite and natural hematite respectively. Data for goethite and natural hematite agree well.

Table 7.4 Reported exchange capacity (EC) and surface coverage (SC) values.

EC umol/g	SC OH/nm^2	SA m^2/g	Reference		Oxides
	10		Micale et al.	C	(H+G)
200	4	28-\	Sigg and Stumm	M	(G)
350	6-7	29/		M	
	2.7		Parfitt et al.	M	(G)
1348	16.74	48.5	Yates	M	(G)
550	3.5-6.9	48-96	Russel et al.	M	(G)
134-269	4.5-9.0	18	Breuwsma	M	(H)
	6.7-7.9		Morimoto et al.	M	(H)
	9			C	
(68)	4.3	9.6	Jurinak	M	(H)
(93)	5.6	10	McAfferty and Zettlemoyer	M	(H)
1316	18	44.1	\	M	(SG)
678	9.26		\	C	"
733.5	10.2	43.2	\ This Study	M	(SH)
664	9.26		/	C	"
498.5	25	12.1	/ measured =	M	(NH)
186	9.26		/ calculated =	C	"

VII. Hydroxide Release vs Sulfate Sorption -

For sorption experiments, known amounts of K_2SO_4 are added to oxide suspensions. During reaction, pH is noticed to rise. To determine how much OH^- is released (or H^+ consumed) during sorption (1) a calculation is made from monitored changes in pH of the solutions and (2) experimental titrations are performed to measure hydroxyl release during reaction.

CALCULATION:

The calculation of hydrogen consumption or hydroxyl release during reaction is performed for several different

initial solution sulfate concentration levels, including the highest levels run for each oxide. Initial pH before reaction (initial moles H^+) and final pH at the end of reaction time (final moles H^+) are compared to determine change in moles H^+ for the reaction.

Samples of suspension are analyzed for remaining sulfate to determine sulfate consumed. Then the ratio (R) of {μmoles H^+ consumed} to {μmoles SO_4 sorbed} is calculated. Notice, in Table 7.5, the decrease in R as the $[SO_4]_i$ increases. Thus the more sulfate sorbed, the less H^+ consumed as the experiment proceeds.

EXPERIMENTAL TITRATION:

During several sulfate sorption experiments, acid is added titrimetrically to maintain the original suspension pH. Acid additions are monitored throughout the time of the experiments in order to determine the amount of OH^- released from the oxide surface and thus neutralized by the added acid. At pH 3 (5), the hydroxyls released during sulfate sorption are 1/10 (1/14), 1/5 (1/6) and 1/5 (1/24) of measured exchange capacity of goethite, hematite and natural hematite respectively.

The ratio (R)={μmoles H^+ consumed}/{μmoles SO_4 sorbed} is determined using sulfate values derived from sorption isotherms (see Table 7.6). Calculation, as in above section, underestimates the actual H^+ consumed during sorption of sulfate. This is reflected in the ({H^+}/{$SO_4^=$})

ratio by exhibition of lower R values when using calculated H^+ consumed divided by isotherm determined values of sorbed sulfate. This difference is noticed for all sorption experiment data, suggesting that there is some buffering in the system which prevents the actual change in $[H^+]$ from being fully exhibited by observed pH changes. Thus only titration shows the true H+ consumed.

Raw sulfate data are obtained from one set of early experiments and used to illustrate changing ratios observed throughout the range of initial sulfate concentrations used (Table 7.5). For these data $[H^+]$ calculated from observed pH changes is used since no titrations were being performed at that time.

The early raw data do not reflect later determined isotherms well nor the isotherm sulfate values reported in Table 7.6. Isotherm values reflect (i) true isotherm sorption maxima or (ii) 'approximate' sorption maxima (labeled ~), meaning maximum sorption values determined for numerous 500 ppm initial sulfate concentration experiments on these oxides. These values are more correct than the initial 'raw' values and show distinctly different influences on $H^+/SO_4^=$ ratio calculations.

Table 7.5 Ratio of hydrogen consumed to sulfate sorbed calculated from early raw data.

OXIDE	ppm $[SO_4]_i$	(R) $\frac{\{\mu mol\ H^{\pm}\}}{\{\mu mol\ SO_4\}}$ (pH 3)	(R) $\frac{\{\mu mol\ H^{\pm}\}}{\{\mu mol\ SO_4\}}$ (pH 5)	
Synthetic Hematite	5	1.28	0.16	¦ d
	20	0.64	0.08	¦ e
	30	0.48	0.08	¦ c
	40	0.58	0.08	¦ r
	50	0.77	0.08	¦ e
	100	0.65	0.07	¦ a
	300	0.55	0.04	¦ s
	500	0.43	0.03	\¦/ e
Synthetic Goethite	5	1.28	0.57	¦ d
	20	0.71	0.08	¦ e
	30	0.66	----	¦ c
	40	0.64	----	¦ r
	50	0.69	0.05	¦ e
	100	0.57	0.04	¦ a
	300	0.56	0.04	¦ s
	500	0.56	0.03	\¦/ e

Table 7.6 Ratio of hydrogen consumed to sulfate sorbed from titration data for 500 ppm initial $[SO_4]$.

OXIDE	pH	$\{\mu mol/g\ H^+\}$ acid used	$\{\mu mol/g\ SO_4\}$ sorbed	(R) $\frac{\{\mu mol\ H^{\pm}\}}{\{\mu mol\ SO_4\}}$
Synthetic Hematite	3	154.6	~ 275	0.56
		(Langmuir gives	~ 284	0.54)
	5	125.6	~ 80	1.57
		(Langmuir gives	~ 82.5	1.52)
Synthetic Goethite	3	147.5	151	0.98
	5	93.8	73	1.28
Natural Hematite	3	106.1	45	2.36
			46 **	2.31
		(Langmuir gives	~ 45.7 **	2.32)
	5	21.2	ND	----
		(Langmuir gives	~ 39.2**	0.54)

** Data from Wootton 1985

CHAPTER 8 MODEL OF SULFATE SORPTION ON FERRIC OXIDES

I. SORPTION SUMMARY

A. General Characteristics

The sorption reaction characteristics observed in this study (Table 8.1) are comparable to literature reports and can be summarized as follows:

a) The process is initiated by a fast reaction followed by a longer, slower one which appears to equilibrate within 24 hours. pH increases observed during the process due to H+ consumption or OH^- release also equilibrate within this time period.

b) Sorption decreases with increasing pH, as is observed in soil and oxide studies in the literature.

c) As the original solution sulfate concentration increases the amount sorbed increases. That is, the total μmol/g

Table 8.1 Sorption reaction characteristics.

	Equilibrium Time in hrs	Sorption With Respect to Increasing pH	Sorption With Respect to Increasing $[SO_4]$	Sorption With Respect to Increasing IS	Sorption With Respect to Increasing S/S	Desorption Activity
Goethite	24	dec	inc	inc @ pH5	nil	some
Hematite	24	dec	inc	nil	nil	some
Natural Hematite	24	dec	inc	nil	nil	some

Table 8.2 Sorption maxima and calculated maximum possible surface coverage by sulfate, in μmol/g (μmol/m^2).

Sample	pH 3	pH 5	pH 7	maximum coverage
Synthetic Goethite	151.0 (3.42)	72.9 (1.65)	20.8 (0.47)	372 (8.44)
Synthetic Hematite	-	-	17.6 (0.41)	364 (8.43)
Natural Hematite	45.0 (3.72)	ND*	ND*	102 (8.43)

* ND = not determined

sorbed increases, although the total percent sorbed decreases. Both synthetic goethite and natural hematite reach sorption maximum (Table 8.2), after which increasing amounts of sulfate cause no further increases in sorption.

d) No effect of ionic strength on the sorption isotherm is observed for hematite. However, goethite exhibits ionic strength effects at pH 5, where sorption increases with ionic strength.

e) No effect on the sorption isotherm is observed when the solid content/solution ratio of solutions is changed.

f) Goethite and hematite show desorption only when sorption reactions are performed at pH 3, but sorption is not fully reversible. Goethite desorbs more sulfate than hematite when the desorbing pH is maintained at pH 3 and larger amounts are released when pH is raised to 7 (see Table 8.3). Sorption on natural hematite is even less reversible than on synthetic hematite.

Table 8.3 Percent desorbed from equilibrium solutions.

	pH 7		pH 3	
	500 ppm	300 ppm	500 ppm	300 ppm
Synthetic Goethite	41	41	11.5	11.5
Synthetic Hematite*	23	29	5.5	6.4
Natural Hematite	6.4	6.4	2.4	2.4

* No sorpn max reached at pH 3 for synthetic hematite

B. Sorption Maxima

Sorption data plots (Figure 6.4) show the curve fitted maxima listed in Table 8.2. Literature goethite values of 150 μmol/g (1.85 μmol/m^2) at pH 3 reported by Hingston et al. (1972) and 75 μmol/g (0.83 μmol/m^2) at pH 5.1 reported by Parfitt and Smart (1977) can be compared with goethite values determined in this study. A maximum of 125 μmol/g (1.39 μmol/m^2) at pH 3.4 was also reported by Parfitt and Smart (1977). Inconsistencies between experimental and literature values arise through differences in surface area measurements.

Literature values for hematite of 67 μmol/g (2.50 μmol/m^2) at pH 4.6 (Aylmore et al. 1967) and 85 μmol/g (3.8 μmol/m^2) at pH 3.5 (Parfitt and Smart 1978) do not match well with data obtained on the synthetic hematite due to lack of adsorption maxima at the lower pH values. The natural hematite maximum observed here appears to be lower than that reported in the literature, but does match closely the work of Wootton (1985) who reported an apparent maximum at 46 μmol/g (3.80 μmol/m^2). As above with goethite, the

differences between literature and experimental values can be attributed to variations in measured surface area.

Calculated maximum surface coverage of oxide samples by sulfate ions, approximately 19.7 $Å^2$ (0.197 nm^2) in size, are also listed in Table 8.2. Data show that only half of the available surface space is actually occupied by sulfate at pH 3 and less at higher pHs. The maximum coverage is not reachable due to factors such as mineral dissolution (which will occur if the pH is lowered more as required for increased sorption), steric hinderance as ions crowd the surface, and location, amount and type of exchange sites.

C. Isotherm Comparison

Experimental data obtained in this study are compared using both the Freundlich and Langmuir isotherms to determine the better fit and in the case of the Langmuir, to see if calculated maxima agree with observed maxima. Isotherm parameters are summarized in Tables 8.4 a and b.

Table 8.4a Langmuir isotherm data fit for oxide samples.

Oxide	pH	r	Slope	I	Max	K
Synthetic Goethite	3	0.99999	0.0066	0.2	152.3	32.9
	5	0.99920	0.0134	2.5	74.6	186.5
	7	0.99800	0.0422	5.5	23.7	130.5
Synthetic Hematite	3	0.98277	0.0036	1.5	278.4	408.3
	5	0.97500	0.0121	7.3	82.4	603.6
	7	0.99768	0.0494	6.3	20.2	127.6
Natural Hematite	3	0.99895	0.0218	3.8	45.9	173.1

Table 8.4b Freundlich isotherm data fit for oxide samples.

Oxide	pH	r	Slope	I
Synthetic Goethite	3	0.95038	0.1047	1.8
	5	0.95669	0.2160	1.1
	7	0.98576	0.4229	0.1
Synthetic Hematite	3	0.94137	0.1961	1.7
	5	0.94330	0.2237	0.8
	7	0.95633	0.4729	0.1
Natural Hematite	3	0.97940	0.1222	1.2

r = correlation coefficient
I = intercept
Max = sorption maximum in μmol/g
K = equilibrium constant

Correlation coefficients show goethite data to have a much better fit to the Langmuir than to the Freundlich equation. Hematite data also show a better fit to Langmuir behavior, but the correlation coefficients are not as good as are seen for goethite.

The Langmuir sorption maxima for goethite for pH levels 3, 5 and 7 (Table 8.4a) agree fairly well with the observed maxima of 151.0, 72.9 and 20.8 μmol/g. No maxima are observed for pH 3 or 5 isotherms of synthetic hematite for the range of concentrations under study (i.e. up to 500 ppm or approximately 5000 μmol/l original solution sulfate concentration). However, a maxima of 17.6 μmol/g is observed at pH 7, which is within range of the Langmuir calculated maxima. For natural hematite, the calculated Langmuir adsorption maxima is in fair agreement with the observed maxima of 45 μmol/g.

D. Sorption in Relation to Surface Area

Aylmore et al. (1967) conclude sorption to be proportional to surface area due to sorption of 0.50 me/m^2 sulfate on hematite and pseudoboehmite (see their Table 1), but their calculations are incorrect. Hematite (surface area 26.7 m^2/g) sorbed 13.4 me/100 g (or 67 μmol/g) of sulfate at pH 4.6, which calculates to 5.0 μeq/m^2 (or 2.51 μmol/m^2). Their pseudoboehmite data (sorption maxima 84.2 me/100 g, surface area 165.5 m^2/g) also gives 5.0 μeq/m^2. Results for the two oxides are expected to be similar since sorption methods on iron and aluminum oxides are similar. Aylmore et al. (1967) report sorption maxima and surface area for two kaolinite samples, but not the adsorption per unit area values of 1.05 and 0.59 μeq/m^2. The clay minerals give different results from the oxides because their sorption mechanisms are different.

Values determined in this study are listed in Table 8.5. Aylmore et al.'s (1967) data (5.0 μeq/m^2 or 2.5094 μmol/m^2 at pH 4.6) are within range of these data. The decrease in sorption per unit area with increasing pH is

Table 8.5 Sorption in relation to surface area.

	pH 3		pH 5		pH 7	
	μmol/m^2	μeq/m^2	μmol/m^2	μeq/m^2	μmol/m^2	μeq/m^2
SG	3.42	6.84	1.65	3.30	0.47	0.94
SH	-	-	-	-	0.41	0.82
NH	3.72	7.44	ND	ND	ND	ND

quite obvious in the present data. This leads to the conclusion that sorption is not directly proportional to surface area in the way Aylmore et al. (1967) believe.

II. OTHER EVIDENCE

A. OH^- Released / SO_4 Sorbed = R

In Chapter 4, models for sulfate sorption on oxide surfaces are illustrated. Figures 4.4, 4.5 and 4.6 list the ratio of number of ligands replaced to the number of anions held (R) beside each model. Table 8.6 summarizes the experimental R values obtained in this study, which can now be compared to Chapter 4 model R values.

Experimentally, synthetic goethite and hematite show decreasing R with pH. This is expected since the surfaces should have fewer hydroxyls, which coincidently are more strongly held, as pH is lowered. If, for argument sake, a fixed amount of sulfate is sorbed at any pH, R would have to decrease with pH due to the decrease in available hydroxyls.

Synthetic goethite ratios indicate mono-ligand exchange (one hydroxyl ion for one sulfate ion) at pH 3 and

Table 8.6 Ratio of hydroxyl released vs sulfate sorbed.
OH/SO4 = (C)/(A) = (R)

	pH 3		pH 5	
	*µmol/g OH released	R	*µmol/g OH released	R
SG	154.6	0.98	125.6	1.28
SH	147.5	0.56	93.8	1.57
NH	106.1	2.36	21.2	ND

* (OH released from 500 ppm initial experiment)

a 75:25 combination of mono and multi-ligand exchange (one to two hydroxyls for one sulfate ion) at pH 5. Synthetic hematite ratios indicate a 50:50 combination of $-OH_2^+$ and -OH mono-ligand exchange at pH 3, and a 50:50 combination of mono and multi-ligand exchange at pH 5. Electrostatic attraction also gives an R value that is compatable with synthetic hematites sorption model at pH 3, but it allows large amounts of desorption, which is not experimentally observed under these conditions. It appears that for the above minerals, as pH changes, the sorption mechanism shifts from a mono to a multi-ligand exchange. That is, at different pHs, different mechanisms come into play according to the availability of various surface sites.

The natural hematite ratio indicates multi-ligand exchange, with one to three hydroxyls exchanged per one sulfate at pH 3. The following two sections, B and C, show natural hematite to possess a large hydroxyl surface coverage and thus the ability to accommodate a high demand for exchange, but there is at present no model for one sulfate ion exchanging with three hydroxyl ions. It must be remembered that this natural hematite sample has been crushed. It may contain impurities which alter its surface activity, and may have surfaces which are not behaving as natural mineral faces.

B. Sample Weight Loss

Oxide weight loss through heat treatment is

indicative of surface and structural waters. Weight losses can be used to calculate surface coverage by hydroxyls when the two types of waters can be distinguished in the weight loss measurement, as in Thermal Gravimetric Analysis (TGA). Table 8.7 lists total percentage of weight lost by the oxide samples when subjected to two types of heat treatment and their approximate hydroxyl surface coverages.

Generally more weight loss is indicated by Loss On Ignition (LOI) over TGA, except in the case of synthetic hematite here, due to its efficiency in complete sample destruction over the latter method. LOI values are total % lost, internally and externally. Increased weight loss after sulfate treatment is expected due to the greater weight of the sulfate ion over the hydroxyl ion.

Theoretical calculations discussed in chapter 7 give a value of 9.2 OH/nm^2 for hydroxyl surface coverage. Literature values range from 2.7 to 16.74 (See Table 7.4). Measured experimental values in Table 8.7 are greater than both calculated and literature values, excepting LOI for

Table 8.7 Weight loss on ignition (L), and by thermal gravimetric analysis before (H) and after(T) sulfate sorption, and resulting OH/nm^2.

	% loss on ignition	* OH/nm^2	% loss before sorpn	OH/nm^2	% loss after sorpn
SG	15.34	16.4	14.3	15.3	14.4
SH	0.85	4.8	3.5	19.7	6.9
NH	6.62	35.6	5.5	29.6	6.5

*Approximate calculation using total % lost, for comparison only.

synthetic hematite data. The TGA and LOI values for natural hematite are twice that of synthetic goethite. TGA natural hematite surface coverage is 50% more than synthetic hematite.

C. Exchange Capacity

Table 8.8 summarizes exchange capacity data with respect to hydroxyl surface coverage and sorption efficiency. Note that synthetic hematite hydroxyl surface coverage determined by exchange capacity methods is not in as close an agreement with the TGA and LOI data discussed above as are the other oxide samples. Exchange capacity data for synthetic hematite lie between TGA and LOI values. Why synthetic hematite data vary so widely is uncertain.

Synthetic hematite has the lowest hydroxyl surface coverage, sorbs the most sulfate of the oxide samples studied and exhibits a high efficiency (hydroxyl released on sorption vs maximum available for release). Goethite has a moderate surface coverage, sorbs a medium amount of

Table 8.8 Exchange capacity and efficiency. (OH released on sorption (C) / max exchange capacity (E) = X)

	OH/nm^2	μmol OH/g	Efficiency (%) pH 3	pH 5
Synthetic Goethite	18.0	1316	11.2	7.1
Synthetic Hematite	10.2	733.5	21.1	17.1
Natural Hematite	24.8	498.5	21.3	-

sulfate and shows lower hydroxyl release efficiency. At pH 3, natural hematite has the highest surface coverage and sorbs the smallest amount of sulfate. It shows an efficiency higher than goethite, but similar to synthetic hematite.

D. Summary

All oxide samples examined sorb sulfate. Sorption increases with sulfate concentration. All the oxides, except synthetic hematite, reach a sorption maximum. Sorption increases with decreasing pH. Under optimum pH and [SO4] conditions, approximately half of the mineral surface will be covered by sulfate ions. The sulfate ion is sorbed irreversibly. Only a fraction of the sulfate can be desorbed, an amount which increases as pH is raised. Thermal analysis indicates the sulfate to be strongly bonded. The presence of four infrared bands indicates direct coordination of the sulfate anion with the iron cation on the oxide surface.

Sulfate is specifically adsorbed by ligand exchange. No evidence was found to support surface precipitation of iron hydroxysulfate minerals as a sulfate sorption mechanism. Sorption characteristics change with pH as different surface sites (OH and OH_2^+) become available to interact with sulfate. It appears that the sorption mechanism shifts from a mono to a multi-ligand exchange as pH increases. Synthetic hematite sorbs the greatest amount

of sulfate per gram of oxide followed by synthetic goethite then natural hematite.

III. SORPTION BEHAVIOR MODELS

The iron oxide and hydroxide minerals prepared in this study were positively identified using X-ray diffraction, Mossbauer spectroscopy and scanning electron microscopy. Mineral surfaces were characterized using surface area, zero point of charge measurements, infrared spectroscopy and thermal analysis. Neutron activation analysis and X-ray fluorescence were used to look for impurities. The structure of the iron oxides can be pictured at the pH_{zpc} as shown in Figure 8.1. Under experimental conditions of pH 3 and constant ionic strength, the structure illustrated in Figure 8.2 will form.

Figure 8.1 Schematic illustrating the internal structure of iron oxides at the pH_{zpc}.

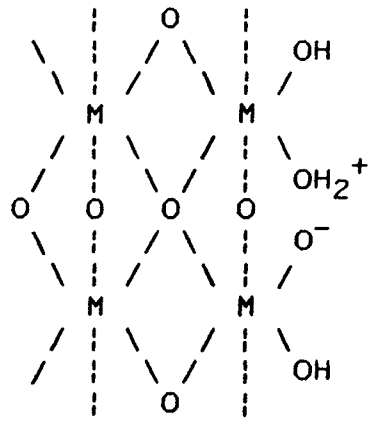

Where M = Fe^{3+}

Figure 8.2 Schematic of oxide surface under the system conditions pH = 3 and constant ionic strength.

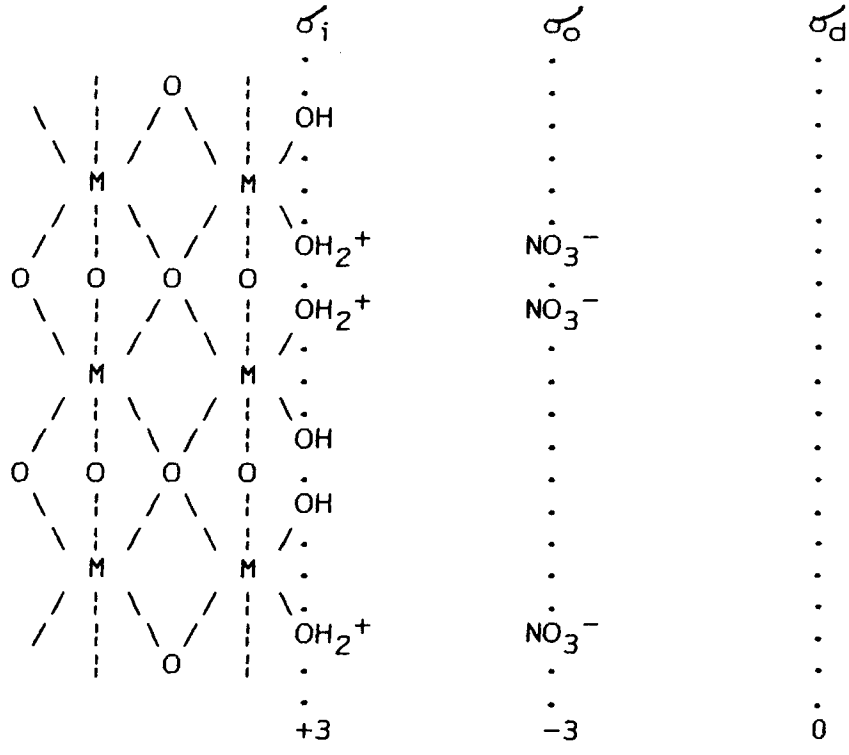

σ_i, σ_o and σ_d are the charge of the inner, outer, and diffuse planes respectively.

The oxide surface exhibits positively charged groups ($-OH_2^+$), negatively charged groups ($-O^-$) and neutral groups (-OH). At pH_{zpc}, positive and negative charges cancel each other out so that the net surface charge equals zero. That is, the surface acts as if it were completely covered by neutral OH groups.

Surface hydroxyls are of three types, which give rise to different types of reactivity. Triply and doubly bonded hydroxyls are held strongly, thus are not likely to be very reactive. Singly bonded hydroxyl groups (A-type)

are held the least strongly, therefore are likely to be the most reactive. Infrared spectroscopy has uncovered evidence in support of this idea for both phosphate and sulfate sorption onto oxide surfaces (Parfitt and Atkinson 1976, Parfitt et al. 1975, 1976, Parfitt and Russell 1977, Parfitt and Smart 1977, 1978).

Studies in the literature give the reaction series HPO_3^- >> $SO_4^=$ $\geq$ NO_3^- ~ Cl^- for anion sorption in soils (Harward and Reisenauer 1966). According to this series, sulfate is expected to react with the iron oxide surface much in the same way that nitrate and chloride do. That is, by forming outersphere complexes through electrostatic attraction. If this is true, the results of experiments performed in this study should be predictable as follows:

a) the reaction should be instantaneous,

b) there should be no pH change during the reaction as no hydroxyl ions should be released to solution (no ligand exchange),

c) there should be no changes in XRD, IR or Mossbauer spectra (no structural changes),

d) there should be no morphological changes visible by SEM,

e) there should be no changes in thermal analysis (DTA/TGA) spectra,

f) there should be a decrease in sorption per unit surface area with increasing pH due to change in

surface charge (and thus +ve sites) with pH,

g) the reaction should be totally reversible,

h) there should be no sorption maxima.

i) the ratio of hydroxyl released to sulfate sorbed (R) should be zero (no ligand exchange).

Figure 4.5 illustrates the possible electrostatic reactions for the above oxide surface model.

Experimental results obtained in this study do not agree with the above "expected" results for outer sphere electrostatic attraction as the mechanism for sulfate sorption. Observations in this study are:

a) sorption is initiated by a rapid reaction which is followed by a longer slow reaction which takes 24 hours to reach apparent equilibrium,

b) pH increases on sorption as some OH^- is released or H^+ consumed on reaction,

c) there are no changes in XRD or Mossbauer spectra, but IR spectra show that some, not all, A-type hydroxyls are replaced on sorption and the sulfate ion symmetry indicates direct coordination with the surface metal cations,

d) no morphological differences are seen in SEM images after the sorption reaction,

e) occurrence of exothermic peaks at temperatures higher than those required for electrostatic attraction after reaction with sulfate indicate

breaking of strong bonds holding sulfate,

f) sorption per unit area decreases with increasing pH due to decreasing number of reaction sites and decreasing surface charge,

g) sorption is only partly reversible, desorption increases with pH of desorbing solution,

h) sorption maxima are observed for each oxide sample studied under specific pH conditions.

i) The ratio of hydroxyl released to sulfate sorbed (R) ranges from 0 to 2, depending on specific conditions.

The above observations suggest something other than nonspecific electrostatic attraction is contributing to the overall behavior of sulfate during sorption. Precipitation of an iron hydroxy sulfate mineral is one possibility as supersaturation conditions for jarosite exist, but no evidence for formation of a precipitant was found. Another possibility is inner sphere specific sorption through ligand exchange. Figure 4.6 illustrates the possible ligand exchange reactions for sulfate on the above oxide surface model. Figure 8.3 illustrates the results of nonspecific and specific sulfate sorption on the surface sites discussed in Figure 8.2.

Although some observations are consistent with nonspecific sorption, others agree better with specific sorption as the sorption mechanism. Thus, it is suggested

Figure 8.3 Schematic illustrating sulfate sorption onto surface sites described in Figure 8.2.

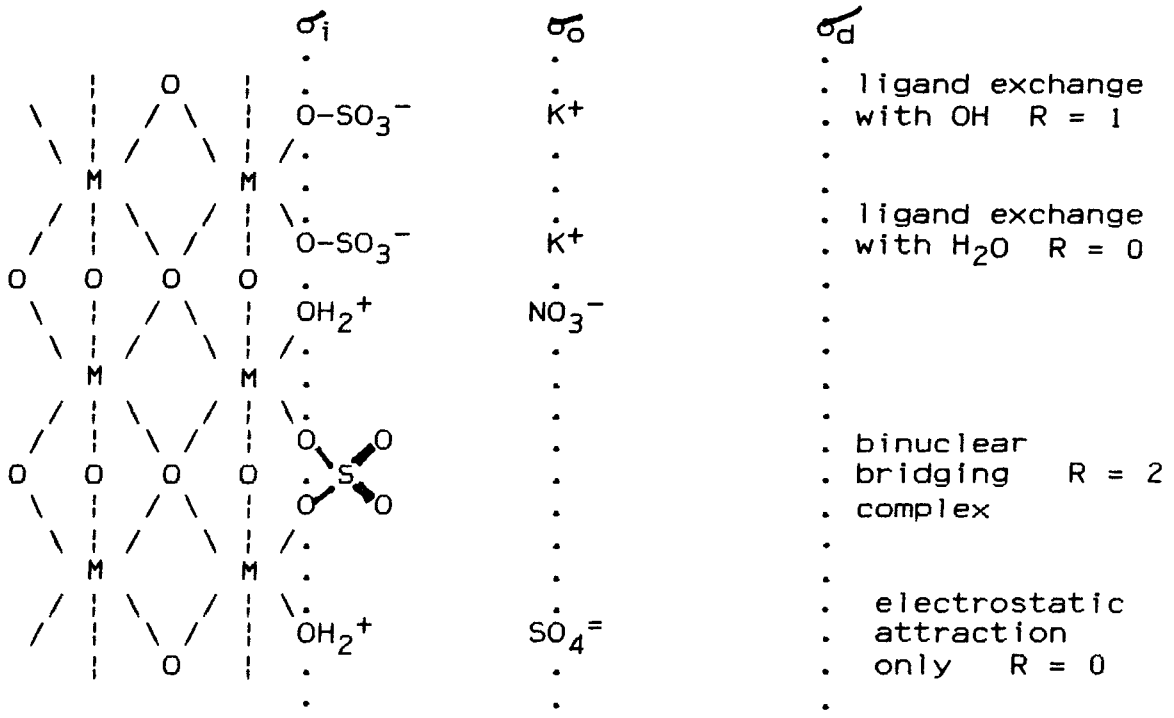

that sulfate sorption on the iron oxide minerals prepared in this study is a combination of the two mechanisms, electrostatic and mono and multi-ligand exchange, which act under different system conditions to form the basis of sulfate sorption behavior.

CHAPTER 9 ENVIRONMENTAL IMPLICATIONS

In the natural environment, soil is a complex mixture of minerals (silicates, oxides and hydroxides), organic matter, liquid (soil solution) and gas. Each phase interacts with the others to help formulate the behavior of the soil complex as a whole. One can get a rough idea of how soil behaves by examining an individual soil phase under set conditions, then combinations of phases. Comparing experimental results with true soil behavior allows formulation of soil behavioral models.

In this study, sorption behavior for three oxide samples is examined. Data can be used to give rough calculations of how soils containing oxides may behave when subject to sulfate inputs.

A. Sulfate Sorption Capacity of Soils:

A simple calculation can be carried out to determine the soil sorption capacity for sulfate by comparing the atmospheric deposition of sulfate to soil sorption.

a) atmospheric deposition:

Lerman (1979) reports the average rainfall on 1 cm^2 of surface to be 86 cm^3/yr (ml/yr). The average concentration of sulfate in rainfall over the Northeastern

United States is 30 μmol/l (Likens 1976). Thus, approximately 2.58 μmol SO_4/yr (86 ml/yr × 0.030 μmol SO_4/ml) falls on 1 cm^2 of soil surface.

b) iron oxide content of soils:

Consider two soils, one with a fairly high content of free iron oxides, the other with a lower amount. For example:

Type	Location	Average % Free Fe_2O_3	Avg. pH
Brown podzolic soil	Falcon, Manitoba	20	5.4
Dark brown/black soil	Waskada, Manitoba	3	7.5

Reference: Ehrlich et al. 1955

In these cases free extractable iron oxides refers to the total soil iron occurring as hydrous oxides and uncombined with layer structures (Buol et al. 1980).

The bulk density of most soils falls in the range <1 to 2 g/cm^3 (Carmichael 1982). If average bulk density of soil is assumed to be that of sandy loam, 1.4 g/cm^3 dry soil weight (Carmichael 1982), then the above soils contain 0.28 and 0.042 g/cm^3 free iron oxides.

c) time required to load soils:

Knowing the average yearly sulfate input through rainfall (section a) (Note: the present calculated value is actully higher than Manitoba receives), the amount of iron oxide in the soil (section b) and the iron oxides sorption capacity (present experimental results), the time required

Table 9.1 Estimated time, in years, required to saturate Manitoba soils with sulfate.

Mineral	pH	Time required to saturate $1cm^3$ Falcon soil	Waskada soil
s-goethite	3	16.39	2.46
	5	7.91	1.19
	7	0.34	0.63
s-hematite	7	1.91	0.29
	5,3	more	more
n-hematite	3	4.88	0.73
	5,7	less	less

to load the iron oxide surfaces of the above example soils is calculated and summarized in Table 9.1.

It is important to note that the results tabulated in Table 9.1 are dependent on the following assumptions:

1. all the free iron oxide is of one type (i.e. in the present calculation, goethite).
2. no sorbed sulfate is desorbed throughout the loading process.
3. system pH is set at 3, 5 or 7.
4. no other soil constituents are pertinent to the sorptive properties of the soil, either positively or negatively.
5. no other system ions are important.
6. soil is a uniform system of components.

Of course all of the above assumptions do not apply to real

world situations:

1. Soil iron oxides are of many types with the percentage of each being dependent on other soil properties (soil type, parent material, age and pH).

2. Soils do not hold all the sulfate permanently. Of that sulfate sorbed, a certain amount is desorbable, an amount which increases with pH of desorption. The sorbed ion may be desorbed through washings with rainfall of lower sulfate concentrations or higher pH, or by replacement by stronger binding ions such as phosphate. Thus in reality, it will take longer to reach the maximum sorption capacity of a soil, if it is ever reached, due to possible repeated 'washing out' of sulfate. In other words, desorption can constantly be occurring causing the sorption maxima to never be reached.

3. The average pH of rainfall in the eastern U.S.A. is 4.13 (Likens, 1976). The soil pH, listed in Table 9.1, also differ from the assumed system pH. The combination of rainfall and soil solution pH will affect the sorption reaction strongly.

4. Anion sorption occurs on several types of oxides (iron and aluminum) as well as on some clay surfaces. In addition, organic materials tend to inhibit the sorption of sulfate by blocking sorption sites.

5. There are many ions in soil solutions, of which phosphate is a much stronger binder then sulfate. Phosphate

oxyanions will block some of the surface sites and may replace sulfate on other sites.

6. Soil is not a uniform mixture of components, but is fairly structured. Different soil types exhibit characteristic profiles. Components in different parts of the profile (horizons) come in varying forms and concentrations. For example, spodosols have an oxide rich horizon and an organic rich horizon. Although the oxide rich horizon should have a high sulfate sorption capacity, there will be interference from the organic rich horizon.

In summary, the calculation of soil sulfate sorption capacity gives only an approximate figure of true sorption capacity and must be interpreted as such. In reality, many factors such as those discussed above, influence the sorption capacity. In environmental studies of catchment basins and related work, many of these factors are dealt with and included in complex models to more closely simulate the natural environment.

B. Relevance to Watershed Acidification Models:

Several models which simulate watershed response to changing inputs of acidic deposition have been used to study watershed recovery processes. One model, the Direct Delayed Response Program Model (DDRP) describes the dynamic response of surface water chemistry as a function of rates of acidic

deposition and a few key soil processes. In particular, it uses soil sulfate adsorption as the controlling factor of long term sulfate dynamics (Galloway et al. 1983, Cosby et al. 1986, Hornberger et al. 1986).

The DDRP model uses a Langmuir type expression to describe the sulfate sorption as a nonlinear function of the equilibrium sulfate concentration in soil solution. It is based on a lumped parameter formulation of hydrological and chemical characteristics and assumes constant soil/soil water contact. Inherent in the model is the assumption of reversibility of sulfate adsorption; equilibrium adsorption and desorption.

The concept behind this model is that if the rate of acid deposition changes in aquatic and terrestrial systems, a variety of constituents will respond, namely sulfate, base cations and alkalinity. This response is not necessarily instantaneous. If the terrestrial system can act as a sink through sulfate adsorption, a time lag will delay the attainment of a new steady state (i.e. direct-delayed response). The response time required is a function of the hydrologic retention time and the amount of sulfate adsorbed by the soil. Soils with small sulfate sorption capacity will respond in a time near to the hydrologic response time (months to years), soils with large sulfate sorption capacity will respond more slowly (decades). When sulfate deposition is reduced through emission controls, recovery is

again delayed by a time lag controlled by hydrologic retention time and sulfate desorption.

The results of the present work have significant implications for the above model and all modelling studies of environmental systems containing soils. This work has shown sulfate sorption to be for the most part irreversible, with desorption only occurring under certain specific conditions.

A soil with a measurable amount of sulfate sorption capacity will follow the DDRP model when amounts of acidic deposition are increased. That is, the (new excess) incoming sulfate will adsorb onto the soil oxides delaying the equilibration of the surface water chemistry with the new system conditions of increased sulfate concentration until the sorption capacity is reached. After reaching sorption capacity, hydrologic retention will determine the remaining time to equilibrium. However, because of the irreversibility of sulfate sorption, the system will not react as predicted by the DDRP model when acidic deposition is decreased.

A neutral or alkaline soil is not likely to adsorb a large amount of sulfate. An acidic soil, on the other hand, will adsorb a larger amount of sulfate and has the best chance of desorbing some of that sulfate. Present data indicate that the amount desorbed will be small if the pH remains low and will only increase if the pH is raised.

Thus, if a small amount of adsorbed sulfate is desorbed, there will be a time lag greater than that of hydrologic response time before equilibrium is again reached. However, if no sulfate is desorbed, as is the case with neutral to alkaline soils, equilibrium will be established according to hydrologic response time alone.

C. Other Aspects

Due to evidence uncovered by this study, it is now known that a certain amount of sorbed sulfate will be permanently bonded to soil iron oxide particles. It is of interest to speculate on the long term role of this sulfate in soil systems.

Investigations into the coordination chemistry of mineral weathering have recently led to the proposal of several pathways for the dissolution of oxide minerals (Furrer and Stumm 1986, Zinder et al. 1986). One is a ligand-promoted dissolution reaction in which ligands exchange with surface hydroxyl groups forming surface complexes which polarize critical iron-oxygen bonds thus facilitating the detachment of surface metal species. The dissolution of reducible oxide minerals, like iron(III) oxides and hydroxides, is facilitated under reducing conditions because the Fe(II)-O bond is more labile than the Fe(III)-O bond. Ligands capable of forming multidentate

complexes are thought to be most effective in this reaction. Since the sulfate anion forms bidentate complexes on iron oxide surfaces, as evidenced by infrared spectra, it is possible that sulfate is involved in the (reductive) dissolution of iron oxide minerals in soil weathering processes.

Another hypothesis, as to the long term role of sulfate in soil systems, deals with the formation of basic ferric sulfate minerals. Although no evidence was found in this study for the precipitation of the iron hydroxy sulfate mineral jarosite, it is possible that in natural soil systems basic ferric sulfates, such as jarosite, could precipitate on oxide surfaces with the aid of microbes such as Thiobacillus ferrooxidans. In acid sulfate soils containing these bacteria, basic ferric sulfates are common (Ross et al. 1982).

REFERENCES

Adams, F. and Z. Rawajfih 1977. Basaluminite and aluminite: a possible cause of sulfate retention by acid soils. Soil Science Society of America, Journal 41:86-692

Ahmed, S.M. and D. Maksimov 1968. Studies of the oxide surface at liquid-solid interfaces. (II) Iron oxides. Canadian Journal of Chemistry 46:3841-3846

Albrethson, A.E. 1963. An electrochemical study of the ferric oxide - solution interface. Ph.D. Thesis. Massachusetts Institute of Technology, Cambridge, Massachusetts.

Amarasirwardena, D.D., E. De Grave, L.H. Bowen and S.B. Weed 1986. Quantitative determination of aluminum substituted Goethite - Hematite mixtures by Mossbauer spectroscopy. Clays and Clay Minerals 34:250-256

Atkinson, R.J., A.M. Posner and J.P. Quirk 1967. Adsorption of potential determining ions at the ferric-oxide aqueous electrolyte interface. Journal of Physical Chemistry 71:550-558

Atkinson, R.J., A.M. Posner and J.P. Quirk 1968. Crystal nucleation in Fe(III) solutions and hydroxide gels. Journal of Inorganic Nuclear Chemistry 30:2371-2381

Atkinson, R.J., A.M. Posner and J.P. Quirk 1972. Kinetics of heterogeneous isotopic exchange reactions. Exchange of phosphate at the α-FeOOH aqueous solution interface. Journal of Inorganic and Nuclear Chemistry 34:2201-2211

Atkinson, R.J., R.L. Parfitt and R.C. Smart 1974. Infrared study of phosphate adsorption on goethite. Journal of the Chemical Society, Faraday Transactions I 70:1472-1479

Aylmore, L.A., G.M. Karim and J.P. Quirk 1967. Adsorption and desorption of sulfate ions from soil constituents. Soil Science 103:10-15

Balistreiri, L.S. and J.W. Murray 1981. The surface chemistry of Goethite (α-FeOOH) in major ion seawater. American Journal of Science 281:788-806

Barrow, N.J., C.J. Asher and P.G. Ozanne 1967. Nutrient potential and Capacity. III. Minimum value of potassium potential for availability to Trifolium subterraneum in soil and solution culture. Australian Journal of Agricultural Research 18:55-62

Barrow, N.J. 1967. Sulfur and developing agriculture in Western Australia. Sulfur Institute Journal 3:2-5.

Barrow, N.J. 1967. Studies on extraction and on availability to plants of adsorbed plus soluble sulfate. Soil Science 104:242-249

Barrow, N.J. 1967. Studies on the adsorption of sulfate by soils. Soil Science 104:342-349

Barrow, N.J. 1969. Effects of adsorption of sulfate by soils on the amount of sulfate present and its availability to plants. Soil Science 108:193-201

Barrow, N.J., K. Spencer and W.M. McArthur 1969. Effects of rainfall and parent material on the ability of soils to adsorb sulfate. Soil Science 108:120-126

Barrow, N.J. 1972. Influence of solution concentration of calcium on the adsorption of phosphate, sulfate, and molybdate by soils. Soil Science 113:175-180.

Barrow, N.J. and T.C. Shaw 1977. On the slow reaction between soil and anions. Effects of time and temperature of contact between an adsorbing soil and sulfate. Soil Science 124:347-354

Bleam, W.F., and M.B. McBride 1985. Cluster formation versus isolated site adsorption. A study of Mn (II) and Mg (II) adsorption on boehmite and goethite. Journal of Colloid and Interface Science 103:124-132

Boehm, H.P. 1971. Acidic and basic properties of hydroxylated metal oxide surfaces. Discussions of the Faraday Society 52:264-275

Bolland, M.D.A., A.M. Posner and J.P. Quirk 1976. Surface charge on kaolinites in aqueous suspension. Australian Journal of Soil Research 14:197-216.

Borggaard, O.K. 1982. The influence of iron oxides on the surface area of soil. Journal of Soil Science 33:433-450

Borggaard, O.K. 1983. Extraction of amorphous Fe oxides by E.D.T.A. from a mixture of Akaganeite (β-FeOOH) and amorphous Fe oxides. Acta Chemica Scandinavica 37A:169-171

Borggaard, O.K. 1983. Effect of surface area and mineralogy of iron oxides on their surface charge and anion-adsorption properties. Clays and Clay Minerals 31:230-232

Bornemisza, E. and R. Llanos 1967. Sulfate movement, adsorption, and desorption in three Costa Rican soils. Soil Science Society of America, Proceedings 31:356-360

Bowen, L.H. and S.B. Weed 1981. Mossbauer spectroscopic analysis of iron oxides in soil IN Advances in Chemistry Series 194:247-261

Bowen, L.H. and S.B. Weed 1984. Mossbauer spectroscopy of soil and sediments. IN Chemical Mossbauer Spectroscopy. Ed. R.H. Herber, Plenium Press N.Y.

Bowden, J.W., M.D.A. Bolland, A.M. Posner and J.P. Quirk 1973. A general model for anion and cation adsorption at oxide surfaces. Nature of Physical Science (London) 245:81-82

Breuwsma, A. and J. Lyklema 1971. Interfacial electrochemistry of Hematite (α-FeOOH). Discussions of the Faraday Society 52:324-333

Breuwsma, A. 1973. Adsorption of ions on Hematite (α-Fe2O3). A colloid - chemical study. Ph.D. Thesis. Agricultural University, Wageningen, Netherlands.

Breuwsma, A. and J. Lyklema 1973. Physical and chemical adsorption of ions in the electrical double layer on hematite (α-Fe2O3). Journal of Colloid and Interface Science 43:437-338

Breuwsma, A. 1973. Adsorption of ions on hematite (α-Fe2O3). Med. Landbowhogeschool. Wageningen 73-1. 124pp.

Brunauer, S., P.H. Emmett and E. Teller 1938. Adsorption of gases in multimolecular layers. Journal of the American Chemical Society 60:309-319

Buol, S.W., F.D. Hole and R.J. McCracken 1980. Soil Genesis and Classification. Second edition. Iowa State University Press, Ames, Iowa.

Cabrera, F., L. Madrid and P. De Arambarri 1977. Adsorption of phosphate by various oxides: Theoretical treatment of the adsorption envelope. Journal of Soil Science 28:30-313

Cabrera, F., P. De Arambarri, L. Madrid and G.G. Toca 1981. Desorption of phosphate from iron oxides in relation to equilibrium pH and porosity. Geoderma 26:203-21

Caillere, S. and S. Henin 1954. Sur quelques mineraux du djebel debar. Bulletin de la Societe Francaise de Mineralogie et de Cristallographie 77:479-490

Cambier, P. 1986. Infrared study of goethite of varying crystallinity and particle size: I. Interpretation of OH and lattice vibration frequencies. Clay Minerals 21:191-200

Cambier, P. 1986. Infrared study fo goethite of varying crystallinity and particle size: II. Crystallographic and morphological changes in a series of synthetic goethites. Clay Minerals 21:201-210

Carmichael, R.S. 1982. CRC Handbook of Physical Properties of Rocks. Volume III. CRC Press.

Chang, M.L. and G.W.Thomas 1963. A suggested mechanism for sulfate adsorption by soils. Soil Science Society of America, Proceedings 27:281-283

Chao, T.T., M.E. Harward and S.C. Fang 1962. Soil constituents and properties in the adsorption of sulfate ions. Soil Science 94:276-283

Chao, T.T., M.E. Harward and S.C. Fang 1962. Movement of S^{35} tagged sulfate through soil columns. Soil Science Society of America, Proceedings 26:27-32

Chao, T.T., M.E. Harward and S.C. Fang 1962. Adsorption and desorption phenomena of sulfate ions in soil. Soil Science Society of America, Proceedings 26:234-237

Cole, D.W. and D.W. Johnson 1977. Atmospheric sulfate additions and cation leaching in a Douglas fir ecosystem. Water Resources Research 13:313-317

Conesa, A.P., J.C. Fardeau and G. Simon-Sylvestre 1982. Phosphorus and Sulfur. IN Constituents and Properties of Soil. Eds. M. Bonneau and B. Souchier. Academic Press.

Cosby, B.J., G.M. Hornberger J.N. Galloway 1985. Modelling the effects of acid deposition: Assessment of a lumped parameter model of soil water and stream water chemistry. Water Resources Research 21:51-63

Cosby, B.J., R.F. Wright, G.M. Hornberger and J.N. Galloway 1985. Modelling the effects of acid deposition: Estimation of long-term water quality responses in a small forested catchment. Water Resources Research 21:1591-1601

Cosby, B.J., G.M. Hornberger, R.F. Wright and J.N. Galloway 1986. Modelling the effects of Acid deposition: Control of long-term sulfate dynamics by soil sulfate adsorption. Water Resources Research 22:1283-1291

Couto, W., D.J. Lathwell and D.R. Bouldin 1979. Sulfate adsorption by two oxisols and an alfisol of the tropics. Soil Science 127:108-116

Deer, W.A., R.A. Howie and J. Zussman 1966. Rock Forming Minerals. Wiley Interscience, New York.

Derie, R., M. Ghodsi and C. Calvo-Roche 1976. DTA study of the dehydration of synthetic goethite (α-FeOOH). Journal of Thermal Analysis 9:435-440

Ehrlich, W.A., H.M. Rice and J.H. Ellis 1955. Influence of the composition of parent material on soil formation in Manitoba. Canadian Journal of Agricultural Science 35:407-421

Ensminger, L.E. 1954. Some factors affecting the adsorption of sulfate by Alabama soils. Soil Science Society of America, Proceedings 18:259-264

Eriksson, E. 1955. Airborne salts and the chemical composition of river waters. Tellus 7:243-250

Eriksson, E. 1960. The yearly circulation of chloride and sulfur in nature meteorological, geochemical, and pedological implications - Part 1. Tellus 11:375-403

Eriksson, E. 1960. The yearly circulation of chloride and sulfur in nature meteorological, geochemical, and pedological implications - Part 2. Tellus 12:63-109

Evans, T.D., J.R. Leal and P.W. Arnold 1979. Interfacial electrical chemistry of goethite and especially the effect of CO_2 contamination. Journal of Electroanalytical Chemistry and Interfacial Electrical Chemistry 105:161-167

Fang, S.C., R.D. Nauca, T.T. Chao and M.E. Harward 1962. A chromatographic approach to the determination of sulfate adsorption and exchange of less retentive soils. Soil Science 94:14-18

Feller, M.C. and J.P. Kimmins 1979. Chemical characteristics of small streams near Haney in southwestern British Columbia. Water Resources Research 15:247-258

Fischer, W.R. and U. Schwertman 1975. The formation of hematite from amorphous iron (III) hydroxide. Clays and Clay Minerals 23:33-37

Fitzgerald, J.W. 1978. Naturally occurring organosulfur compounds in soils. IN Sulfur in the Environment, Part II. Ecological Impacts. Ed. J.O. Nriagu. John Wiley and Sons, New York. p. 391-444

Fitzpatrick, R.W. and U. Schwertman 1982. Al-substituted goethites - an indication of pedogenic and other weathering environments in South Africa. Geoderma 27:335-347

Forbes, E.A., A.M. Posner and J.P. Quirk 1974. The specific adsorption of inorganic Hg (II) species and Co (II) complex ions on goethite. Journal of Colloid and Interface Science 49:403-409

Furrer, G. and W. Stumm 1986. The coordination chemistry of weathering. I. Dissolution kinetics of -Al2O3 and BeO. Geochimica et Cosmochimica Acta 50:1847-1860

Galloway, J.N., S.A. Norton and M.R. Church 1983. Freshwateracidification from atmospheric deposition of sulfuric acid: A conceptual approach. Environmental Science and Technology 17:541A-545A

Garrels, R.M. and C.L. Christ 1965. Solutions, Minerals, and Equilibria. Harper and Row, 450 p.

Gast, R.C., E.R. Landa and G.W. Meyer 1974. The interaction of water with goethite (α-FeOOH) and amorphous hydrated ferric oxide surfaces. Clays and Clay Minerals 22:31-39

Gebhardt, H. and N.T. Coleman 1974. Anion adsorption by allophanic tropical soils: (I) Chloride adsorption. Soil Science Society of America, Proceedings 38:255-259

Gebhardt, H. and N.T. Coleman 1974. Anion adsorption by allophanic tropical soils: (II) Sulfate adsorption. Soil Science Society of America, Proceedings 38:259-262

Gebhardt, H. and N.T. Coleman 1974. Anion adsorption by allophanic tropical soils: (III) Phosphate adsorption. Soil Science Society of America, Proceedings 38:263-266

Goldberg, E.D. 1963. Chemistry - the oceans as a chemical system. IN The Sea Vol. 2: Composition of Seawater, Comparative and Descriptive Oceanography. Ed. M.N. Hill. Interscience Publishers, New York. p 3-25

Goodman, B.A. 1980. MossbauerSpectroscopy. IN Advanced Chemical Methods for Soil and Clay Minerals Research. Eds. J.W. Stucki and W.L. Banwart. D. Reidel, Dordrecht, 1-92

Goodman, B.A. and D.G. Lewis 1981. Mossbauer Spectroscopy of aluminous goethites (α-FeOOH). Soil Science 32:351-364

Harrison, J.B. and V.E. Berkheiser 1982. Anion interactions with freshly prepared hydrous iron oxides. Clays and Clay Minerals 30:97-102

Haque, I. and D. Walmsley 1973. Adsorption and desorption of sulfate in some soils of the West Indies. Geoderma 9:269-278

Harward, M.E. and H.M. Reisenauer 1966. Reactions and movements of inorganic sulfur. Soil Science 101:326-335

Hasan, S.M., R.L. Fox and C.C. Boyd 1970. Solubility and availability of sorbed sulfate in Hawaiian soils. Soil Science Society of America, Proceedings 34:897-901

Hazel, F. and G.H. Ayres 1931. Migration studies with ferric oxide sols. I. Positive sols. Journal of Physical Chemistry 35:2930-2942

Heinrichs, H. and R. Mayer 1977. Distribution and cycling of major and trace elements in two central European forest ecosystems. Journal of Environmental Quality 6:402-407

Hem, J.D. 1960. Some chemical species relationships among sulfur species and dissolved ferrous iron. United States Geological Survey Water Supply Paper 1459-C

Hem, J.D. 1970. Study and interpretation of the chemical characteristics of natural water. Geological Survey Water Supply Paper 1473, 2nd edition.

Hingston, F.J., A.J. Atkinson, A.M. Posner and J.P. Quirk 1967. Specific adsorption of anions. Nature 215:1459-1461

Hingston, F.J., A.J. Atkinson, A.M. Posner and J.P. Quirk 1968. Specific adsorption of anions on goethite. International Congress on Soil Science, 9th Transactions (Adelaide Australia) 1:669-678

Hingston, F.J., A.M. Posner and J.P. Quirk 1972. Anion adsorption by goethite and gibbsite.(I) The role of the proton in determining adsorption envelopes. Journal of Soil Science 23:177-192

Hingston, F.J., A.M. Posner and J.P. Quirk 1974. Anion adsorption by goethite and gibbsite. (II) Desorption of anions from hydrous oxidesurfaces. Journal of Soil Science 25:16-26

Horn, M.K. and J.A.S. Adams 1966. Computer - derived geochemical balances and element abundances. Geochimica et Cosmochimica Acta 30:279-297

Hornberger, G.M., B.J. Cosby and J.N. Galloway 1986. Modelling the effects of acidic deposition: uncertainty and spatial variability in estimation of long term sulfate dynamics in a region. Water Resources Research 22:1293-1302

Ivarson, K.C. 1982. Microbiological transformations of iron and sulfur and their applications to acid sulfate soils and tidal marshes. IN Acid Sulfate Weathering. Soil Science Society of America Spec. Publn. 10. Madison, Wisconsin

Ivarson, K. C. 1986. Private Communication.

Johnson, D.W. and G.S. Henderson 1979. Sulfate adsorption and sulfur fractions in a highly weathered soil under a mixed deciduous forest. Soil Science 128:34-40

Johnson, D.W., D.W. Brewer and D.W. Cole 1979. The influence of anion mobility on ionic retention in wastewater - irrigated soils. Journal of Environmental Quality 8:246-250

Johnson, D.W., D.W. Cole and S.P. Gessel 1979. Acid precipitation and soil sulfate adsorption properties in a tropical and temperate forest soil. Biotropica 11:38-42

Johnson, D.W. and D.W. Cole 1980. Anion mobility in soils: relevance to nutrient transport from forest ecosystems. Environment International 3:79-90

Joint Committee on Powder Diffraction Standards (JCPDS) 1974. Selected powder diffraction data for minerals. Swarthmore, Pennsylvania

Jurinak, J.J. 1964. Interaction of water with Fe and Ti oxide surfaces: goethite, hematite and anatase. Journal of Colloid and Interface Science 19:477-487

Jurinak, J.J. 1966. Surface chemistry of hematite: anion penetration effect on water adsorption. Soil Science Society of America, Proceedings 30:559-562

Kamprath, E.J., W.L. Nelson and J.W. Fitts 1956. The effect of pH, sulfate,and phosphate concentration on the adsorption of sulfate by soils. Soil Science Society of America, Proceedings 20:463-466

Kerr, P.F. and J.L. Kulp 1948. Multiple differential thermal analysis. American Mineralogist 33:387-419

Kulp, J.L. and H.H. Adler 1950. Thermal study of jarosite. American Journal of Science 248:475-487

Landa, E.R. and R.G. Gast 1974. Mineralogical characterization and adsorptive properties of amorphous and crystalline hydrated ferric oxides. Tr. Mezhdunar. Kongr. Pochvoved 10th 7:132-8

Langmuir, D. 1964. Stability of carbonates in the system $CaO-MgO-CO_2-H_2O$: Unpublished Ph.D. dissertation, Harvard University, 142 p.

Langmuir, D. 1971. Particle size effect on the reaction Goethite = Hematite + Water. American Journal of Science 271:147-156

Langmuir, D. and D.O. Whittemore 1971. Variations in the stability of precipitated ferric oxyhydroxides. IN Advances in Chemistry Series, Nonequilibrium systems in natural water chemistry 106:209-234. American Chemical Society, Washington, D.C.

Lerman, A. 1979. Geochemical Processes in Water and Sedimentary Environments. John Wiley and Sons.

Likens, G.E., F.H. Bormann, R.S. Pierce, J.S. Eaton and N.M. Johnson 1977. Biogeochemistry of a Forested Ecosystem. Springer-Verlag, Berlin - New York

Likens, G.E. 1976. Acid precipitation. Chemical and Engineering News November 22:29-44

Liu, M. and G.W. Thomas 1961. The nature of sulfate retention by acid soils. Nature 192:384

Lowe, L.E. and W.A. Delong 1961. Aspects of the sulfur status of three Quebec soils. Canadian Journal of Soil Science 41:141-146

Lumsdon, D.G., A.R. Fraser, J.D. Russell and N.T. Livesey 1984. New infrared band assignments for the arsenate ion adsorbed on synthetic goethite (α-FeOOH). Journal of Soil Science 35:381-386

MacIntre, W.H., W.M. Shaw and B. Robinson 1941. Influence of limestone and dolomite upon sulfate retention from annual additions of potassium sulphate. Soil Science 51:73-84

MacIntre, W.H., W.M. Shaw and B. Robinson 1952. Nitrogen recoveries from applications of ammonium chloride, phosphate, and sulfate and outgo of complimentary ions in rainwater leachings through a six-foot soil-subsoil column. Soil Science Society of America, Proceedings 16:301-306

Mackenzie, R.C., E. Paterson and R. Swaffield 1981. Observation of surface characteristics by DSC and DTA. Journal of Thermal Analysis 22:269-274

Madrid, L.E. and P. De Arambarri 1978. Adsorption isotherms and hysteresis of H+ adsorption by goethite. Geoderma 21:199-208

Madrid, L.E., and A.M. Posner 1979. Desorption of phosphate from goethite. Journal of Soil Science 30:697-707

Madrid, L., E. Diaz, F. Cabrera and P. De Arambarri 1983. Use of a three-plane model to describe charge properties of some Fe oxides and soil clays. Journal of Soil Science 34:57-67

Madrid, L., E. Diaz and F. Cabrera 1984. Charge properties of mixtures of minerals with variable and constant surface charge. Journal of Soil Science 35:373-380

Martin, C.W. 1979. Precipitation and streamwater chemistry in an undisturbed forested watershed in New Hampshire. Ecology 60:36-42

McCafferty, E. and A.C. Zettlemoyer 1970. Entropy of adsorption and the mobility of water vapor on α-Fe_2O_3. Journal of Colloid and Interface Science 34:452-460

McCafferty, E. and A.C. Zettlemoyer 1971. Adsorption of water vapor on α-Fe2O3. Discussions of the Faraday Society 52:239-254

McFee, W.W., J.M. Kelley and R.H. Beck 1976. Acid precipitation effects on soil pH and base saturation of exchange sites. IN Proceedings of the First International Symposium on Acid Precipitation and Forest Ecosystems, May 12-15 1975, Columbus, Ohio.

Eds L.S. Dochinger and T.A. Seliga. U.S. Forest Service Technical Report NE-23

McFee, W.W., J.M. Kelley and R.H. Beck 1976. Acid precipitation effects on soils in the humid temperate zone. U.S. Department of Agriculture, Forest Service Technical Report NE-23

McKay, H.A.C. 1971. Kinetics of exchange reactions. Nature 142:997-998

McKay, H.A.C. 1971. Principles of Radiochemistry. CRC Press

McKell, C.M. and W.A. Williams 1960. A lysimeter study of sulfur fertilization of an annual-range soil. Journal of Range Management 13:113-117

McLaughlin, J.R., J.C. Ryden and J.K. Syers 1977. Development and evaluation of a kinetic model to describe phosphate sorption by hydrous ferric oxide gel. Geoderma 18:295-307.

McLaughlin, J.R., J.C. Ryden and J.K. Syers 1981. Sorption of inorganic phosphate by iron- and aluminum- containing soil components. Journal of Soil Science 32:365-378

Mekaru, T. and G. Uehara 1972. Anion adsorption in ferruginous tropical soils. Soil Science Society of America, Proceedings 36:296-300

Micale, F.J., D. Kiernan and A.C. Zettlemoyer 1985. Characterization of the surface properties of iron oxides. Journal of Colloid and Interface Science 105:570-576

Morimoto, T., M. Nagaro and F. Tokuda 1969. The relation between the amounts of chemisorbed and physisorbed water on metal oxides. Journal of Physical Chemistry 73:243-248

Muljadi, D., A.M. Posner and J.P. Quirk 1966. The mechanism of phosphate adsorption by kaolinite, gibbsite, and pseudoboehmite. (I) The isotherms and the effect of pH on adsorption. Journal of Soil Science 17:212-229

Muljadi, D., A.M. Posner and J.P. Quirk 1966. The mechanism of phosphate adsorption by kaolinite, gibbsite, and pseudoboehmite. (II) The location of the adsorption sites.Journal of Soil Science 17:230-237

Muljadi, D., A.M. Posner and J.P. Quirk 1966. The mechanism of phosphate adsorption by kaolinite, gibbsite, and pseudoboehmite. (III) The effect of temperature on adsorption. Journal of Soil Science 17:238-247

Murad, E. 1979. Mossbauer Spectra of goethite, evidence for structural imperfections. Mineralogical Magazine 43:355-361

Murad, E. 1982. The characterization of goethite by Mossbauer spectroscopy. American Mineralogist 67:1007-1011

Nakamoto, K. 1978. Infrared and Raman Spectra of Inorganic and Coordination Compounds. 2nd edition. Wiley, New York, 448 pp.

Nahon, D., C. Janot, A.M. Karpoff, H. Paquet and Y. Tandy 1977. Mineralogy, petrography and structures of iron crusts (ferricretes) developed on sandstones in the western part of Senegal. Geoderma 19:263-277

Nickel, E.H. 1984. An unusual pyrite - sulfur - jarosite assemblage from Arlcaroola, Southern Australia. Mineralogical Magazine 48:139-142

Nodvin, S.C., C.T. Driscoll G.C. Likens 1968. The effect of pH on sulfate adsorption by a forest soil. Soil Science 142:69-75

Nordstrom, D.K. 1982. The effect of sulfate on aluminum concentrations in Natural waters. Some stability relations in the system Al_2O_3-SO_3-H_2O at 298 K. Geochimica et Cosmochimica Acta 46:681-692

Nordstrom, D.K. 1982. Aqueous pyrite oxidation and the consequent formation of secondary iron minerals. IN Acid Sulfate Weathering. Soil Science Society of America (1979) Symposium Proceedings Publication No. 10:37-56

Norrish, K. and R.M. Taylor 1961. The isomorphous replacement of iron by aluminum in soil goethites. Journal of Soil Science 12:294-306

Onoda, G.Y. and P.L. DeBruyn 1966. Proton adsorption at the ferric oxide aqueous solution interface. (I) Kinetic study of adsorption. Surface Science 4:48-3

Parfitt, R.L., A.D. Thomas, R.J. Atkinson and R. St. C. Smart 1974. Adsorption of phosphate on imogolite. Clays and Clay Minerals 22:455-456

Parfitt, R.L., R.J. Atkinson and R.C. Smart 1975. The mechanism of phosphate fixation by iron oxides. Soil Science Society of America, Proceedings 39:837-841

Parfitt, R.L. and R.J. Atkinson 1976. Phosphate adsorption on goethite. Nature 24-740-742

Parfitt, R.L., J.D. Russell and V.C. Farmer 1976. Confirmation of the surface structures of goethite (α-FeOOH) and phosphated goethite by infrared spectroscopy. Journal of the Chemical Society, Faraday Transactions I 72:1082-1087

Parfitt, R.L., V.C. Farmer and J.D. Russell 1977. Adsorption on hydrous oxides. (I) Oxalate and benzoate on goethite. Journal of Soil Science 28:29-39

Parfitt, R.L., A.R. Fraser, J.D. Russell and V.C. Farmer 1977. Adsorption on hydrous oxides. (II) Oxalate, benzoate, and phosphate on gibbsite. Journal of Soil Science 28:40-47

Parfitt, R.L. and J.D. Russel 1977. Adsorption on hydrous oxides. (IV) Mechanism of adsorption of various ions on goethite. Journal of Soil Science 28:297-305

Parfitt, R.L. and R.St.C. Smart 1977. Infrared spectra from binuclear bridging complexes of sulfate adsorbed on goethite (α-FeOOH). Journal of the Chemical Society, Faraday Transactions 73:796-802

Parfitt, R.L. and R.St.C. Smart 1978. The mechanism of sulfate adsorption on iron oxides. Soil Science Society of America, Journal 42:48-50

Parks, G.A. and P.L. DeBruyn 1962. The zero point of charge of oxides. Journal of Physical Chemistry 66:967-973

Parks, G.A. 1965. The isoelectric points of solid oxides, solid hydroxides, and aqueous hydroxo complex systems. Chemical Reviews 65:177-198

Parks, G.A. 1967. Aqueous surface chemistry of oxides and complex oxide minerals. Isoelectric point and zero point of charge. IN Advances in Chemistry Series 67:121-160

Parker, R.L. 1967. Composition of the earths crust. IN Data of Geochemistry. United States Geological Survey Professional Paper 440-D, 19 p.

Paterson, E. 1980. Use of thermal methods of analysis in the study of surface phenomena. Analytical Proceedings 17:234-236.

Paterson, E. and R. Swaffield 1980. Influence of adsorbed anions on the dehydroxylation of synthetic goethite. Journal of Thermal Analysis 18:161-167

Pratt, P.F. and H.D. Chapman 1961. Gains and losses of mineral elements in an irrigated soil during a 20-year lysimeter investigation. Hilgardia 30:445-467

Pritchard, D.T. and E.C. Ormerod 1976. The effect of heating on the surface area of iron oxide. Clay Minerals 11:327-329

Rajan, S.S.S., K.W. Perrott and W.M.H. Saunders 1974. Identification of phosphate reactive sites of hydrous alumina from proton consumption during phosphate adsorption at constant pH values. Journal of Soil Science 25:438-447

Rehm, G.W. and A.C. Caldwell 1968. Sulfur supplying capacity of soils and the relation to soil type. Soil Science 105:355-361

Rendon, J.L. and C.J. Serna 1981. Infrared spectra of powder hematite: Effects of particle size and shape. Clay Minerals 16:375-381

Rochester, C.H. and S.A. Topham 1979. Infrared study of surface hydroxyl groups on hematite. Journal of the Chemical Society, Faraday Transactions I 75: 1073-1088

Ross, G.J., K.C. Ivarson and N.M. Miles 1982. Microbial formation of basic ferric sulfates in laboratory systems and in soils. IN Acid Sulfate Weathering. Soil Science Society of America Spec. Publn. 10. Madison, Wisconsin

Russel, J.D., P.L. Parfitt, A.R. Fraser and V.C Farmer 1974. Surface structure of gibbsite, goethite, and phosphated goethite. Nature 248:220-221

Russel, J.D., E. Paterson, A.R. Fraser and V.C. Farmer 1975. Adsorption of carbon dioxide on goethite (α-FeOOH) surfaces and its implications for anion adsorption. Journal of the Chemical Society, Faraday Transactions I 71:1623-1630

Ryden, J.C. and J.K Syers 1975. Rationalization of ionic strength and cation effects on phosphate sorption by soils. Journal of Soil Science 26:395-406

Ryden, J.C. and J.K. Syers 1975. Charge relations of phosphate sorption. Nature 255:51-53

Sanders, F.E. and P.B.H. Tinker 1975. Adsorption of sulfate by a sandy loam soil (Calcic Cambisol). Geoderma 13:317-324

Schwertmann, U., P. Cambien and E. Murad 1985. Properties of goethites of varying crystallinity. Clays and Clay Minerals 33:369-378

Shriner, D.J. and G.S. Henderson 1978. Sulfur distribution and cycling in a deciduous forest watershed. Journal of Environmental Quality 7:392-397

Sibanda, H.M. and S.D Young 1986. Competitive adsorption of humic acids and phosphate on goethite, gibbsite, and two tropical soils. Journal of Soil Science 37:197-204

Sigg, L. and W. Stumm 1981. The interactions of anions and weak acids with the hydrous goethite surface. Colloids and Surfaces 2:101-117

Sillen, L.G. and A.E. Martell 1964. Stability constants of metal-ion complexes. Special Publication # 17. The Chemical Society, London.

Sillen, L.G. and A.E. Martell 1971. Stability constants of metal-ion complexes. Supplement #1. Special Publication #25. The Chemical Society, Burlington House, London

Simon-Sylvestre, G. 1969. Soluble sulfate in soils. Ann. Agron. 20:435-447

Simon-Sylvestre, G. 1969. The total sulfur content of the cultivated soils of France. Ann. Agron. 30:609-625

Stauffer, R.S. and R.H. Rust 1954. Leaching losses in rainfall and percolation from 8 Illinois soils. Agronomy Journal 47:207-211

Stumm, W. and J.J. Morgan 1970. Aquatic Chemistry. First edition. Wiley-Interscience, New York, N.Y. 583 pp.

Stumm, W. and J.J. Morgan 1981. Aquatic Chemistry: An Introduction Emphasizing Chemical Equilibrium in Natural Waters. Second edition. Wiley-Interscience, New York, N.Y. 780 pp.

Swank, W.T. and J.E. Douglas 1977. Nutrient budgets for undisturbed and manipulated hardwood forest ecosystems in the mountains of North Carolina. IN Watershed Research in Eastern North America. Vol 1. p343-363. Ed. D.L. Correll. Smithsonian Institute, Washington, D.C.

Tipping, E. 1981. The adsorption of aquatic humic substances by iron oxides. Geochimica Cosmochimica Acta 45:191-199

Troelstra, S.A. and H.R. Kruyt 1942. Electrophoretic measurements on hydrophobic colloids. Kolloid Zeitschrift 101:182-189

Van Breeman, N. 1982. Genesis, morphology, and classification of acid sulfate soils in coastal plains. IN Acid Sulfate Weathering. Soil Science Society of America Special Publication No. 10:95

Verdonck, L., S. Hoste, F.F. Roeland and G.P. Van Der Keln 1982. Normal coordinate analysis of α-FeOOH. A molecular approach. Journal of Molecular Structure 79:273-279

Vlek, P.L.G., J.M. Blom, J. Beek and W.L. Lindsay 1974. Determination of solubility products of various iron hydroxides and jarosite by the chelation method. Soil Science Society of America, Proceedings 38:429-432

Williams, C.H. 1975. The chemical nature of sulfur compounds in soil. IN Sulfur in Australian Agriculture. p 21-31

Wootton, R.S. 1985. Sorption of sulphate by iron oxides. BSc Thesis, McMaster University, Hamilton, Ontario

Yates, D.E. 1975. The structure of the oxide - aqueous electrolyte interface. Ph.D. Thesis, University of Melbourne, Melbourne, Australia

Yates, D.E. and T.W. Healy 1975. Mechanism of anion adsorption at the ferric and chromic oxide/ water interfaces. Journal of Colloid and Interface Science 52:222-228

Yopps, J.A. and D.W. Fuerstanau 1964. The zero point of charge of alpha-alumina. Colloid Science 19:61-71

Zinder, B., G. Furrer, and W. Stumm 1986. The coordination chemistry of weathering: II. Dissolution of Fe(III) oxides. Geochimica et Cosmochimica Acta 50:1861-1869

APPENDIX A

SUMMARY OF OXIDE RESEARCH (Preparation, Sulfate Sorption)

HEMATITE STUDIES	SA	ZPC	SM	IS	pH	T
Ahmed Maksimov 1968	451	5.3±0.05	--	0.001M KNO_3	--	--
Natural Sample	cm^2/g	5.4±0.05	--	0.1 M KNO_3	--	--
- interface study	308	5.7±0.1	--	1 M KNO_3	--	--
		6	--	KCl	--	--
Albrethson 1963	23	8.70	--	NaCl	--	25
Atkinson et al. 1967	43.5	8.60±0.2	--	KNO_3	--	20±1.5
Reflux $Fe(NO_3)_3$ 18	44.6	9.27±0.1	0--	KCl	--	20±1.5
days at b.p. pH 0-1	34.1	8.45±0.2	--	KNO_3	--	20±1.5
- p.d.i. adsorption	36.4	8.90±0.15	--	KCl	--	20±1.5
Aylmore et al. 1967	26.7	NR	67 [(2.50)]	NR	4.6	20
Reflux $Fe(NO_3)_3$ 18 days at b.p. pH 0-1						
- adsorption/desorption by soil constituents						
Boehm 1971	56	---	--	---	--	--
Calcination of precipitated a-FeOOH						
-amphoteric propeties of hydroxylated surfaces						
Borggaard 1983	14	7.3	--	NaCl	--	--
heated goethite @ 560°C for 20 hrs						
heated feroxyhite @ 560°C for 20 hrs	6	7.1	--	NaCl	--	--
-surface charge/anion adsorption wrt surface area and mineralogy						
Breuwsma Lyklema 1973/71	18	8.5±0.2	--	KCl	--	20±0.3
boil @ pH 7, age at 140-150°C in an autoclave for 8 hrs						
- ion and H_2O adsorption, A/B titration.						
Cabrera et al. 1977	1.2	6.45	--	---	--	--
Precip $FeCl_3$ at b.p., filter, heat 1000°C for 1 hr						
heat $Fe(NO_3)_3$ $9H_2O$ at 150°C for 1 hr	17.3	6.77	--	---	--	--
- phosphate adsorption envelope						
Jurinak 1964/1966	9.60	9.9	--	---	--	30
Fischer Co.(Thermal decomposition of $FeSO_4$)					Activation	
- H_2Oadsorption					Temperature	

Madrid et al. 1983	110	6.7	--	NaCl	--	--
2 hr. decomposition of lepidocrocite @ 350°C						
- adsorption of p.d.i. and electrolyte ions						
McCafferty Zettlemoyer	10	---	--	---	--	--
1971 Fischer Co.						
- adsorption of H_2O						
McLaughlin et al. 1981	18.0	---	--	---	--	--
reflux $Fe(NO_3)_3$ at b.p. for 18 days pH 0-1						
- phosphate adsorption						
Morimoto et al. 1969	14.5 (heat treated 250°C)				--	25
calcination of $FeSO_4$ $7H_2O$ @ 800°C for 7 hrs						
calcination of a-FeOOH @ 800°C in air for 5 hrs, then immersed in hot water at 80°C for 3 days	21.2 (heat treated 250°C)				--	25
- water on metal oxides						
Onoda DeBruyn 1966	21	8.3 fast	--	NaClO4	--	35
hydrolyze $Fe(NO_3)_3$ at b.p. pH 0-1		8.5 slow titration				
- H+ adsorption and kinetics						
Parfitt et al. 1975	22	---	--	---	--	--
Reflux $Fe(NO_3)_3$ at b.p, pH 0-1 for 2 weeks						
- adsorption of phosphate and infrared work						
Parfitt Smart 1978	22	---	85	KCl	3.5	26
reflux $Fe(NO_3)_3$ at the b.p. for 2 weeks			[(3.86)]			
- sulfate sorption, infrared work						
Parks DeBruyn 1962	22	8.5	--	KNO_3	--	21
reflux $Fe(NO_3)_3$ at the b.p. pH 0-1						
- hydrogen/hydroxyl adsorption, A/B titration						
Pritchard Ormerod 1976	113	---	--	---	--	--
ignite goethite for 2 hrs at (i) 275°C and (ii) 600°C	27	---	--	---	--	--
- effects of heating on surfaces						
Rochester Topham 1979	68	(NaOH, <673 °C)		---	--	--
$FeCl_3$ + base, aged overnight @ pH 7-8	38	(NaOH, 673 °C)		---	--	--
	27	(NH3, <623 °C)		---	--	--
filtered, dried = ferigel. Heat in O_2 at Temp > 573°C	117	(NH3, 713 °C)		---	--	--
	57	(NH3, 773 °C)		---	--	--
- infrared study of OH groups						

Tipping 1981	63	(6.3)	--	---	--	--
reflux $Fe(NO_3)_3$ at the b.p., pH 0-1						
- adsorption of Humic Substances						
Troelstra Kruyt 1942	---	8.3	--	---	--	--
react $FeCl_3$ $6H_2O$ with NH_4OH,						
heat precip in autoclave at 150-160°C in H_2O at 5 atm.						
Wootton 1985	12.0	---	46	0.01 NaCl	3	RT
Natural Sample			[(3.83)]			
	---	---	35	0.01 NaCl	5	RT
- sulfate sorption			[(2.92)]			

GOETHITE STUDIES	SA	ZPC	SM	IS	pH	T
Atkinson et al. 1967	70.9	7.55±0.15	--	KCl	--20.3±0.4	
aged $Fe(NO_3)_3$ pH 12 for 24 hrs. at 60°C						
- p.d.i. adsorption						
Atkinson et al. 1972	13.8	---	--	---	--	--
aged $Fe(NO_3)_3$ pH 12	38.2	---	--	---	--	--
for 24 hrs. at 60°C	57.5	---	--	---	--	--
- isotopic exchange	64.3	---	--	---	--	--
of phosphate (kinetics)						
Balistreri Murray 1979	48.5	7.5	--	NaCl/KCl	--	--
aged $Fe(NO_3)_3/FeClO_4$	±0.2					
pH 12 for 24 hrs. at 60°C						
- surface chemistry in seawater						
Balistreri Murray 1981	51.8	7.1	--	seawater	--	--
aged $Fe(NO_3)_3$ at pH 12 for 24 hrs. at 60°C						
- surface chemistry in seawater						
Bleam McBride 1985	82	---	--	---	--	--
aged $FeClO_4$ (OH:Fe = 1)at pH = 12 for 24 hrs at 60°C						
- metal (Mn, Mg) adsorption and changes in surface charge						
Borggaard 1983	16	7.2	--	NaCl	--	--
aged $Fe(NO_3)_3$ 2 days at 60°C and OH/Fe = 3.5						
aged $Fe(NO_3)_3$ at	82	7.6	--	---	--	--
OH/Fe = 1.0 for 3 days at RT then age 2 days						
@ pH 12.3 and 55°C						
- surface charge/anion adsorption wrt surface area & mineralogy						
Cabrera et al. 1977	87.4	8.45	--	---	--	--
$Fe(NO_3)_3$ + NaOH to pH 11.7, age 10 days at RT						
- phosphate adsorption envelope/phosphate precipn from $CaHPO_4$ solutions by Fe and Al oxides						

Cabrera et al. 1981	54.4	8.4	--	---	--	--
$Fe(NO_3)_3$ + NaOH to pH 11.7, age 10 days at RT	87.4					
- phosphate adsorption wrt porosity/equilibrium pH						
Cambier 1986 and	153	(4°C for 68 days)	---		--	--
Schwertman et al 1985	119	(10°C for 35 days)	---		--	--
$Fe(NO_3)_3$ + KOH aged at X temp Y days	101	(15°C for 28 days)	---		--	--
	92	(25°C for 13 days)	---		--	--
	85	(30°C for 13 days)	---		--	--
- infrared study wrt particle size and crystallinity	60	(40°C for 13 days)	---		--	--
	41	(50°C for 13 days)	---		--	--
	16	(60°C for 7 days)	---		--	--
	13	(70°C for 6 days)	---		--	--
Evans et al. 1979	112	8.75	--	NaI	--	--
aged $Fe(NO_3)_3$ pH 12 for 24 hrs. at 60°C						
- H+, OH-, and CO_2 adsorption/surface charge density, A/B titn						
Forbes et al. 1974	89	{7.6}	--	---	--	--
aged $Fe(NO_3)_3$ at pH 1.9 for 48 hrs at 60°C, then at pH 11.7 for 3 days at 60°C						
- metal (Hg and Co) adsorption						
Gast et al. 1974	32	---	--	---	--	--
aged ferric oxide gel ($FeCl_3$ + KOH) @ pH 12, at 60°C						
- interaction of water with oxide surfaces						
Hingston et al. 1972 and 1974	81	8.0	150 [(1.85)]	0.1 NaCl	3.0	20-23
	---	---	110 [(1.36)]	0.1 NaCl	4.0	20-23
- anion adsorption and desorption	---	---	60 [(0.74)]	0.1 NaCl	5.0	20-23
	32	7.8	--	NaCl	--	--
	28	8.3	--	NaCl	--	--
	17	8.0	--	NaCl	--	--
Jurinak 1964	16.2	---	--	---	--	30
Fischer Co.					Activation	
- H_2O adsorption					Temperature	
Lumsdon et al. 1984	86	---	--	---	--	--
- Arsenite adsorption, infrared work						
Madrid Arambarri 1978	70.5	8.71	--	NaCl	--	20±1
aged $Fe(NO_3)_3$ at 60°C for 24 hrs.						
- H+ adsorption and desorption						

Madrid Posner 1979	84	8.0	--	NaCl	--	25
method of Hingston et al 1968						
- phosphate desorption						
Madrid et al. 1983	74	8.5	--	NaCl	--	--
method of Hingston et al 1968						
- adsorption of p.d.i. and electrolyte ions						
McLaughlin et al.1981	17.0	---	--	---	--	--
aged $Fe(NO_3)_3$ @ RT at pH 11 for 2 days, then heat at 90°C for 16 hrs						
- phosphate adsorption						
Murad 1982	30	---	--	---	--	--
ferrihydrate transformation in 0.4 M KOH at 70°C for 14 days						
	88	---	--	---	--	--
ferrihydrate transformation in 2 M KOH at 70°C for 8 days						
	89	---	--	---	--	--
lepidocrocite transformation in 2 M KOH / 1.23×10^{4} M Si @ Room Temp.						
	167	---	--	---	--	--
oxidation of 0.05 M $FeCl_3$ in O_2/CO_2 at pH 6-7 and RT						
- Mossbauer studies						
Parfitt et al. 1974 and Parfitt Smart 1976	90	---	--	---	--	--
aged $Fe(NO_3)_3$ for 50 hrs. at pH 12 and 28°C						
- phosphate adsorption, infrared studies						
Parfitt et al. 1975 and Parfitt Atkinson 1976	80	---	--	---	--	--
aged $Fe(NO_3)_3$ for 50 hrs. at pH 12 and 28°C						
- phosphate adsorption, infrared studies						
Parfitt Russell 1977	90	---	--	---	--	--
aged $Fe(NO_3)_3$ for 50 hrs. at pH 12 and 28°C						
- ion adsorption, isotopic exchange, and infrared work						
Parfitt Smart 1977/78	90	---	125 [(1.39)]	KCl	3.4	26
aged $Fe(NO_3)_3$ @ pH 12 for 50 hrs. 28°C	---	---	75	KCl	5.1	26
- sulfate sorption, infrared work [(0.83)]						
Parfitt et al. 1977	90	---	--	---	--	--
aged $Fe(NO_3)_3$ 50 hrs, adjust to pH 11.8, age 4 days at 60 °C						
- organics adsorption envelope, infrared studies						

Pritchard Ormerod 1976	50	---	--	---	--	--
$Fe(NO_3)_3$ + NaOH stir 1 hr., age at pH 12, 60°C for 90 hrs						
- heating effects on surface						
Rendon Serna 1981	50	---	--	---	--	--
aged $Fe(NO_3)_3$ at pH 12 for 24 hrs at 60°C						
- infrared study						
Russel et al.1974/75	60	---	--	---	--	--
age $Fe(NO_3)_3$ hrs at RT, adjust to pH 11.8, then						
age at 60°C for 4 days						
- surface structure infrared studies, CO_2 adsorption						
Sibanda Young 1986	96.2	---	--	---	--	--
method of Hingston et al 1968						
-competetive adsorption between Humic Acids and phosphate						
Sigg Stumm 1981	28	7.0	--	$NaClO_4$	--	--
aged $Fe(NO_3)_3$ 24 hrs	29	---	--	---	--	--
at pH 12 and 60°C						
- A/B titration, anion adsorption work						
Tipping 1981	11	{8.4}	--0.002 M NaCl		--	--
aged $Fe(NO_3)_3$ 24 hrs	15	{8.2}	--0.002 M NaCl		--	--
at pH 12 and 60°C	18	{7.0}	--0.002 M NaCl		--	--
- adsorption of humic substances						
Yates Healy 1975	48	7.5	--	KNO_3	--	25±1
aged $Fe(NO_3)_3$ for 24 hrs at pH 12 and 60°C						
- anion and H_2O sorption, A/B titration						

SA = Surface Area (m^2/g)
IS = Ionic Strength
T=Temperature °C
{IEP} = Isoelectric Point
ZPC = Zero Point of Charge
SM = Sorption Maxima (μmol/g)
[(SS)] = SORBED SULFATE(μmol/m^2)